Universidad Autónoma de Madrid
Facultad de Ciencias
Departamento de Biología Molecular

STUDY OF THE FUNCTIONS OF SHELTERINS AND TELOMERASE IN AGING AND NUCLEAR REPROGRAMMING

DOCTORAL THESIS

IANIRE GARROBO CALLEJA

Madrid, 2014

Universidad Autónoma de Madrid
Facultad de Ciencias
Departamento de Biología Molecular

STUDY OF THE FUNCTIONS OF SHELTERINS AND TELOMERASE IN AGING AND NUCLEAR REPROGRAMMING

Ianire Garrobo Calleja
BSc, Biochemist; MSc

The entirety of the work presented in this Thesis has been carried out at the Telomeres and Telomerase Group in the Spanish National Cancer Research Centre (CNIO, Madrid), under the direction and supervision of Dr. Maria Antonia Blasco Marhuenda
Madrid, 2014

Acknowledgements

Gracias **Maria** por darme la oportunidad de realizar mi tesis en tu laboratorio y en un centro como el CNIO.

Gracias **Nani** por tu supervisión todos estos años.

Gracias también a todos los miembros del grupo de **Telómeros y Telomerasa** y **Supresión Tumoral**, pasados y presentes, por vuestra ayuda y apoyo todo este tiempo.

Abstract

Mammalian telomeres are nucleoprotein structures consisting of TTAGGG tandem repeats bound to a protein complex called shelterin, which protect chromosome ends from degradation, fusions and fragility. TRF1, one of the components of the shelterin that binds to dsDNA, has been shown to be essential for telomere protection and replication. Telomerase is an enzyme composed of a reverse transcriptase (TERT) and a RNA template (*Terc*) that has the ability to add telomere repeats *de novo*. Telomerase is expressed during embryonic development and in adult stem cell compartments of several tissues, but its activity is not sufficient to compensate for the accumulative telomere erosion associated aging.

Telomeric repeats can also be found throughout the genome, as Internal or Interstitial Telomeric Sequences (ITSs). Furthermore, several shelterins have been described to bind to ITSs as well as to other extra-telomeric regions, some of them having key roles in transcriptional regulation. Here, we set to address whether TRF1 can be found at extra-telomeric sites in cells with both normal and critically short telomeres, contributing to the transcriptional alterations associated with aging. In particular, we performed a ChIP-sequencing technique to map TRF1 binding sites in wild-type and *Terc*$^{-/-}$ MEFs, concluding that TRF1 is exclusively located at telomeres in this type of cells.

In 2006, Takahashi and Yamanaka achieved the nuclear reprogramming of somatic cells by the ectopic addition of the transcription factors *Oct3/4*, *Sox2*, *Klf4* and cMYC, giving rise to the so-called induced pluripotent stem (iPS) cells. IPS cells closely resemble ES cells in their global gene expression and epigenetic patterns. Besides they overcome the ethical and immune-compatibility issues that limit the clinical use of ES cells. Telomerase activity, telomere length and TRF1 levels are increased in iPS cells and this increase correlates with higher pluripotency. In this way, knowledge of telomere remodeling during reprogramming is crucial for the possible applications of iPS cells in regenerative medicine. In this thesis, we demonstrated that the shelterin TRF1 is essential for the acquisition and maintenance of pluripotency, highlighting the importance of telomere protection and replication in stem cells biology.

Resumen

Los telómeros de mamíferos son estructuras nucleoproteicas que consisten en repeticiones TTAGGG unidas al complejo proteico *shelterin* y que protegen los extremos de los cromosomas de la degradación, fusiones y fragilidad. TRF1, uno de los componentes del *shelterin* de unión a DNA de doble hebra, es esencial para la protección y replicación telomérica. La telomerasa es una enzima compuesta por una transcriptasa reversa (TERT) y un RNA molde (*Terc*) que tiene la capacidad de añadir repeticiones teloméricas *de novo* a los extremos de los cromosomas. La telomerasa se expresa durante el desarrollo embrionario y en los compartimentos de células madre adultas en varios tejidos, pero su actividad no es suficiente para compensar la erosión telomérica asociada al envejecimiento.

Las repeticiones teloméricas también se encontran a lo largo del genoma, como "sequencias teloméricas intersticiales" o ITSs. Además, se ha descrito que ciertas shelterinas se unen tanto ITSs como a otras regiones extra-teloméricas, teniendo papeles clave en la regulación transcripcional. En esta tesis, nos propusimos estudiar si TRF1 puede unirse a sitios extra-teloméricos en células con telómeros normales y críticamente cortos, contribuyendo así a las alteraciones transcripcionales asociadas con el envejecimiento. En concreto, realizamos un ChIP-sequencing con el fin de mapear los lugares de unión de TRF1 en MEFs *wild-type* y *Terc*$^{-/-}$, concluyendo que TRF1 está exclusivamente localizada en telómeros en este tipo celular.

En el 2006 Takahashi y Yamanaka lograron la reprogramación nuclear de células somáticas mediante la adición de los factores de transcripción *Oct3/4*, *Sox2*, *Klf4* y *c-Myc*, dando lugar a las células madre pluripotentes inducidas (iPS). Las células iPS son similares a las células madre embrionarias (ES) en su expresión génica global y patrones epigenéticos. Adicionalmente, anularían los problemas éticos y de inmunocompatibilidad que limitan el uso clínico de las células ES. La actividad telomerasa, la longitud telomérica y los niveles de TRF1 aumentan en células iPS, estando este aumento correlacionado con la pluripotencia. De este modo, un conocimiento de la remodelación telomérica durante la reprogramación es crucial para las posibles aplicaciones de las células iPS en medicina regenerativa. En esta tesis, hemos demostrado que la proteína TRF1 es esencial para la adquisición y mantenimiento de la pluripotencia, enfatizando la importancia de la protección y replicación telomérica en la biología de las células madre.

Index

Abbreviations

3F/ 4F	3/4 reprogramming factors
4-OHT	4-hydroxytamoxifen
AB	antibody
ADP	adenosine-diphosphate
ALT	Alternative Lengthening of Telomeres
AP	Alkaline Phosphatase
ATM	Ataxia Telangiectasia Mutated
ATR	Ataxia Telangiectasia Related
a.u.	Arbitrary units
BER	Base Excision Repair
BLM	Bloom protein
bp	Base pairs
BSA	Bovine serum albumin
CDK1	Cyclin-dependent kinase 1
cDNA	Complementary DNA
cm	centimeters
CFS	Common Fragile Site
ChIP	Chromatin Immunoprecipitation
CHK1	Checkpoint kinase 1
CHK2	Checkpoint kinase 2
c-MYC	myelocytomatosis
Ctrl	Control
Dapi	4',6-Diamidino-2-phenylindole dihydrochloride
DC	Dyskeratosis Congenita
DDR	DNA Damage Response
D-loop	Displacement loop
DNA	Deoxyrribonucleic acid
DNA-PK	DNA-activated Protein Kinase

DKC1	Dyskerin1
DMEM	Dulbecco's Modified Eagle's Medium
DMSO	Dimethyl sulfoxide
dox	Doxycycline
DSBs	Double Strand Breaks
dsDNA	Duble-strand DNA
E	Exon
(e)GFP	(Enhanced) Green Fluorescent Protein
ERT2	Estrogen Receptor T2 variant
ES(Cs)	Embryonic Stem (cells)
EV	Empty Vector
FACS	Fluorescence-activated cell sorting
FBS	Foetal bovine serum
FDR	False discovery rate
Fig.	Figure
Fw	Forward
G1/3	First/ Third Generation
G4	Guanine cuadruplex
Gapdh	Glyceraldehyde-3-phosphate
GSK3	Glycogen synthase kinase-3
h	hours
HEK	Human Embryonic Kidney
Helt	hTERT immortalized BJ fibroblasts
HR	Homologous Recombination
hTEP1	Human telomerase-associated protein 1
I	intron
I4F	Inducible four factors
ICM	Inner-cell Mass
iPS	Induced Pluripotent Stem

IR	Ionizing Radiation
ITSs	Internal/ Interstitial Telomeric sequences
K5	Keratin 5 (promoter)
Kb	Kilo-bases
kD	Kilo-Daltons
Klf4	Krüppel-like factor 4
KO	Knockout
KSR	Knockout Serum Replacement
LIF	Leukaemia Inhibitory Factor
MACS	Model-based Analysis of ChIP-seq
Mbp	Megabase-pairs
MEF	Mouse Embryonic Fibroblast
min	minutes
mRNA	Messenger Ribonucleic Acid
MTS	Multitelomeric Signals
Neo	Neomycin selection cassette
NER	Nucleotide Excision Repair
NHEJ	Non-Homologous End Joining
NLS	Nuclear Localisation Signal
nt	nucleotides
OCT3/4	Octamer3/4
o/n	overnight
OSK/OSKM	*Oct3/4*, *Sox2*, *Klf4*; *Oct3/4*, *Sox2*, *Klf4*, *c-Myc*
P	Passage
PAGE	polyacrylamide gel electrophoresis
PARP1/2	poly-ADP-ribose polymerase 1/2
PBS	Phosphate buffer saline
PCR	Polymerase chain reaction
PFA	Paraformaldehyde

p.i.	Post-infection
PINX1	PIN2-Interacting protein1
POT1	protection of telomeres 1
Q-FISH	Quantitative Fluorescence *in situ* Hybridization
qRT-PCR	Quantitative Real Time PCR
RAP1	Repressor Activator Protein 1
RB	Retinoblastoma-Protein
RT	Room Temperature
RTEL1	regulator of telomere elongation helicase 1
rtTA	Transcriptional activator
Rv	Reverse
S	Subtelomeres
SAC	Spindle Assembly Checkpoint
SCNT	Somatic-cell nuclear transfer
SDS	Sodium dodecyl sulfate
sec	seconds
S.e.m.	Standard error of the mean
shRNA	Short-hairpin RNA
SMC-1	Structural Maintenance of Chromosomes 1
SSB	Single-strand breaks
ssDNA	Single-strand DNA
SSEA-1	Stage-Specific Embryonic Antigen 1
SOX2	Sry-related, HMG box-containing protein
Sp	Super
TANK1	Tankyrase 1
TANK2	Tankyrase 2
Terc	Telomerase RNA Component
TERT	Telomerase Reverse Transcriptase
Tg	Transgenic
TIF	Telomere dysfunction Induced Foci

TIN2	TRF1 Interacting Protein 2
T-loop	Telomere loop
TOPOIIα	Topoisomerase II alpha
TPP1	POT1-TIN2 organizing protein
TRF1/TERF1	Telomere Repeat binding Factor 1
TRF2/TERF2	Telomere Repeat binding Factor 2
TRFH	Telomere Repeat binding Factor Homology domain
T-SCE	telomeric sister-chromatid exchange
TSS	transcription start sites
TTF	tail-tip fibroblast
UTR	Untranslated region
WRN	Werner
WT	Wild-type
XPF	Xeroderma Pigmentosum group F
γH2AX	Gamma phosphorylated histone Histone 2 variant A.X

Introduction

1. Telomere structure

"Telomere" is a term that derives from the Greek words *telos* (end) and *meros* (part). Telomeres are specialized ribonucleoprotein structures at the end of eukaryotic chromosomes that protect them from being detected as double-strand DNA (dsDNA) breaks (DSBs) by the DNA damage response (DDR) machinery, preventing fusions, recombination and degradation (Chan and Blackburn, 2002; de Lange, 2005) . In vertebrates, telomeres are composed of heterochomatic tandem arrays of TTAGGG repeats bound to a complex of proteins called shelterin or telosome, which contributes to the telomere protection and capping (de Lange, 2005). On average, human telomeres are 10-15 kb long, while in mice telomeres span between 25 and 40 kb, depending on the genetic background (Blasco, 2005). At the end of the telomere sequences, there is a single-stranded DNA (ssDNA) 3' overhang of the G-rich strand (G-strand overhang) of approximately 150 to 200 nt, which is a direct consequence of the "end-replication problem" (explained later) **(Fig. 1A)**. In order to prevent degradation of chromosomal ends by exonucleases or processing as DSBs, the G-strand overhang folds back and invades the double-stranded telomeric region forming the so-called telomere loop (T-loop) and generating a displacement loop or D-loop (Griffith et al., 1999) **(Fig. 1B)**. Some shelterin components have been shown to influence this T-loop formation (de Lange, 2005). Because of its G-rich content, G-strand overhangs can form G-cuadruplexes (G4 DNA), where each G serves as a donor and acceptor for hydrogen bond formation **(Fig. 1C)**. In humans, G-cuadruplexes have been implicated in telomere protection and inhibition of telomere elongation by telomerase (Lipps and Rhodes, 2009).

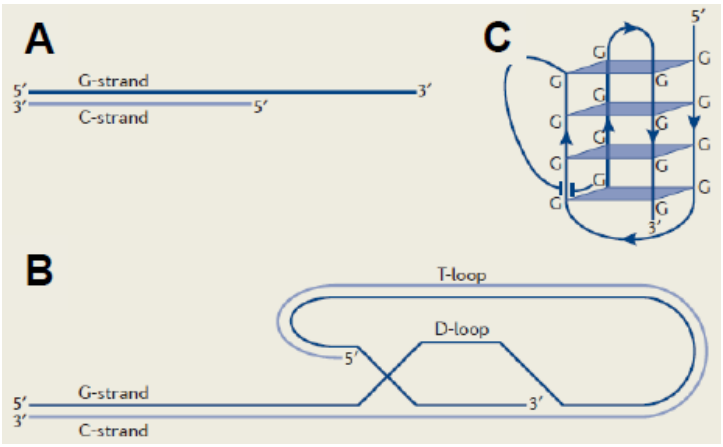

Figure 1: The structure of mammalian telomeres. (A) Mammalian chromosomes end in an array of TTAGGG repeats. The telomere terminus contains a single-stranded G-rich 3'-overhang of 150-200 nt. (**B**) Scheme of the T-loop structure showing the invasion of the dsDNA by the G-overhang, leading to the formation of the D-loop. (**C**) Structure of the G-cuadruplex (G4) DNA (Adapted from Nandakumar and Cech, 2013).

2. The shelterin complex

Mammalian shelterin complex is composed of six proteins: telomeric or TTAGGG repeat binding factors 1 (TERF1 or TRF1) and 2 (TERF2 or TRF2), TRF1-interacting protein 2 (TIN2), protection of telomeres 1 (POT1), the POT1-TIN2 organizing protein (TPP1, TINT1, PTOP or PIP1) and repressor/activator protein 1 (RAP1) (de Lange, 2005) **(Fig. 2A)**. From these six proteins only three of them bind directly to DNA: TRF1 and TRF2 to dsDNA and POT1 to the single-stranded 3' overhang. TRF1 and TRF2 bind independently to the 5'-YTAGGGTTR-3' sequence, forming homodimers or oligomers (Broccoli et al., 1997; Court et al., 2005). POT1 also has strong sequence specifity binding single-stranded 5'-TAGGGTTAG-3' sites at the G-strand overhang and the displaced G-strand at the D-loop (Baumann and Cech, 2001; Lei et al., 2004; Loayza et al., 2004) **(Fig. 2B)**. POT1 interacts with TRF1 and this interaction is proposed to affect the loading of POT1 on the ssDNA (Loayza and De Lange, 2003). While humans contain only one *POT1* gene, mouse *Pot1* has two paralogs, *Pot1a* and *Pot1b*, which carry out different functions (Hockemeyer et al., 2006). POT1 is recruited to telomeres by its binding to TPP1 (Liu et al., 2004), which is also able to bind to TIN2 protein (Ye et al., 2004b). TIN2 binds to TRF1 and TRF2 via different domains and is necessary for

the stabilization of these proteins at telomeres. Besides, it recruits the TPP1-POT1 complex to the rest of the shelterins, acting as a bridge that links the double-stranded and single-stranded binding proteins of the shelterin complex (Chen et al., 2008; Kim et al., 2004; Ye et al., 2004a). Lastly, RAP1 is recruited to telomeres by its binding to TRF2 (Celli and de Lange, 2005; Li and de Lange, 2003).

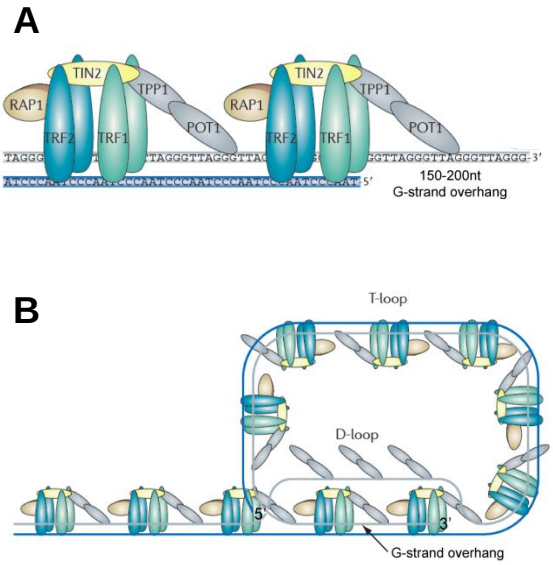

Figure 2: Shelterin complex and T-loop structure. (A) Schematic depiction of the nucleoprotein structure of a telomere and the binding pattern and partners of the shelterin proteins. Of note is that only TRF1, TRF2 and POT1 are directly binding to telomeric DNA. RAP1, TIN2 and TPP1 are localized at the telomere via a linker protein. **(B)** Telomere nucleoprotein structure forming the T-loop and binding of the corresponding shelterins (Adapted from Martinez and Blasco, 2011).

Complete abrogation of each of these proteins leads to early embryonic lethality in mice, with the exception of RAP1 and POT1B. Shelterins have fundamental roles in telomere biology, associated with T-loop formation (TRF2 and TRF1), protection and recombination (TRF2, TRF1, TIN2, TPP1 and RAP1), inhibition of DDR (TRF2, TRF1, TPP1, POT1, RAP1), G-strand overhang protection (POT1), telomerase recruitment (TPP1), telomere length regulation (TRF2, TRF1, TIN2, TPP1 and RAP1) or telomere replication (TRF1) (Martinez and Blasco, 2011).

In addition to the core proteins that form the shelterin complex, accessory factors are transiently associated with telomeres. Some examples are the TRF1-interacting ankyrin-related poly-ADP-ribose polymerase (PARP) Tankyrase 1 (TNK1) and 2 (TNK2), which regulate TRF1 binding to telomeres (Cook et al., 2002; Smith et al., 1998), PIN2/TERF1 interacting protein (PINX1), which directly

binds and inhibits telomerase (Soohoo et al., 2011), MRE11/ NBS1/ RAD50 complex, involved in the detection of DSBs and repair by homologous recombination (HR) (Zhu et al., 2000), XPF/ERCC1 endonucleases complex, a component of the nucleotide-excision repair (NER) pathway (Zhu et al., 2003), the DNA-PKs complex, which are kinases implicated in non-homologous end joining (NHEJ) (d'Adda di Fagagna et al., 2001; Yang et al., 1999), the RecQ helicases WRN and BLM, associated with unwinding DNA during the replication process (Opresko et al., 2002), the ADP-ribosylases 1 (PARP1) and 2 (PARP2), implicated in base excision repair (BER) (Dantzer et al., 2004) and Apollo, a 5'-exonuclease involved in telomere end modulation) (Wu et al., 2012). The majority of these factors are recruited to telomeres through their interaction with the shelterin components, mostly TRF1 and TRF2 (Chen et al., 2008), having essential roles in the maintenance, protection and function of telomeres.

3. Telomere protection and DDR

Mammalian cells respond to the presence of DNA lesions by activating a DDR that consists in signaling cascades including the detection, degradation or repair of the fragments, cell cycle arrest and/or death. DNA breaks can activate two signaling pathways: ataxia telangiectasia mutated (ATM) kinase pathway, primarily activated by DSBs, and ATM-RAD3-related (ATR) kinase pathway, activated by ssDNA breaks (SSBs). Once any of these two kinases are activated, they phosphorylate the histone variant H2AX on Serine 139 (γH2AX), inducing the accumulation of detectable DNA damage foci. ATM and/or ATR activation induces the checkpoint proteins CHK1 and CHK2 and ultimately leads to the activation of the tumor suppressors p53 and p21, triggering cell cycle arrest, senescence and/or apoptosis. In parallel, recognition of DSBs also drives the repair of these DNA fragments by two different pathways, HR and NHEJ (Denchi, 2009).

Telomeres are potential sites of genome instability, hence its maintenance and protection requires the inhibition of DDR signals. Some of the shelterins contribute to this inhibition and, hence to the protection of telomeres. Abnormal or impaired

telomeres that are critically short or unprotected due to shelterin deficiencies are recognized as DSBs by the DDR machinery, triggering the accumulation of DNA damage foci known as telomeric-induced damage foci (TIF) and chromosomal aberrations (de Lange, 2009; Denchi, 2009; Martinez et al., 2009; Tejera et al., 2010), ultimately resulting in cell cycle arrest, senescence and/or apoptosis. The non proper inhibition of NHEJ pathway can lead to chromosome or sister chromatid end-to-end fusions, while the activation of HR would lead to recombination between telomeres (telomeric sister-chromatid exchanges, T-SCE) or telomeres and other sequences in the genome. Chromosome end-to-end fusions are tremendously deleterious for the cell because they give rise to dicentric chromosomes that are unstable during mitosis, promoting genome instability and eventually, cancer.

4. Telomere shortening and replicative senescence

During the DNA replication that takes place every cell division, telomeres shorten around 50 to 200 bp as a result of the "end-replication problem". This "end-replication problem" resides in the notion that conventional DNA polymerases need a primer to initiate the synthesis and can only add bases to the 3' end, causing the discontinuous and incomplete replication of the lagging strand (3'→ 5') of linear chromosomes (Ohki et al., 2001; Okazaki et al., 1967). It has been postulated that additional telomere loss occurs due to post-replicative processing of the C-rich strand, giving rise to the 3' G-overhangs (Makarov et al., 1997).

"Replicative senescence" is a phenomenon that was first described by Hayflick in the sixties and is based on the idea that most cell types have a limited proliferative capacity, becoming senescent after a number of divisions (Hayflick, 1965). These senescent cells are metabolically active but unable to proliferate. It is very well established that telomere shortening is the major mechanism that induces replicative senescence (Bodnar et al., 1998). Progressive erosion of telomeres is propagated into daughter cells and as a consequence of this telomere loss, less shelterin complex can be recruited to the end of the chromosomes. This would eventually results in critically short or uncapped telomeres, which would ultimately lead to cell cycle

arrest, apoptosis or senescence (d'Adda di Fagagna et al., 2003). This cell cycle arrest in response to telomere dysfunction differs from humans to mice. While in humans it is mediated by p53 and RB pathways, in mice the activation of p53 suffices to induce cell cycle arrest (Smogorzewska et al., 2000).

5. Telomere elongation

5.1. Telomerase

In 1985, Greider and Blackburn demonstrated the existence of an enzymatic activity that added telomere sequences to the 3' ends of chromosomes, the so-called telomerase (Greider and Blackburn, 1985). Telomerase, the main regulator of telomere length in mammalian cells (Chan and Blackburn, 2002), is able to re-elongate telomeres *de novo*, compensating for the telomere loss associated with cell division (Blackburn, 2001; Collins and Mitchell, 2002). This enzyme is a ribonucleoprotein complex that consists of two molecules each of a telomerase reverse transcriptase component (encoded by *Tert* gene) and a telomerase RNA component (encoded by the *Terc* gene), which serves as a template for telomere elongation. In addition, a single molecule of dyskerin 1 (DKC1) is retained in the core telomerase complex, binding and stabilizing *Terc* (Blasco, 2007) **(Fig. 3)**.

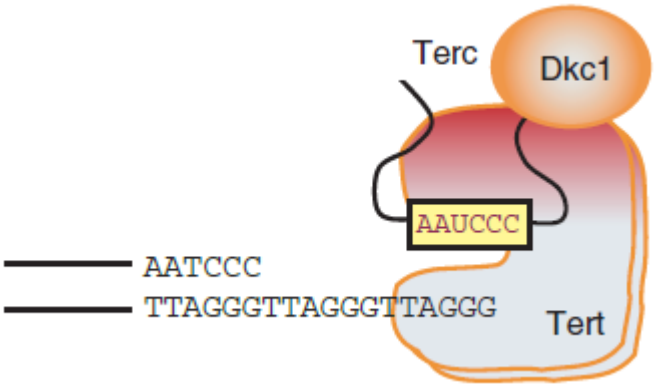

Figure 3: Telomerase structure and telomere elongation. The telomerase enzyme consists of two molecules of TERT and *Terc* subunits and a molecule of DKC1. Telomerase recognizes the 3' end of the G-rich telomere strand and adds telomeric repeats *de novo* (Blasco, 2007).

In humans, telomerase activity is restricted to embryonic development, embryonic stem (ES) cells, germ cells, adult stem cell compartments, certain types of

somatic cells (e.g. lymphocytes) and most cancer cells (85-90%), allowing them to maintain telomere length and escape cellular crisis (Allsopp et al., 2003; de Lange and DePinho, 1999; Greenberg et al., 1998; Hiyama and Hiyama, 2002; Hoffmeyer et al., 2012; Montgomery et al., 2011; Schepers et al., 2011). In contrast, telomerase is active at low levels in a large repertoire of somatic mouse cells (Forsyth et al., 2002; Greenberg et al., 1998). Although *Terc* expression can also be regulated, a major determinant of telomerase activity is the transcriptional regulation of the catalytic subunit *Tert. Tert* transcription is influenced by several factors associated with cell cycle, TGF-β, PI3K/AKT or NF-κB pathways (Cifuentes-Rojas and Shippen, 2012; Daniel et al., 2012). Some examples are SP1, WT1 or the oncogenic transcription factors c-MYC (Greenberg et al., 1999), NF-κB (Yin et al., 2000) and β-catenin (Zhang et al., 2012). Nevertheless, TERT can also be modulated by post-translational modifications like phosphorylation or ubiquitylation. Besides, telomerase activity can be regulated by interaction with other proteins. For instance, the C-terminus of p53 interacts with the N-terminus of human telomerase-associated protein 1 (hTEP1) and inhibits telomerase activity *in vitro* (Li et al., 1999). Finally, some shelterins affect the recruitment of telomerase to telomeres. Specifically, TPP1 contains a telomerase-interacting N-terminal domain and it has been involved in the recruitment of telomerase to chromosome ends (Tejera et al., 2010; Xin et al., 2007). In contrast, TRF1 and TRF2 are thought to be negative regulators of telomere length by hampering the access of telomerase to telomeres (Smogorzewska et al., 2000).

It is well established that telomerase has non-canonical functions unrelated to telomere lengthening, some of them dependent on its catalytic activity. It has been demonstrated that TERT can regulate cell growth and proliferation, independent of its role on telomeres. It is also involved in the transcriptional or post-transcriptional regulation of NF-κB, β-catenin, VEGF or TGF-β pathways, which are master regulators of many oncogenic pathways (Low and Tergaonkar, 2013). In fact, *Tert* overexpression increments the proliferative potential of Mouse Embryonic Fibroblasts (MEFs) by targeting TGF-β pathway in a telomere-length independent manner, even if it requires the formation of TERT/*Terc* complexes (Geserick et al., 2006). Moreover, it has been reported that telomerase contains mitochondria

targeting signals and that exogenously expressed telomerase can localize to the mitochondria, regulating apoptotic responses to oxidative stress (Kovalenko et al., 2010; Santos et al., 2004; Santos et al., 2006).

5.2. Alternative Telomere Lengthening (ALT)

In the absence of functional telomerase, some immortal cell lines and tumors (Henson et al., 2002), cells from the early embryo cleavage stage (Liu et al., 2007) and even some normal mouse somatic cells (Neumann et al., 2013) present other strategies to maintain telomere length, such as Alternative Telomere Lengthening (ALT). ALT mechanism involves HR between telomeres and subtelomeres (S), the chromosomal regions immediately adjacent to telomeres that expand around 3 Mbp from telomeres and also contain repetitive stretches of DNA. Cells that use this pathway are characterized by highly heterogeneous telomere lengths, with the simultaneous presence of long and short telomeres in the same nucleus (Dunham et al., 2000).

6. Telomeres in aging and cancer

Progressive telomere attrition is observed during normal aging both in humans and mice (Collins and Mitchell, 2002), being one of the hallmarks of this process (Blasco, 2005; Lopez-Otin et al., 2013). As we mentioned before, telomerase is active in adult stem cell compartments, which contain the cells with the longest telomeres in an organ and efficiently repair lesions and repopulate tissues in young or adult organisms. In contrast, in old organisms progressive telomere shortening compromises the ability of adult stem cells to repair tissues, preventing the mobilization of stem cells from their niches and leading to tissue degeneration (Flores et al., 2008). A number of age-related pathologies and premature aging syndromes, such as Werner and Bloom syndromes or ataxia telangiectasia, are characterized by a faster-than-normal rate of telomere shortening, reinforcing the idea that telomere loss is a cause of organism aging. Furthermore, mutations in the

different components of telomerase as well as in some of the shelterins (e.g. TIN2) have been linked to rare human genetic degenerative diseases (Armanios and Blackburn, 2012). These telomere syndromes are associated with the presence of short or dysfunctional telomeres, exhibiting a characteristic failure in the regenerative capacity of tissues (Donate and Blasco, 2011). For instance, mutations in any of the components of telomerase (*Tert*, *Terc* or *Dkc1*) can lead to a severe form of bone marrow deficiency known as dyskeratosis congenita (DC). DC is characterized by mucosal leukoplakia, nail dystrophy and abnormal skin pigmentation (Dokal, 2000). Other examples of telomere syndromes are aplastic anaemia and idiopathic pulmonary fibrosis (Armanios et al., 2007; Tsakiri et al., 2007).

Cancer and aging share common origins and both are intimately associated with the accumulation of DNA damage. Tumor cells with insufficient telomerase activity that divide without control would undergo telomere erosion that could have a dual role in cancer progression. On the one hand, dysfunctional telomeres can trigger a DDR and act as a tumor suppressor inducing apoptosis and/or senescence. On the other hand, in the absence of a functional DDR, dysfunctional telomeres would give rise to genome instability, favoring transformation and tumor development (Artandi et al., 2000; McClintock, 1941). In both human and mouse cancer cells *Tert* is transcriptionally activated to maintain telomere length and to enable "replicative immortality", which is one of the hallmarks of cancer (Hanahan and Weinberg, 2000, 2011). Besides, non-canonical functions of telomerase have also been associated with promotion of the rest of the hallmarks of cancer, underlining the determinant role of telomerase in cancer (Low and Tergaonkar, 2013).

6.1. Telomerase mouse models

The generation of telomerase-deficient mice (*Terc*$^{-/-}$ mice) was decisive to demonstrate the importance of telomerase in the maintenance of telomeres *in vivo*, both in cancer and aging. In contrast to knockout mice for most of the shelterins, telomerase deficient mice (*Terc* and *Tert* KO mouse models) survive to adulthood.

Terc$^{-/-}$ mice exhibit an accelerated telomere shortening, leading to the loss of telomere protection and end-to-end fusions (Blasco et al., 1995; Blasco et al., 1997; Herrera et al., 1999a; Lee et al., 1998). Successive generations of *Terc*$^{-/-}$ mice (G1 to G3) display a progressive telomere shortening linked to a progressive decrease in both median and maximum longevity (Herrera et al., 1999b). Similar phenotypes were described in *Tert* knockout mice (Sahin et al., 2011). Transgenic mice overexpressing *Tert* in stratified epithelia (K5-*Tert*) show a decreased lifespan compared to wild-type cohorts associated with a higher incidence of preneoplastic and neoplastic lesions in various tissue types (Gonzalez-Suarez et al., 2002). Additionally, they are more susceptible than wild-type mice to develop tumors when subjected to chemical carcinogenesis of the skin (Gonzalez-Suarez et al., 2001). However, when *Tert* is overexpressed in a context of cancer-resistant mice, by combination with overexpression of the tumor suppressors *p53*, *p16* and *p19ARF* (*Sp53/ Sp16/ SpArf/TgTert*), mice show a retardation in the onset of degenerative lesions, attenuation of the symptoms of aging and a significant extension of median and maximum lifespan. Furthermore, they have longer telomeres than wild-type mice with less DNA damage (Tomas-Loba et al., 2008). Recently, two studies in mice demonstrated that *Tert* overexpression is able to delay aging without increasing cancer incidence (Bernardes de Jesus et al., 2012; Jaskelioff et al., 2011).

7. Telomere repeat binding factor 1 (TRF1)

TRF1, the first mammalian telomeric protein identified, binds to dsDNA as a homodimer or oligomer (Zhong et al., 1992). Murine TRF1 is a 56 kD and 421 aminoacids protein that contains four functional domains: the amino-terminal N-domain, the TRF homology (TRFH) domain, which facilitates the homodimerization and interaction with TIN2 protein, the nuclear localization signal (NLS) domain and the highly conserved cSANT/MYB DNA binding domain (Bianchi et al., 1997; Broccoli et al., 1997; Fairall et al., 2001; Poulet et al., 2012; Smith and de Lange, 1997) **(Fig. 4)**. The structure of TRF1 protein only differs from that of TRF2 in the N-terminal domain, which is acidic in TRF1 and basic in TRF2.

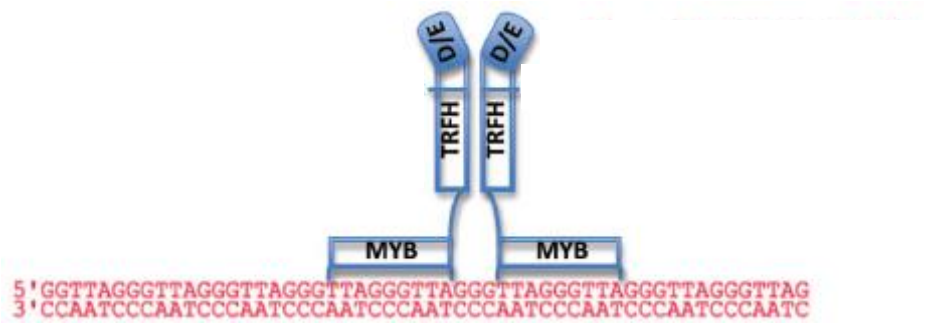

Figure 4: TRF1 protein structure. TRF1 binds to dsDNA as a dimer or oligomer through its C-terminal MYB domain. The binding sequence of each MYB domain consists in the half-site 5'-YTAGGGTTR-3'. Dimerization is mediated by the TRFH domains. The N-terminal acidic domain is indicated (D/E) (Adapted from Diotti and Loayza, 2011).

TRF1 protein is implicated in several functions as T-loop formation and telomere capping, telomere replication, telomere protection from DDR, telomere length maintenance, resolution of sister telomeres or mitosis. Cell-based *in vitro* studies in humans using overexpression of *TRF1* or dominant-negative *TRF1* mutant alleles suggested a role for TRF1 as a negative regulator of telomere length, by inhibition of telomerase access to telomeres (Ancelin et al., 2002; Smogorzewska et al., 2000; van Steensel and de Lange, 1997). Equally, *Trf1* overexpression in the context of mouse epidermis (K5-*Trf1* mice) was reported to lead to telomere shortening *in vivo*, by augmenting XPF nucleolytic activity at chromosome ends (Munoz et al., 2009). A similar but more severe phenotype was also described for targeted *Trf2* overexpression to mouse epithelia (Munoz et al., 2005). Complete *Trf1* deletion in mouse leads to early embryonic lethality, at day 5 to 6 post-coitus, without any defects in telomere length or capping (Karlseder et al., 2003). Conditional *Trf1* knockout mouse models showed a critical role of TRF1 in telomere capping, protection and replication, preventing telomere fusions and fragility (Martinez et al., 2009; Sfeir et al., 2009). Subsequently, *Trf1* deleted MEFs show chromosomal aberrations and massive TIF induction, triggering a p53 and RB mediated senescence. *Trf1* deletion in stratified epithelia ($Trf1^{\Delta/\Delta}$ *K5-Cre* mice) causes perinatal death in mice and severe skin degeneration effects such as hyperpigmentation, lack of mature hair follicles and missing sebaceous glands. *P53* deletion in these mice rescues mouse survival, indicating that the observed

phenotype is p53 mediated (Martinez et al., 2009). TRF1 has also been reported to be necessary for the efficient replication of telomeres, preventing fork stalling (Sfeir et al., 2009). Telomeres challenge the DNA replication machinery due to their repetitive sequences and enrichment in G-cuadruplexes. In fact, they can resemble common fragile sites (CFS), which are chromosomal loci known to be hotspots for DNA breakage under conditions that induce replication stress and prone to replication fork stalling (Sutherland et al., 1998). It has been suggested that TRF1 facilitates telomere replication by recruitment of BLM and RTEL1, two helicases that have been implicated in the removal of G-cuadruplexes (Sfeir et al., 2009). Likewise, topoisomerase IIα (TOPOIIα), an enzyme essential for resolution of DNA replication intermediates, was recently shown to bind to telomeres in a TRF1-dependent manner (d'Alcontres et al., 2014).

On top of that, TRF1 has been reported to carry out additional functions in mitosis. Overexpressed TRF1 in K5-*Trf1* mice was also shown to co-localize with the spindle assembly checkpoint (SAC) proteins BUBR1 and MAD2 and to result in aberrant mitosis (Munoz et al., 2009). In fact, TRF1 is necessary for the telomeric localization of these SAC proteins In mitosis, sister telomeres associate and the resolution of this association is required for progression through mitosis (Dynek and Smith, 2004). In this sense, TRF1 has been described to mediate telomere associations, since *Trf1* overexpression prevents proper resolution of telomeres during mitosis. Cyclin b-dependent kinase 1 (CDK1), a key mediator of mitotic entry, regulates TRF1 to modulate the resolution of telomeres. CDK1 phosphorylates TRF1 at T371, keeping TRF1 free of telomere chromatin and protected from proteasome-induced protein degradation. This phosphorylation is upregulated during mitosis and it facilitates temporal telomere deprotection, essential for sister telomere resolution (McKerlie and Zhu, 2011). Lastly, *Trf1* overexpression is also connected with increased telomere recombination in K5-*Trf1* mice and in ES cells (Lisaingo et al., 2014; Munoz et al., 2009).

The abundance of TRF1 as well as its binding to DNA and other proteins for the execution of its multiple roles is subjected to a complex post-translational regulation, which is cell-cycle dependent. For instance, TNK1 and TNK2 bind to

TRF1 N-terminus and negatively regulate TRF1 binding to telomeres by ADP-ribosylation (Cook et al., 2002; Donigian and de Lange, 2007; Smith et al., 1998). This post-translational modification of TRF1 leads to its release from telomeres, promoting ubiquitylation and consequent degradation of this protein. As it is explained above, CDK1 can phosphorylate TRF1 protecting it from degradation. PINX1 is also able to interact with and stabilize TRF1(Yoo et al., 2014) . Furthermore, TRF1 has been reported to be phosphorylated by other several kinases including AKT, ATM, Aurora A, CK2 and PLK1 (Walker and Zhu, 2012).

8. Interstitial Telomeric Sequences (ITSs)

In addition to their location at telomeres, TTAGGG repeats can be found at internal chromosomal sites, the so-called Internal or Interstitial Telomeric Sequences (ITSs) (Meyne et al., 1990). Alike telomeres, ITSs also resemble fragile sites. Two classes of ITSs exist in mammals: long blocks of mainly pericentromeric, heterochromatic ITSs (het-ITSs), present only in some species, such as the Chinese Hamster, and short ITSs, present at internal positions of ostensibly all vertebrate genomes. Some of these short ITSs are part of subtelomeric regions. In humans and mice, 83 and 244 non-subtelomeric short ITSs have been characterized, respectively. However, no het-ITSs have been detected in these two species. ITSs in rodents are longer than in primates, what is probably connected with their longer telomeres (Nergadze et al., 2007; Ruiz-Herrera et al., 2008). The origin of ITSs seems to be related with chromosome fusions or telomeric hexamers insertions in the genomes during the repair of DSBs (Messier et al., 1996). However, their biological role still remains unknown.

9. Extra-telomeric binding of shelterins

Aside from their fundamental role in telomere biology, recent evidence suggests additional functions of some of the shelterins by binding to extra-telomeric DNA regions. In particular, the ortholog of mammalian RAP1 in budding yeast,

scRap1, binds to not only telomeric but also extra-telomeric DNA, acting as a transcription factor (Buchman et al., 1988; Capieaux et al., 1989) and this is conserved in mammals. It was recently reported that mouse RAP1 is able to bind to inter-genic and intra-genic extra-telomeric sites, some of them ITSs. RAP1 shows enrichment at S regions, where its binding induces gene silencing. Akin to what happens at telomeres, TRF2 mediates binding of RAP1 to DNA in ITS regions (Martinez et al., 2010). Similarly, a recent study in humans described that TRF2 and RAP1 proteins occupy a limited number of interstitial regions throughout the genome and also regulate gene expression (Yang et al., 2011). Taz1, the fission yeast ortholog of mammalian TRF1 and TRF2, involved in telomere protection and recruitment of Rap1 to telomeres (Cooper et al., 1997; Kanoh and Ishikawa, 2001), binds ITSs and plays an essential role in the "replication timing control" (Tazumi et al., 2012). In agreement with this, a recent study reported restricted abilities of TRF1 and TRF2 proteins in binding extra-telomeric sites of the genome in human tumor cell lines, most of them ITSs (Simonet et al., 2011). In addition, TRF1 and other shelterins can bind to an ITS present at human chromosome 2q14 that forms a CFS, stabilizing it (Bosco and de Lange, 2012). Furthermore, in Chinese hamster cells, which contain long blocks of het-ITSs representing about 5% of their genome (Day et al., 1998). TRF1 is involved in protection of these internal $(TTAGGG)_n$ repeats from breaks and chromosome rearrangements (Krutilina et al., 2001; Krutilina et al., 2003).

10. Nuclear reprogramming

ES cells (ESCs) are pluripotent stem cells that have self-renewal capability and can differentiate into all of the three germ layers of the embryo (ectoderm, mesoderm and endoderm). ES cells were first isolated from the mouse inner cell mass (ICM) of blastocysts in 1981 (Evans and Kaufman, 1981; Martin, 1981) . During development, cells gradually lose their self-renewal and differentiation capacities. Remarkably, differentiated cells can be reverted to a more pluripotent state by nuclear reprogramming, which involves genome-wide changes in chromatin structure and gene expression (Gurdon and Melton, 2008; Hochedlinger and Plath, 2009; Rideout

et al., 2001; Yang and Smith, 2007). Nuclear reprogramming can be achieved by three different approaches. The first one is somatic cell nuclear transfer (SCNT), which is based on the insertion of the nucleus of a differentiated somatic cell into an enucleated, unfertilized oocyte of the same species (Wilmut et al., 1997). Another strategy is the fusion of differentiated cells with ES cells (Tada et al., 2001). The most recent approach was described in 2006 by Takahashi and Yamanaka, consisting in the direct reprogramming to a state of pluripotency through the ectopic expression of defined transcription factors which give rise to the so-called induced pluripotent stem (iPS cells or iPSCs) (Takahashi and Yamanaka, 2006).

11. Induced Pluripotent Stem (iPS) Cells

The achievement of iPS cells was a breakthrough in the field of regenerative medicine, as they represent a new source of patient-specific stem cells with great potential for the study and treatment of human diseases. These cells overcome the ethical and technical problems associated with the use of human embryos, as well as the potential rejection by the immune system.

Like ES cells, iPS cells have the properties of self-renewal and differentiation into all three germ layers. They can also contribute to chimeric mice, go to germ line transmission (Takahashi and Yamanaka, 2006) and directly develop into mice by tetraploid complementation assay (Kang et al., 2009; Zhao et al., 2009). Mouse and human iPS cells possess morphological, growth, molecular and developmental features that closely resemble those of ES cells, including similar global gene expression and epigenetic patterns (Amabile and Meissner, 2009; Huang et al., 2014). IPS cells are also similar to ES cells in their shortened cell cycle compared to somatic cells. They show a shorter G1 phase with the loss of G1/S checkpoint, promoting rapid progression through successive rounds of replication (Becker et al., 2006; Momcilovic et al., 2010). Because of the major risk of suffering replication errors, both iPS and ES cells have more stringent mechanisms to protect genome stability like G2/M cell cycle arrest, hypersensitivity to DNA damage, efficient DSBs

repair mechanisms and highly proficient antioxidant defense (Giachino et al., 2013; Huang et al., 2014; Momcilovic et al., 2010).

The two main limitations for the clinical use of this technology reside in the inefficient and stochastic characteristics of the reprogramming process and the oncogenic potential of the viral integration in the host genome. Since the original publication, much effort has been made in the field of reprogramming trying to unveil the mechanisms of this process and to ameliorate the technique, so as to bring iPS cells closer to clinical applications. The initial cocktail used to obtain iPS cells from mouse and human fibroblasts comprised the following transcription factors, typical of ES cells: *Oct3/4* (*Pou5f1*, Octamer3/4), *Sox2* (SRY box-containing gene 2), *Klf4* (Krüppel-like factor 4) and *c-Myc* (myelocytomatosis oncogene) (Takahashi et al., 2007; Takahashi and Yamanaka, 2006). Other researchers utilized different cocktails including the cellular factors *Oct3/4*, *Sox2*, *Nanog* and *Lin28*, achieving a similar outcome (Yu et al., 2007). Some of the relevant advances of the last years in the iPS field are the removal of the oncogenic factor *c-Myc* from the reprogramming cocktail, reported to be dispensable for the reprogramming of both mouse and human fibroblasts (Nakagawa et al., 2008; Wernig et al., 2008), the obtaining of integration-free iPS cells (Anokye-Danso et al., 2012; Kaji et al., 2009; Miyoshi et al., 2011; Okita et al., 2011; Okita et al., 2008; Stadtfeld et al., 2008b; Wang et al., 2011; Woltjen et al., 2009; Yu et al., 2009), the characterization of p53, p21 and INK4/ARF tumor suppressors as a barrier for reprogramming (Hong et al., 2009; Kawamura et al., 2009; Li et al., 2009; Marion et al., 2009a; Utikal et al., 2009), the chemical reprogramming using small-molecules (Hou et al., 2013; Li et al., 2012; Li et al., 2011; Zhu et al., 2011) and the achievement of *in vivo* reprogramming in mice (Abad et al., 2013). Regarding the dynamics of the reprogramming process, it is known that while downregulation of Thy1 and subsequent upregulation of SSEA-1 occur at early time points, reactivation of endogenous *Oct3/4*, *Sox2*, *Nanog* and *Tert* and the silent X chromosome mark late events in the reprogramming process (Stadtfeld et al., 2008a) **(Fig. 5)**.

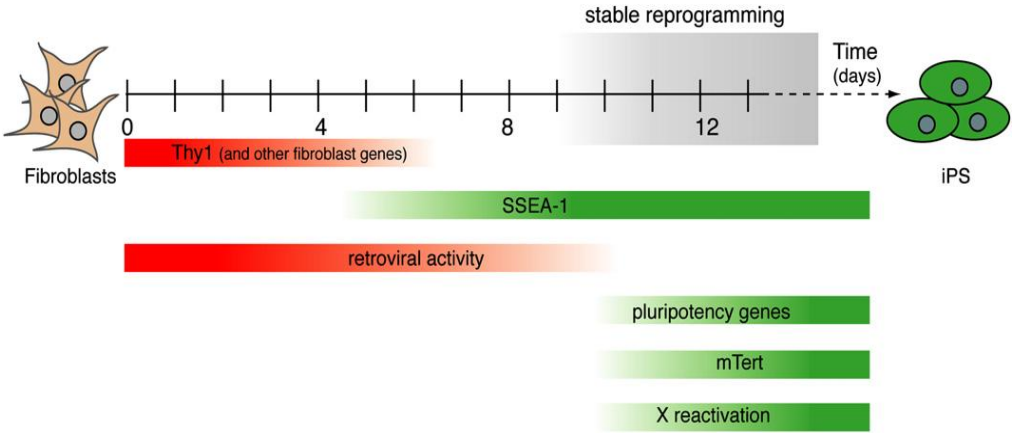

Figure 5: Kinetics of marker expression during reprogramming

11.1. iPS cells and telomeres

The successful use of iPS cells in regenerative medicine requires unlimited proliferative potential of these cells, genomic integrity and differentiation capacity of these cells. In this regard, maintenance of telomere length and function is critical. One of the main characteristics of iPS cells is their high telomerase activity, similar to that of ES cells (Takahashi et al., 2007; Takahashi and Yamanaka, 2006). Reprogramming factors have been associated with the regulation of telomerase components transcription, inferring that they could be directly implicated in the activation of telomerase during reprogramming. C-MYC transcriptionally upregulates *Tert* expression (Drissi et al., 2001; Flores et al., 2006; Wu et al., 1999), but its ectopic expression is not necessary for efficient reprogramming or telomerase activation during this process both in mice (Marion et al., 2009b) and humans (Suhr et al., 2009). KLF4 activates the expression of human *TERT* by binding to its promoter in cancer and ES cells (Wong et al., 2010). In mouse ES cells, recruitment of β-catenin is necessary for *Tert* transcription and KLF4 promotes this binding (Hoffmeyer et al., 2012). Likewise, enhanced binding of OCT3/4 and NANOG has been described in the *Terc* locus in human iPS cells and murine ES cells (Agarwal et al., 2010). Nevertheless, it has been reported that mouse *Tert* gene expression is moderately increased during reprogramming in comparison with the human *TERT*,

whose transcription is strongly upregulated in this process (Mathew et al., 2010). Thus, post-translational mechanisms are also presumed to regulate telomerase activation during reprogramming.

Telomerase activation during reprogramming triggers a telomere elongation both in mice and humans that takes place mainly post-reprogramming (Agarwal et al., 2010; Marion et al., 2009b). Mouse iPS cells show a moderate telomere elongation compared to parental fibroblasts at early passages (P8), but these length is progressively increased upon passages, achieving a telomere length similar to mouse ES cells (Marion et al., 2009b). Apparently, unlike the slow and progressive telomere elongation in mouse iPS cells, human iPS cell telomeres achieve the 14-15 kb length characteristic of human ES cells as early as P5 (Suhr et al., 2009). Telomerase activity and telomere length differ between humans and laboratory mice, which could explain the differences in telomerase activation and telomeres lengthening during the process of reprogramming between these two species. Nevertheless, it has become evident that iPS cells can exhibit heterogeneity in both telomerase activity and telomere length (Mathew et al., 2010; Suhr et al., 2009; Vaziri et al., 2010). While telomere elongation during reprogramming is mainly telomerase dependent, independent mechanisms like ALT have now been reported to be relevant for continuous self-renewal of iPS cells via the maintenance or extension of telomere length, contributing to the mentioned heterogeneity (Wang et al., 2012; Yehezkel et al., 2011). In fact, higher telomere recombination frequencies were observed in iPS cells and ES cells compared to differentiated MEFs (Marion et al., 2009b). It has been reported that not only telomere length but also telomere chromatin is altered during the reprogramming process. While telomeres in differentiated somatic cells are usually composed of heterochromatin, recent studies have shown that iPS and ES cells contain relatively “open” telomeric chromatin. It is likely that reprogramming allows the elongation of telomeres to a length characteristic of ESCs by making them more accessible for telomerase. Therefore, the telomeric chromatin of pluripotent stem cells is likely in a unique and dynamic state that can undergo remodeling during differentiation (Huang et al., 2014; Marion et al., 2009b; Wong et al., 2009).

In the last years, studies in pluripotent stem cells and during nuclear reprogramming based on the overexpression or deletion of components of telomerase have been crucial to unravel the link between telomeres and pluripotency. Both human and mouse ES and iPS cells with short telomeres due to *Tert* or *Terc* deletion show imparment of differentiation and loss of pluripotency (Huang et al., 2011; Marion et al., 2009b; Pucci et al., 2013; Yang et al., 2008). In contrast, *Tert* overexpression in both mouse and human ES cells confers proliferative advantage, resistance to oxidative stress and enhanced differentiation (Armstrong et al., 2005; Yang et al., 2008). MEFs from increasing generation of *Terc*$^{-/-}$ mice (G1 to G3) present a decrease in reprogramming efficiency that is restored by the reintroduction of telomerase (Marion et al., 2009b). Similarly, *Tert*$^{-/-}$ tail-tip fibroblasts (TTFs) have recently been reported to show a reduced reprogramming ability independent of telomere shortening, suggesting extra-telomeric functions of TERT during this process (Kinoshita et al., 2014). IPS cell studies using fibroblasts from DC patients with mutations in different components of telomerase have also shed light on the interplay between telomerase and pluripotency establishment, highlighting the importance of telomere maintenance for the viability of iPS cells (Agarwal et al., 2010; Batista et al., 2011). In contrast, TERT overexpression in human keratinocyte lines was described to enhance reprogramming efficiency, since it leads to immortalization of these cells (Utikal et al., 2009).

In mice, TPP1 shelterin has been described to be necessary for telomere elongation by facilitating the recruitment of telomerase (Tejera et al., 2010). Alike TERT, TRF1 and TRF2 have also been characterized as stem cell markers, since they are overexpressed in ES or iPS cells (Ginis et al., 2004; Schneider et al., 2013). In particular, human *TRF1* is one of the genes most consistently highly expressed in ES and iPS cells compared to the starting populations (Boue et al., 2010; Hosseinpour et al., 2013). High expression of TRF1 is associated with early stages of ES-cell generation (cultivated ICM cells) coincidental with high SOX2 and OCT3/4 levels and before telomere elongation (Varela et al., 2011). Recently, a publication from our lab showed that the reprogramming factor OCT3/4 binds directly to *Trf1* promoter, modulating its expression in pluripotent cells (Schneider et al., 2013). Besides, *Trf1* is in the group of genes downregulated after *Oct3/4* supression in

mouse ES cells (Sharov et al., 2008), highlighting the connection between TRF1 and stem cell biology. Knowing the relevance of telomere remodeling and maintenance during the acquisition of pluripotency, it becomes interesting to study the possible implications of shelterins during this process, as they have essential roles in telomere length regulation, protection and replication.

Objectives

1. Identification of putative extra-telomeric binding of TRF1

1. To identify TRF1 binding sites in MEFs by ChIP- sequencing analysis

2. To address whether telomere shortening can influence TRF1 binding to extra-telomeric regions by ChIP-sequencing.

2. Dissecting reprogramming process: shelterin and telomerase during iPS cells generation

1. To enlighten the role of TRF1 protein during the process of reprogramming by gain and loss of function experiments in MEFs during this process.

2. To study the effect of *Trf1* excision on mouse iPS cells.

3. To analyze the effect of *Tert* overexpression on the acquisition of pluripotency by reprogramming to iPS cells.

4. To unveil the dynamics of shelterins and telomerase during reprogramming.

Objetivos

1. Identificación de lugares de unión de TRF1 extra-teloméricos.

1. Identificar lugares de unión de TRF1 en MEFs mediante la técnica de *ChIP-sequencing*

2. Averiguar si el acortamiento telomérico puede influir en la unión a regiones extra-teloméricas de TRF1 mediante *ChIP-sequencing*

2. El proceso de reprogramación: shelterinas y telomerasa durante la generación de células iPS

1. Elucidar el papel de la proteína TRF1 durante el proceso de reprogramación por medio de experimentos de ganancia o pérdida de función en MEFs durante este proceso

2. Estudiar el efecto de la escisión de *Trf1*en células iPS de ratón

3. Analizar el efecto de la sobreexpresión de *Tert* en la adquisición de pluripotencia mediante reprogramación a células iPS

4. Desvelar la dinámica de expresión de shelterinas y telomerasa durante la reprogramación

Experimental Procedures

1. Culture conditions

Cells were maintained in an incubator at 37ºC with 16% O_2 and 5% CO_2. Mouse Embryonic Fibroblasts (MEFs) and HEK293T cells (ATCC® Number CRL-11268™) were cultured in Dulbecco's Modified Eagle's medium (DMEM; Gibco) supplemented with 10% heat inactivated fetal bovine serum (FBS, Gibco) and 1% antibiotic/antimycotic (Gibco). iPS cells were grown in iPS medium (high-glucose DMEM (Invitrogen) supplemented with 15% Knockout Serum Replacement (KSR; Gibco, 10828028), Leukemia Inhibitory Factor (LIF, 1000 U/ml; ESGROTM, Millipore ESG1107), non-essential aminoacids (MEM Non-Essential Aminoacids Solution; 1X; Invitrogen), β-mercaptoethanol (0.5 mM; Invitrogen), Penicillin/Streptomycin (1X; Gibco) and Glutamax (Gibco) on feeders or gelatin coated plates.

2. Extraction and culture of MEFs

MEFs were isolated from 13.5 embryos. Uterus was removed and put into PBS with antibiotic/antimycotic at 37ºC. Embryo's head and guts were taken out and the head was used for genotyping. The embryo was minced with a razorblade in 0.1% trypsin (10X diluted in PBS; Invitrogen) and incubated for 20 min at 37ºC, dispersed with a Pasteur pipette and incubated for another 20 min. Cells were transferred to a 10 cm-diameter dish and grown with 10 ml of the aforementioned medium.

MEFs of the following genotypes were isolated: C57BL/6 wild-type, $p53^{-/-}$, $Terc^{-/-}$ of first and third generation G1 and G3) (Blasco et al., 1997), $Trf1^{lox/lox}$ $p53^{-/-}$ and $Trf1^{+/+}p53^{-/-}$ (Martinez et al., 2009), $Trf1^{lox/lox}$ $Cre\text{-}ERT2^{+/ki}$ ($Trf1^{lox/lox}$ $RERT^{n}$) and $Trf1^{+/+}$ $Cre\text{-}ERT2^{+/ki}$ ($Trf1^{+/+}$ $RERT^{n}$) and *Rosa26:rtTA*; *tet-O-Fug-OSKM* (i4F) (Abad et al., 2013).

3. Retroviral and lentiviral infections

Retroviral supernatants were produced in HEK293T cells (5 x 10^6 cells per 100 mm-diameter dish) transfected with the ecotropic packaging plasmid pCL-Eco (4 µg) together with either one of the following constructs (4 µg): pBabe-GFP, pBabe-Cre, pBabe-EV, pBabe-*Trf1*, pMXs-*Oct3/4* (Addgene, plasmid #13366), pMXs-*Sox2* (Addgene, plasmid #13367), pMXs-*Klf4* (Addgene, plasmid #13370) or pMXs-c-*Myc* (Addgene, plasmid #13375). Transfections were performed using Fugene-6 transfection reagent (Roche) according to the manufacturer's protocol. For infections with Cre recombinase, $Trf1^{lox/lox}$ $p53^{-/-}$ and $Trf1^{+/+}$ $p53^{-/-}$ MEFs were seeded the following day (2 x 10^6 cells per 150 mm-diameter dish) and infected after 24 hours with the diluted retroviral supernatants (2:5). Infected cells were selected by addition of puromycin (2 µg/ml, Sigma) after 48 h. For ChIP-seq experiment, $Trf1^{\Delta/\Delta}$ $p53^{-/-}$-Cre and $Trf1^{+/+}$ $p53^{-/-}$-Cre MEFs were amplified and maintained in puromycin selection for one week before cross-linking.

Lentiviral supernatants were produced in HEK293T cells transfected with the packaging plasmids pLP1 (1.95 µg), pLP2 (1.3 µg), pLP/VSVG (1.65 µg) (Invitrogen), and either one of the following lentiviral constructs (5 µg), pLKO.1-puro-scramble shRNA (Addgene), pLKO.1-puro-sh*Trf1* (bacterial glicerol stock TRCM0000071298, Sigma-Aldrich), pLVX-EV (Clontech), pLVX-*Tert* or pLVX-*Tpp1*.

4. PCR

$Trf1^{+/+}p53^{-/-}$ and $Trf1^{lox/lox}$ $p53^{-/-}$ were genotyped by PCR with the following primers: E1-F2 (Forward, 5'-GGATGCTCGACTTCCTCT-3') and SA1 (Reverse, 5'-GCTTGCCAAATTGGGTTGG-3') for *Trf1* genotyping and p53F-12B7 (5'-TGGTTTGTGCGTCTTAGAGACAGT-3'),p53R-1B3 (5'-AAGGATAGGTCGGCGGTTCAT-3') and pPNTF-2B5 (5'-CCAGCTCATTCCTCCCACTCA-3') for *p53* genotyping. The removal of exon 1 of *Trf1* in $Trf1^{lox/lox}$ MEFs upon retroviral infection with Cre recombinase and in iPS

cells obtained from *Trf1*$^{\Delta/\Delta}$ *p53*$^{-/-}$ -Cre MEFs was checked by PCR with E1-Popout (Forward, 5'-ATAGTGATCAAAATGTGGTCCTGGG-3') and SA1 (Reverse, 5'-GCTTGCCAAATTGGGTTGG-3') primers as previously described (Martinez et al., 2009).

I4F MEFs were genotyped by three different PCR reactions. *Rosa26-rtTA* insertion in MEFs was confirmed with primers 125B (5´-AAAGTCGCTCTGAGTTGTTAT-3') and 126B (5'-GCGAAGAGTTTGTCCTCAACC-3') rendering a band of approximately 300 bp, while Rosa26-wt allele was confirmed with 125B and 127B (5'-GGAGCGGGAGAAATGGATATG-3') primers, rendering a band of around 500 bp. The Tet-O-FUW-OSKM insertion was confirmed by PCR with the following primers: ORF2-Fw (5'-GGATGGAGTGGGACAGAGAA-3') and ORF2-Rv (5'-GTGCCGATCCGTTCACTAAT-3'), which renders a fragment of 378 bp.

5. Taqman qPCR

Trf1$^{lox/lox}$ *RERT*^{n} and *Trf1*$^{+/+}$ *RERT*^{n} MEFs were genotyped by Transnetyx company using a qPCR based system and Taqman® probe technology with the following primers and probes (**Table 1**).

Table 1: Primers and probes used for Taqman qPCR genotyping

Allele	Primer and Probe Sequence 5'→ 3'	
Cre	Fw:	TTAATCCATATTGGCAGAACGAAAACG
	Rv:	CAGGCTAAGTGCCTTCTCTACA
	Probe:	CCTGCGGTGCTAACC
Trf1$^{\Delta}$	Fw:	GCTATACGAAGTTATTCGAGGTCGAT
	Rv:	GGTGGCGGCCGAAGT
	Probe:	CTCTAGAAAGTATAGGAACTTC
Trf1^{lox}	Fw:	GCTATACGAAGTTATTCGAGGTCGATC
	Rv:	TGTTTTGCCAAGTTCTAATTCCATCAGA
	Probe:	CCGTCGAGGAAGTTC
Trf1^{+}	Fw:	GAGACGGCGCGAAACC
	Rv:	GCGGGAGCCAGGACTTC
	Probe:	CCGCTTCCTGTTTGCTG

6. Protein extracts and Western blot

Total and nuclear protein extracts were used for Western blot analysis. To prepare nuclear extracts, the cell pellets were lysed by hypotonic buffer A (10 mM Hepes-KOH [pH 7.9], 10 mM KCl, 0.1 mM EDTA, 0.1 mM EGTA and protease inhibitors) by gentle pipetting. The cells were incubated on ice for 15 min, 25 µl of 10% NP-40 were added and cells were vigorously vortexed for 15 sec. Nuclei were collected by centrifugation (1 min; 14,000 rpm; 4°C) and gently resuspended in nuclear extraction buffer B (20 mM HEPES [pH 7.9], 25% glycerol, 0.4 M NaCl, 0.1 mM EDTA, 0.1 EGTA and protease inhibitors). The samples were vigorously rocked at 4ºC for 15 min and centrifuged (5 min; 14,000 rpm; 4°C). For total extracts preparation we resuspended pellets in RIPA buffer and protease inhibitors, incubated the cells on ice for 30 min and sonicated them for 5 min. Total extracts were collected by centrifugation (15 min; 14,000 rpm; 4ºC). Protein concentration was determined using Bradford assay (Sigma) for nuclear extracts or Bio-Rad DC protein assay for total extracts. 30 µg of protein per extract were loaded in a NuPAGE 4-12% Bis-Tris gel 1.0 mm (Invitrogen) and electrophoresed in MES SDS Running Buffer (Invitrogen) before Western blotting. The following antibodies were used: mouse anti-TRF1 (Abcam; ab-10579; 1:1000), mouse anti-β-actin (Sigma; a2228; 1:10,000), rabbit anti-SMC1 (Bethyl Laboratories; # A300-055A; 1:1000).

7. ChIP assays and telomere dot-blots

Chromatin Immunoprecipitation (ChIP) were carried out essentially as described previously (Garcia-Cao et al., 2004), with some modifications. We cross-linked the cells by adding formaldehyde (Sigma) directly to tissue culture medium to a final concentration of 1% and incubated cultures for 15 min at RT on a shaking platform. We stopped the cross-linking by adding glycine to a final concentration of 0.125 M and incubated the cells for 5 min. We washed cross-linked cells twice with cold PBS, scrapped, centrifuged (4,000 rpm; 5 min; 4ºC) and resuspended them with lysis buffer (1% SDS, 50 mM Tris-HCl [pH 8.0] and 10 mM EDTA and protease inhibitors) at a density of 20×10^6 cells/ml for 10 min on ice. We sonicated lysates to

obtain chromatin fragments <1 kb and centrifuged them for 15 min in a microcentrifuge at RT. We sonicated each sample for 50 min using the Bioruptor sonication system (Diagenode) in order to shear the DNA into small fragments. Chromatin from 4 x 10^6 cells was used per immunoprecipitation. We diluted 400 µl of lysate 1:10 with dilution buffer (1.1% Triton X-100, 0.01% SDS, 1.2 mM EDTA [pH 8.0], 167 mM NaCl and 16.7 mM Tris-HCl [pH 8.0] and protease inhibitors). We pre-cleared each immunoprecipitation with 50 µl of protein A/G Plus agarose beads (Santa Cruz Biotechnology, sc-2003) for 1 h and incubated with 4 µl of rabbit polyclonal anti-mouse TRF1 serum antibody (generated in our laboratory) (Garcia-Cao et al., 2004) or preimmune serum at 4ºC o/n on a rotating platform. We then added 50 µl of protein A/G Plus agarose beads and incubated for 1 h. We washed the immunoprecipitated pellets with low salt immune complex wash buffer (0.1% SDS, 1% Triton X-100, 2 mM EDTA, 20 mM Tris-HCl [pH 8.0] and 150 mM NaCl) (one wash), high salt immune complex wash buffer (0.1% SDS, 1% Triton X-100, 2 mM EDTA, 20 mM Tris-HCl [pH 8.0] and 500 mM NaCl) (one wash), LiCl immune complex wash buffer (0.25 M LiCl, 1% NP-40, 1% sodium deoxycholate, 1 mM EDTA and 10 mM Tris-HCl [pH 8.0]) (one wash) and TE buffer (10 mM Tris-HCl [pH 8.0] and 1 mM EDTA) (two washes). We then eluted the chromatin from the beads twice by incubation with 250 µl of elution buffer (1% SDS and 50 mM $NaHCO_3$) during 15 min at RT with rotation. After adding 20 µl of 5 M NaCl, we reversed the cross-links for 4 h at 65 °C. Samples were supplemented with 20 µl of 1 M Tris-HCl [pH 6.5], 10 µl of 0.5 M EDTA, 20 µg of RNase A and 40 µg of proteinase K and incubated for 1 h at 45 °C to remove RNA and proteins. Inputs correspond to the total DNA sample, 1:10 dilution of the amount of lysate used in the immunoprecipitation. After phenol/chloroform DNA extraction, the precipitated DNA was eluted and transferred to a Hybond+ membrane by dot-blotting. The membrane was then hybridized with either a telomeric probe recognizing TTAGGG repeats or a probe recognizing major satellite sequences, characteristic of pericentric heterochromatin.

8. ChIP-sequencing

For each sample we used around 100 x 10^6 cells. Each sample was independently processed into sequencing libraries with a ChIP-Seq sample preparation kit (Illumina) in accordance with the manufacturer's instructions (Quail et al., 2008). Input samples from *Trf1*$^{+/+}$ *p53*$^{-/-}$-Cre and *Trf1*$^{\Delta/\Delta}$ *p53*$^{-/-}$-Cre MEFs were pooled in a single library (input pool 1) and inputs from wild-type, *Terc*$^{-/-}$ G1 and *Terc*$^{-/-}$ G3 MEFs in another library (input pool 2). 29, 37, 40, 16, 15, 26 and 40 ng of DNA (as quantitated by PicoGreen Fluorometry) were respectively used for *Trf1*$^{+/+}$ *p53*$^{-/-}$-Cre, *Trf1*$^{\Delta/\Delta}$ *p53*$^{-/-}$-Cre, input pool 1, wild-type, *Terc*$^{-/-}$ G1, *Terc*$^{-/-}$ G3 and input pool 2 samples. Each sample was electrophoresed on agarose gel and a fraction of 100-150 bp was taken. Extracted DNA was processed through subsequent enzymatic treatments of end-repair, dA-tailing, and ligation to adapters as in Illumina's "ChIP Sequencing Sample Prep Guide" (part # 11257047 Rev. A), with the exception that no further gel extraction was performed. Adapter-ligated library was PCR amplified with Illumina PE primers. The resulting purified DNA libraries were applied to an Illumina flow cell for cluster generation and sequenced on a Genome Analyzer IIx (GA2) by following manufacturer's protocol and using 40 (first ChIP-seq experiment) or 42 (second experiment)-base read run.

9. ChIP-sequencing data analysis

Image analysis was performed with Illumina Real Time Analysis software (RTA1.8 for *Trf1*$^{\Delta/\Delta}$ *p53*$^{-/-}$-Cre, *Trf1*$^{+/+}$ *p53*$^{-/-}$ -Cre and input pool 1 samples and RTA1.6 for wild-type, *Terc*$^{-/-}$ G1, *Terc*$^{-/-}$ G3 and input pool 2 samples). Sequence alignment to the reference genome (NCBI m37/mm9 mouse assembly, April 2007, strain C57BL/6J) was made with Illumina's ELANDv2 algorithm on its "eland_extended" mode from CASAVA-1.7 package. ELANDv2 performs multiseed alignment with consecutive read substrings of 16 to 32 bases separately. The seeds are aligned to multiple candidate positions in the reference genome, with a maximum of two mismatches allowed per 32 bases seed; then they are extended to the full read using gapped alignment, allowing for any number of mismatches and potential gaps

(indels) of up to 20 bases. The best alignment among the multiple candidate positions is chosen based on quality scores. Uniquely aligned 40 or 42-bp-length reads were pooled into seven datasets: *Trf1*$^{+/+}$ *p53*$^{-/-}$-Cre, *Trf1*$^{\Delta/\Delta}$ *p53*$^{-/-}$-Cre, input pool 1, wild-type, *Terc*$^{-/-}$ G1 and *Terc*$^{-/-}$ G3 and input pool 2. Peak detection was performed with MACS version 1.4 software (*p* value= 1 x 10^{-5}; FDR= 10%; 300 bp window).

10. Validation of ChIP-seq results by qRT-PCR

For ChIP-seq validation, quantitative real-time PCR (qRT-PCR) was performed using an ABI PRISM 7700 thermocycler (Applied Biosystems) and the Power SYBR Green PCR Master mix (Life technologies) according to the manufacturer's protocol. Immunoprecipitated and input DNA from independent ChIP experiments in *Trf1*$^{+/+}$ *p53*$^{-/-}$ -Cre and *Trf1*$^{\Delta/\Delta}$ *p53*$^{-/-}$-Cre samples were quantified by qRT-PCR with oligos designed to amplify DNA fragments corresponding to the following peaks: 603 (chr2: 28,039,717- 28,040,535), 620 (chr2: 57,481,892- 57,482,277), 874 (chr6: 52,133,777- 52,134,592), 980 (chr8: 73,956,797- 73,957,467), 1073 (chr9: 95,326,167- 95,326,779), 804 (chr4: 153,217,553- 153,218,190), 805 (chr4: 154,765,741- 154,766,224), 806 (chr4: 155,161,073- 155,161,670), 807 (chr4: 155,334,959- 155,335,528), 1014 (chr8: 128,849,051-128,849,629), 1015 (chr8: 129,108,238- 129,108,707) and 1016 (chr8: 129,423,259- 129, 423,839). The primer sequences are listed in **Table 2**. The results were normalized to the value obtained in the input DNA, by calculating de ΔC_t values between the levels obtained in input DNA and that of the precipitated DNA. The results were relativized to wild-type levels. All values were obtained in triplicates.

Table 2: Sequences of primers used for ChIP-qPCR experiments.

Name	Sequence 5'→ 3'
Peak603-Fw	AACCCTAACCCCAACCCTAA
Peak603-Rv	GAGGCCAAGTCAGGTTCATC
Peak620-Fw	GGGTTAGGGTTAGGGTTAGGG
Peak620-Rv	CACAGAAGTGGATGCTCACAG
Peak874-Fw	GGCAGCAGACCACAACCT
Peak874-Rv	AGGGTTAGAGGGTTAGGG
Peak980-Fw	TATGGGCCTGTTAGGGTTAGG
Peak980-Rv	CACACACCAAAGTTAAATCAAGAGC
Peak1073-Fw	TGGACTTAGTGCAGCCAATG
Peak1073-Rv	TCAGTTTTCCAAGGGTTAGGG
Peak804-Fw	GGGGAAGTCGGGCTTCTCTAT
Peak804-Rv	TCATGCCTGTCCATCTGTCCT
Peak805-Fw	TAACTTTGGGCATGGTCTCCA
Peak805-Rv	AGAGGAGCAGAGCCAGGTAGGT
Peak806-Fw	TGCTGAGCCATTTCTCTAGGC
Peak806-Rv	CAGAGGCAGGTGGATTTCTGA
Peak807-Fw	TGAGTCCATCCCTAGCCACAA
Peak807-Rv	CAAAGATGCAGCACCCTGTTC
Peak1014-Fw	GGGCTCCAGCAAATGAGGTAG
Peak1014-Rv	TTTCCTGATGCCTATCGCTGA
Peak1015-Fw	ACGAGGCGAGTTCAATTCCAT
Peak1015-Rv	GGGCTCTTCCTTTTCCCCTTT
Peak1016-Fw	GAGTCACGCATACCCCTCCTT
Peak1016-Rv	TGACCTGTCCTGTGAGGTGGT

11. Preparation of feeders

Primary wild-type B6 MEFs were expanded up to passage 4-5 and grown to confluence. After washing, cells were trypsinized and pelleted by centrifugation (1,200 rpm; 5 min). Cell pellets were irradiated at 80 greys and frozen in aliquots of

5 x 10^6 cells. Plates were pre-coated with gelatin and feeders were seeded the day before culturing the iPS cells.

12. Cloning

Mouse *Trf1* cDNA was obtained in Addgene (pBluescript SK +/- -m*Trf1*, plasmid #12303). *Trf1* cDNA was cut from pBluescript plasmid by digest with EcoRI and XhoI restriction enzymes and treated with Mung Bean nuclease to obtain blunt ends. It was then cloned in pBabe-puro-EV retroviral backbone, previously linearized with SnabI. Sequence was confirmed with pBabe-Fw (5'-AAGCCCTTTGTACACCCTAAGC-3') and pBabe-Rv (5'-GGACTTTCCACACCTGGTTGC-3') primers.

Mouse *Tpp1* cDNA was obtained by PCR with the following primers: *Tpp1*cDNA-Fw (5'-ATATACGTAATGTCCGATTCAGGGTTGCT-3') and *Tpp1*cDNA-Rv (5'- ATAGAATTCTCATACCTGGGTTAACTCAG-3') and ensuing digest. The resulting PCR product was gel purified, ligated with the linearized pLVX-puro-EV lentiviral backbone and transformed into DH5α *Escherichia coli* cells. Individual clones were sequenced.

13. Reprogramming and maintenance of iPS cells

One day after seeding (2 x 10^5 MEFs per 35 mm-diameter dish), MEFs were infected four times (twice a day) with a cocktail of the three or four retroviral Yamanaka factors pMXs-*Oct3/4*, pMXs-*Sox2*, pMXs-*Klf4* and pMXs-*c-Myc* (OSK or OSKM cocktails). The following day, medium was changed to iPS cell medium, which was changed daily for around two weeks until the appearance of iPS colonies. iPS colonies were picked 2-3 weeks after infection and expanded on feeder fibroblasts. iPS medium was changed daily and at 70-80 % of confluence cells were trypsinized and passed onto a new dish with a 1:5 dilution.

***Trf1* KO MEFs:** *Trf1*$^{lox/lox}$*p53*$^{-/-}$ and *Trf1*$^{+/+}$*p53*$^{-/-}$ MEFs were infected once with retroviral Cre recombinase, selected and reprogrammed one week after Cre infection, as described above. Colonies obtained from *Trf1*$^{\Delta/\Delta}$ *p53*$^{-/-}$- Cre MEFs were picked 2-3 weeks after infection and expanded on feeder fibroblasts. *Trf1* deletion in these iPS cells was checked by PCR with primers E1-popout and SA1.

***Trf1* KD MEFs:** For the reprogramming of *Trf1* KD cells, *p53*$^{-/-}$ MEFs were used. The following viral cocktails were used: pBabe-EV and pLKO.1-puro-scramble (mock-scramble), pBabe-EV and pLKO.1-puro-sh*Trf1* (mock-sh*Trf1*), OSK and pLKO.1-puro-scramble (OSK-scramble), OSK and pLKO.1-puro-sh*Trf1* (OSK-sh*Trf1*). After 4 infections, medium was replaced by iPS medium with puromycin to select for the shRNA vectors. Cultures were maintained in the presence of drug selection with daily medium changes.

Trf1* conditional KO MEFs:* we reprogrammed *Trf1*$^{lox/lox}$ *RERT*^{n} and *Trf1*$^{+/+}$ *RERT*^{n} MEFs as described above. *Trf1* excision in the resultant iPS cells is explained in section 15.

***Trf1* overexpressing MEFs:** we infected wild-type MEFs with the three reprogramming factors (OSK) in combination with either pBabe-puro-EV or pBabe-puro-*Trf1*. Infected MEFs were maintained in puromycin selection during reprogramming. For the Yamanaka factors replacement assay, we infected at the same time with two of the factors (OK, OS or SK) in combination with either pBabe-puro-EV or pBabe-puro-*Trf1* and waited around 1 month for the appearance of colonies, changing the iPS medium every 2 days.

***Tert* and/or *Tpp1* overexpressing MEFs:** wild-type MEFs were infected with different combinations of retroviral and lentiviral viruses: OSK + pLVX-EV, OSK + pLVX-*Tert*, OSK + pLVX-*Tpp1*, OSK + pLVX-*Tert* + pLVX-*Tpp1*, OSKM + pLVX-EV, OSK + pLVX-*Tert*, OSK + pLVX-*Tpp1*, OSK + pLVX-*Tert* + pLVX-*Tpp1*.

Reprogrammable i4F MEFs: 5 x 10^5 i4F MEFs were plated in gelatin-coated 35 mm-diameter dishes. The following day the i4F cassette was activated by

doxycycline (1 μg/ml). Medium was changed every day until iPS cell colonies appeared after approximately one week.

14. Reprogramming efficiency

The infection efficiency during reprogramming was determined by measuring the percentage of GFP^+ cells after infection with pBabe-GFP. Cells infected with OSK or OSKM + pBabe-GFP were trypsinized at day 2 post-infection, washed with PBS and resuspended in 300 μl of PBS for flow cytometry analysis in FACSCalibur (BD Biosciences). TO-PRO-3 dye was added to the cells to stain for dead cells. Pulse processing was used to exclude cell aggregates and debris. At least 20,000 events were collected per sample. Data was analyzed using FlowJo Software v.9.1 (Treestar, Eugene, OR). Reprogramming efficiency was determined by alkaline phosphatase (AP) activity (AP detection kit, Chemicon International or AP Blue Membrane Solution, Sigma-Aldrich), following the manufacturer's instruction. After around of reprogramming AP^+ colonies were counted and the results were normalized to the respective efficiencies of retroviral infection.

15. *Trf1* excision in iPS cells

We reprogrammed $Trf1^{lox/lox}$ and $Trf1^{+/+}$ $RERT^n$ as described above. The resulting iPS cells were picked and clones of each genotype were used for the treatment with 4-hydroxytamoxifen (4-OHT; Sigma-Aldrich), in order to obtain $Trf1^{\Delta/\Delta}$ and $Trf1^{+/+}$ iPS cells, respectively. The iPS from both genotype were seeded at low density (50,000 cells per 35 mm-diameter dish) in feeders or gelatin coated (for qRT-PCR analysis) dishes and treated with 4-OHT at a final concentration of 0.2 μM in complete iPS medium, which was replaced every day.

16. SSEA-1 staining

SSEA-1 expression during reprogramming was assessed by flow cytometry, as described elsewhere (Li et al., 2009). 2 x 10^5 seeded cells were used for each assay. Cells were trypsinized and washed once with PBS. A second wash was done with PBS/0.5% BSA (Sigma) before incubation with the antibody. Cells were incubated with 10 µl of anti-human/anti-mouse APC-conjugated SSEA-1 antibody (R&D) in 50 µl of PBS-0.5% BSA for 30 min at 4ºC. Afterwards, cells were washed by PBS-0.5% BSA once to remove antibody and resuspended in 300 µl of PBS for flow cytometry analysis. Cells were stained with DAPI to exclude for dead cells. Samples were analyzed on the BD LSRII Fortessa cell analyzer (BD Biosciences) using pulse processing to exclude cell aggregates and debris. At least 20,000 events were collected per sample. Data was analyzed using FlowJo Software v.9.1 (Treestar, Eugene, OR).

17. Apoptosis assay

At day 0 (Ctrl), 3 and 6 of 4-OHT treatment iPS cells were collected, washed in PBS, resuspended in 1X annexin V binding buffer (BD Biosciences) and stained with FITC annexin V (BD Biosciences). Cells were incubated for 15 min in the dark at RT. DAPI was added to discriminate dead cells. Apoptotic cells (Annexin V^+, $DAPI^-$ cells) were quantified using the BD FACSCanto system (BD Biosciences), using pulse processing to exclude cell aggregates and debris. At least 20,000 events were collected per sample. Data was analyzed using FlowJo Software v.9.1 (Treestar, Eugene, OR).

18. Immunofluorescence

At day 0, 3 and 6 of 4-OHT treatment iPS cells were collected and plated in glass bottom dishes (24 well plates; MatTek) with feeders. Cells were fixed in 4% paraformaldehyde (PFA) in PBS for 15 min at RT, permeabilized twice in 0.1%

Triton X-100/PBS for 15 min and blocked with 100% Australian FBS (Genycell) for 1 h at RT. Samples were incubated o/n at 4ºC with primary antibodies for TRF1 (rabbit polyclonal home-made antibody; 1:500) and γH2AX (Upstate Biotechnology; 1:500) in diluents with background reducing agents (Invitrogen). Secondary antibody incubation (1 h; RT) was performed after 3washes of 5 min each with PBS. The nuclei were counterstained in a 4 μg/ml DAPI/PBS solution for 10 min before mounting with Vectashield (Vector Laboratories).

19. RNA extraction, cDNA synthesis and qRT-PCR

Total RNA from reprogramming cells at days 9, 11 and 14 was extracted with Trizol (Invitrogen). Samples were treated with DNAse I (DNA free kit; Ambion). Reverse transcription was carried out using Ready-To-Go You-Prime First-Strand Beads kit (GE Healthcare) with random primers (Invitrogen) or iScript Advanced cDNA synthesis kit (Bio-Rad) according to the manufacturer's protocols. qRT-PCR was performed using DNA Master SYBR Green mix (Applied Biosystems) and 7500 Fast Real-time PCR System (Applied Biosystems) according to the manufacturer`s instructions. Primers used are listed in **Table 3**. All values were obtained in triplicates. Calculations were made using the ΔΔ*C*t method as described in (Yuan et al., 2006), using *Gapdh* as reference gene. The values were normalized to WT levels.

20. Q-FISH

In order to analyze telomeric aberrations, cells were arrested in metaphase by treatment with colcemid (0.1 μg/ml; Gibco) for 3 h at 37ºC. Cells were swollen in hypotonic buffer (10 mM Tris-HCl [pH 7.5], 10 mM NaCl, 5 mM $MgCl_2$), fixed with methanol/acetic acid as described elsewhere (Samper et al., 2000) and dropped onto slides. Slides were washed in PBS and further fixed in 4% formaldehyde/PBS for 2 min followed by a 3 x 5 min washing step with PBS. Slides were incubated in 0.1% porcine pepsine (Sigma), 0.01 M HCl (Merck) for 10 min at 37°C, washed with PBS and another fixing and washing step was performed. After dehydratation in 70%,

90% and 100% ethanol dilutions, slides were further air dried and the Q-FISH labelling probe mix (10 mM Tris, 25 mM MgCl, 9 mM citric acid, 82 mM Na_2HPO_4 [pH 7], 70% deionised formamide (Sigma), 0.25% blocking reagent (Roche) and 0.5 µg/ml Telomeric PNA-probe) was applied. Telomeric PNA-probe was generated at Panagene directed against telomeric repeats. The PNA sequence is Cy3-00-CCCTAACCCTAACCCTAA-Lys. Slides were further covered with a coverslip and the DNA was denatured on a pre-warmed heating plate at 85°C for 3 min. Slides were then incubated for 3 h in a wet chamber at RT , followed by a 2 x 15 min washing step in 70% formamide, 10 mM Tris and 0.1% BSA (Sigma). After another 2 x 15 min of washing with 0.08% Tween20 (Sigma)/TBS slides were incubated in a 4 µg/ml DAPI (Sigma) solution and mounted with Vectashield. Around 40 metaphases per genotype from a total of two independent iPS clones per genotype were scored for chromosomal aberrations by superimposing the telomere image on the DAPI chromosomes image.

Table 3: Sequences of primers used for qRT-PCR experiments

Name	Sequence 5'→ 3'
Nanog-Fw	AGGGTCTGCTACTGAGATGCTCTG
Nanog-Rv	CAA CCA CTG GTT TTT CTG CCA CCG
Oct3/4-Fw	TCTTTCCACCAGGCCCCCGGCTC
Oct3/4-Rv	TGCCGGGCGGACATGGGGAGATCC
Tert-Fw	GGATTGCCACTGGCTCCG
Tert-Rv	TGCCTGACCTCCTCTTGTGAC
Terc-Fw	TCATTAGCTGTGGGTTCTGGT
Terc-Rv	TGGAGCTCCTGCGCTGACGTT
Trf1-Fw	TCTAAGGATAGGCCAGATGCCA
Trf1-Rv	CTGAAATCTGATGGAGCACGT
Trf2-Fw	AGAGCCAGTGGAAAAACCAC
Trf2-Rv	ATGATGGGGATGCCAGATTA
Tin2-Fw	TGCCCTGAAGCATCACTTCC
Tin2-Rv	GGCAACTAGAAAGGATTCCCC
Rap1-Fw	AAGGACCGCTACCTCAAGCA
Rap1-Rv	TGTTGTCTGCCTCTCCATTC
Tpp1-Fw	ACTTGTGTCAGACGGAACCC
Tpp1-Rv	CAACCAGTCACCTGTATCC
Pot1a-Fw	AAACTATGAAGCCCTCCCCA
Pot1a-Rv	CGAAGCCAGAGCAGTTGATT
Pot1b-Fw	AGTTATGGTCGTGGGATCAGAG
Pot1b-Rv	GAGGTCTGAATGGCTTCCAA
Gapdh-Fw	TTCACCACCATGGAGAAGGC
Gapdh-Rv	CCCTTTTGGCTCCACCCT

Results

1. Identification of putative extra-telomeric binding of TRF1

1.1. Restricted binding of TRF1 to telomeres in MEFs

Several studies in the last years have reported binding of shelterins to extra-telomeric DNA regions in a variety of species. TRF1 is a component of the shelterin complex that binds to dsDNA at telomeres by recognition of 5'-YTAGGGTTR-3' sequences through its C-terminal SANT/MYB DNA-binding domain. However, this protein has also been implicated in protection of Interstitial Telomeric Sequences (ITSs) in humans and Chinese hamster (Bosco and de Lange, 2012; Krutilina et al., 2003; Simonet et al., 2011). Recent studies reported that TRF1 protein is able to bind to extra-telomeric sites of the genome, most of them ITSs, in human cell lines (Bosco and de Lange, 2012; Simonet et al., 2011). Furthermore, TRF1 is involved in protection of ITSs from breaks and chromosome rearrangements in Chinese hamster cells, which contain long blocks of het-ITSs representing about 5% of the genome (Day et al., 1998; Krutilina et al., 2001; Krutilina et al., 2003). Together, these data suggest that mouse TRF1 could also show *in vivo* extra-telomeric binding and have crucial roles in genome stability.

To address this, we performed a whole-genome ChIP-sequencing (chromatin immunoprecipitation (ChIP) coupled with high-throughput sequencing) analysis. We took advantage of the conditional *Trf1* knockout mouse model from our lab, the $Trf1^{lox/lox}$ mice (Martinez et al., 2009), to obtain *Trf1*-null MEFs that could be use as a negative control for TRF1 peak specificity. In this model, *Trf1* gene exon 1 (E1) is flanked by two *lox*P sites and is excised upon Cre recombinase addition **(Fig. 6A)**. The resulting $Trf1^{\Delta/\Delta}$-Cre MEFs fail to proliferate due to a rapid induction of senescence, which is bypassed by canceling of the p53 and RB pathways. As for ChIP-seq experiments we needed a huge number of cells, we used *p53*-null MEFs for both $Trf1^{+/+}$ and $Trf1^{lox/lox}$ genotypes, as *p53* deficiency rescues cell proliferation in *Trf1*-null MEFs. We infected $Trf1^{+/+}$ $p53^{-/-}$ and $Trf1^{lox/lox}$ $p53^{-/-}$ MEFs with a retroviral vector carrying the Cre recombinase (pBabe-puro-Cre) once, amplified and selected them with puromycin for one week. *Trf1* excision in $Trf1^{\Delta/\Delta}$ $p53^{-/-}$-Cre was checked by PCR **(Fig. 6B)** and the decrease in TRF1 protein was confirmed by Western blot **(Fig. 6C).**

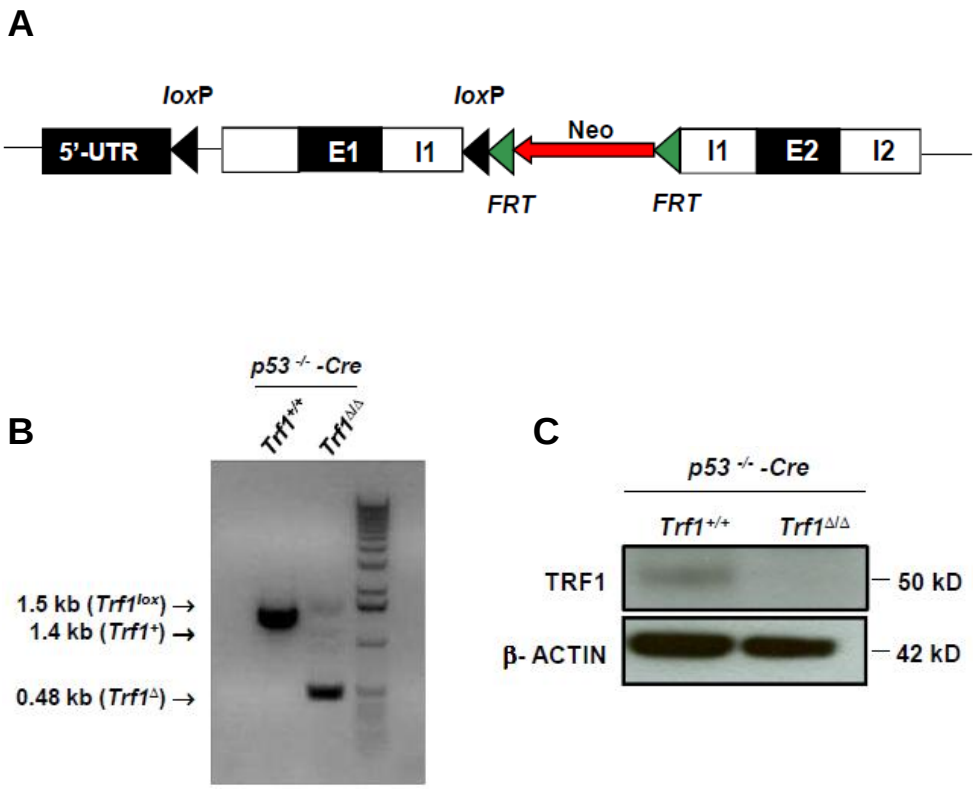

Figure 6: ***Trf1* deletion in *Trf1*$^{lox/lox}$ *p53*$^{-/-}$ MEFs.** (**A)** Scheme of the *Trf1*^{lox} allele. (**B)** *Trf1* deletion *in Trf1*$^{\Delta/\Delta}$ *p53*$^{-/-}$ -Cre infected MEFs was confirmed by PCR. (**C)** Western blot analysis demonstrating the decrease in TRF1 protein upon infection with retroviral Cre recombinase.

We next tested our home-made rabbit polyclonal antibody against full-length mouse TRF1 protein (Garcia-Cao et al., 2004) for its ability to pull down TRF1 protein in MEFs by dot-blot analysis after ChIP in *Trf1*$^{+/+}$*p53*$^{-/-}$-Cre and *Trf1*$^{\Delta/\Delta}$ *p53*$^{-/-}$-Cre MEFs. As shown in **Fig. 7**, the antibody was able to specifically immunoprecipitate TRF1, which is bound to telomeric but not centromeric DNA. "No ab" corresponds to the DNA obtained from immunoprecipitation (IP) without antibody, with the preimmune-serum. Input DNA sample corresponds to the sheared chromatin before incubation with the anti-TRF1 antibody.

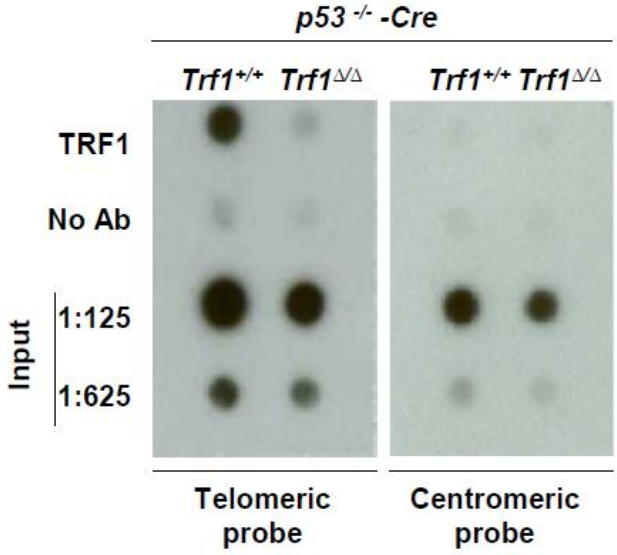

Figure 7: **ChIP experiment with TRF1 antibody immunoprecipitation.** The co-precipitated DNA was analyzed by dot-blotting with a telomere probe to detect telomeric sequences. The same blot was hybridized with a probe against centromeric DNA (major satellite) to test the ChIP specifity, as TRF1 is bound to telomeres but not centromeres. "No ab" corresponds to the same cross-linked DNA incubated with the pre-immune TRF1 antibody serum. "Input" corresponds to the chromatin fraction before incubation with the antibody.

Factors such as GC content, read mappability, DNA repeats, copy number variations and local chromatin structure can influence sequencing and read distribution at different locations in the genome (Feng et al., 2012). Therefore, input DNA was used as a sequencing control sample of sonicated chromatin to eliminate background and to identify reliable read-enriched regions by ChIP-seq. Illumina Genome Analyzer IIx was used for the high-throughput sequencing. The enrichment in telomeric repeats was corroborated before alignment with the mouse genome by the strong over-representation of raw 40 bp sequences containing the telomeric $(TTAGGG)_5$ or the complementary $(CCCTAA)_5$ repeats in *Trf1*$^{+/+}$ *p53* $^{-/-}$-Cre MEFs compared to that in *Trf1*-null control (*Trf1*$^{\Delta/\Delta}$ *p53*$^{-/-}$-Cre MEFs) (7-fold increase in both $(TTAGGG)_5$ and $(CCCTAA)_5$ repeats) and the input DNA (input pool 1), which is a combination of inputs from *Trf1*$^{+/+}$ *p53* $^{-/-}$-Cre and *Trf1*$^{\Delta/\Delta}$ *p53*$^{-/-}$-Cre samples (28-fold increase for $(TTAGGG)_5$ repeats and 34-fold increase for $(CCCTAA)_5$ repeats) **(Fig. 8)**. The enrichment in reads containing 2, 3, 4 and 6 repeats of the TTAGGG or CCCTAA sequences was also

noticeable in the *Trf1*$^{+/+}$ *p53* $^{-/-}$-Cre sample compared to *Trf1*-null and input samples (**Table 4)**. These results demonstrate *in vivo* binding of TRF1 to telomeric repeats.

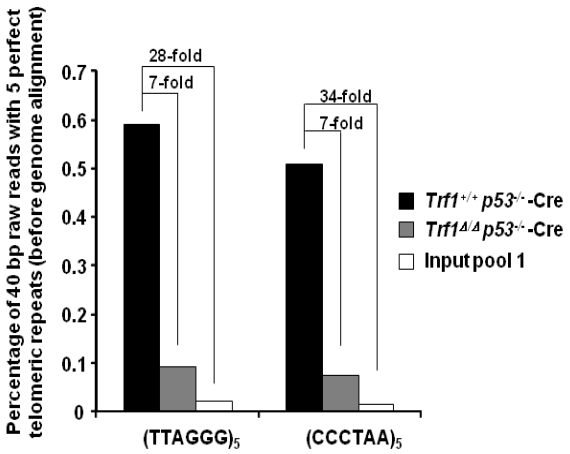

Figure 8: **Enrichment of telomere sequences bound to TRF1 in ChIP-seq experiment**. The percentage of 40-bp raw reads containing perfect $(TTAGGG)_5$ or $(CCCTAA)_5$ repeats before alignment with mouse genome is shown for the different samples. Input pool 1 is a combination of equal amounts of input DNA from *Trf1*$^{+/+}$ *p53*$^{-/-}$-Cre and *Trf1*$^{\Delta/\Delta}$ *p53*$^{-/-}$-Cre samples.

Our ChIP-seq experiment yielded >11 x 10^6 uniquely mapped short reads for *Trf1*$^{+/+}$ *p53*$^{-/-}$-Cre, >32 x 10^6 for *Trf1*$^{\Delta/\Delta}$ *p53*$^{-/-}$ -Cre and almost 20 x 10^6 for input pool 1 **(Table 5)**. In ChIP-seq experiments, although many mapped reads are dispersed throughout the genome, others are found in clusters constituting read-enriched regions, which represent the locations of putative binding of the protein of interest. MACS (Model-based Analysis of ChIP-seq) software is a computational method that was designed to identify read-enriched regions from ChIP-seq data. Significantly read-enriched peaks were detected using this MACS software, version v1.4 with a *P* value cut-off of 1 x 10^{-5}.

Table 4: Total number of reads with $(TTAGGG)_{1,2,3,4,5,6}$ or $(CCCTAA)_{1,2,3,4,5,6}$ repeats and % of enrichment in samples *Trf1*$^{+/+}$*p53*$^{-/-}$-Cre, *Trf1*$^{\Delta/\Delta}$ *p53*$^{-/-}$*-Cre* and input pool 1 from ChIP-seq experiment before alignment with mouse genome.

	Trf1$^{+/+}$*p53*$^{-/-}$-Cre		*Trf1*$^{\Delta/\Delta}$*p53*$^{-/-}$*-Cre*		Input pool 1	
Repeats	**Nº of reads**	**%**	**Nº of reads**	**%**	**Nº of reads**	**%**
$(TTAGGG)_1$	217,345	1.135	185,292	0.665	175,448	0.630
$(TTAGGG)_2$	117,560	0.614	26,550	0.095	6,769	0.024
$(TTAGGG)_3$	116,975	0.611	26,142	0.094	6,372	0.023
$(TTAGGG)_4$	115,084	0.601	25,569	0.092	6,091	0.022
$(TTAGGG)_5$	112,688	0.589	24,930	0.089	5,798	0.021
$(TTAGGG)_6$	97,075	0.507	21,311	0.076	4,818	0.017
$(CCCTAA)_1$	206,359	1.078	212,93	0.764	180,765	0.649
$(CCCTAA)_2$	100,976	0.528	21,473	0.077	4,849	0.017
$(CCCTAA)_3$	100,426	0.525	21,112	0.076	4,438	0.016
$(CCCTAA)_4$	98,964	0.517	20,751	0.074	4,278	0.015
$(CCCTAA)_5$	97,062	0.507	20,327	0.073	4,142	0.015
$(CCCTAA)_6$	76,033	0.397	15,734	0.056	3,166	0.011
$(TTAGGG)_1$ + $(CCCTAA)_1$	423,704	2.214	398,222	1.429	356,213	1.279
$(TTAGGG)_2$ + $(CCCTAA)_2$	218,536	1.142	48,023	0.172	11,618	0.042
$(TTAGGG)_3$ + $(CCCTAA)_3$	217,401	1.136	47,254	0.170	10,810	0.039
$(TTAGGG)_4$ + $(CCCTAA)_4$	214,048	1.118	46,320	0.166	10,369	0.037
$(TTAGGG)_5$ + $(CCCTAA)_5$	209,750	1.096	45,257	0.162	9,940	0.036
$(TTAGGG)_6$ + $(CCCTAA)_6$	173,108	0.904	37,045	0.133	7,984	0.029
Total nº of reads	**19,141,798**		**26,522,663**		**27,857,611**	

To define extra-telomeric TRF1 binding sites, we only retained the peaks that were present in *Trf1*$^{+/+}$ *p53*$^{-/-}$-Cre sample but not in *Trf1*-null sample (*Trf1*$^{+/+}$ *p53*$^{-/-}$-Cre vs *Trf1*$^{\Delta/\Delta}$ *p53*$^{-/-}$-Cre). In the comparisons with the controls, the statistical significance of enriched sites is measured by empirical False Discovery Rate (FDR), which is the expected proportion of incorrectly identified sites among those found to be significant. MACS software calculates the FDR by exchanging the ChIP-seq and control samples. In our experiment, a FDR of 10 was applied for this software. 1,165 peaks were found in the comparison *Trf1*$^{+/+}$ *p53*$^{-/-}$-Cre vs *Trf1*$^{\Delta/\Delta}$ *p53*$^{-/-}$ -Cre. We also did the comparison

Trf1$^{+/+}$ *p53*$^{-/-}$-Cre vs input pool 1, in this case obtaining 1,288 peaks. Out of the 1,165 peaks from the comparison with the *Trf1*-null control, 290 were discarded by the comparison with the input. Remarkably, all the 875 remaining peaks showed a FDR of 100%, meaning that TRF1 specific peaks did not have enough statistical support in the comparison with *Trf1*-null sample.

Table 5: Summary of ChIP-seq experiment. Overall number of reads obtained and their size. % of alignment (PF) is the percentage of filtered reads that were uniquely aligned to the reference. The read length is 40 bp.

Sample	Raw sequenced reads	Size of raw sequenced reads (bp)	% of alignment (PF)	Uniquely mapped reads	Size of uniquely mapped reads (bp)
Trf1$^{+/+}$ *p53*$^{-/-}$-Cre	21,493,914	859,756,560	58.36	11,170,552	446,822,080
Trf1$^{\Delta/\Delta}$ *p53*$^{-/-}$-Cre	52,426,641	2,097,065,640	91.51	32,673,672	1,306,946,880
Input Pool 1	37,408,510	1,496,340,400	71.53	19,932,267	797,290,680

Contrary to what was reported for mouse RAP1 (Martinez et al., 2010) and human RAP1, TRF2 and TRF1 (Simonet et al., 2011; Yang et al., 2011), mouse TRF1 peaks were not enriched in subtelomeric regions (**Fig. 9**), as we only found 29 peaks (2.36% from the total of peaks) in S regions. If the same analysis was done randomly, the expected enrichment in peaks at subtelomeres would be of 2.27%. We observed a slight enrichment in chromosomes 4 and 8, of 6% and 5.4% respectively. Besides, most of the peaks were not associated with genes, as they mapped in regions at more than 10 kb from genes transcription start sites (TSS), with just 13% of the peaks (117 peaks out of 875) at less than 10 kb from genes TSS (**Fig. 10A**). From the peaks that mapped inside a gene, 90% of them were intronic (**Fig. 10B**).

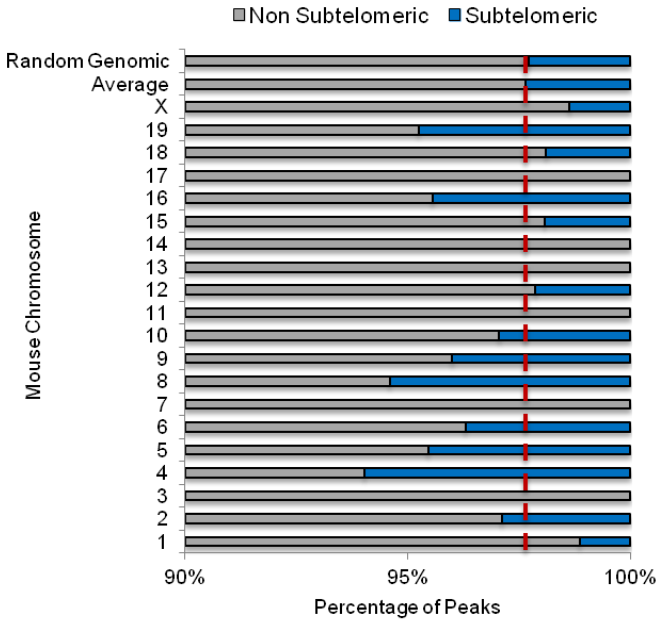

Figure 9: Percentage of peaks from *Trf1*$^{+/+}$ *p53*$^{-/-}$-Cre vs *Trf1*$^{\Delta/\Delta}$ *p53*$^{-/-}$-Cre comparison that are located in non subtelomeric and subtelomeric regions (-3 Mbp from telomeres). Note that there is no enrichment in peaks in subtelomeres comparing with the random average of enrichment in the rest of the genome. The chromosomes with higher percentage of peaks in S regions are 4 and 8.

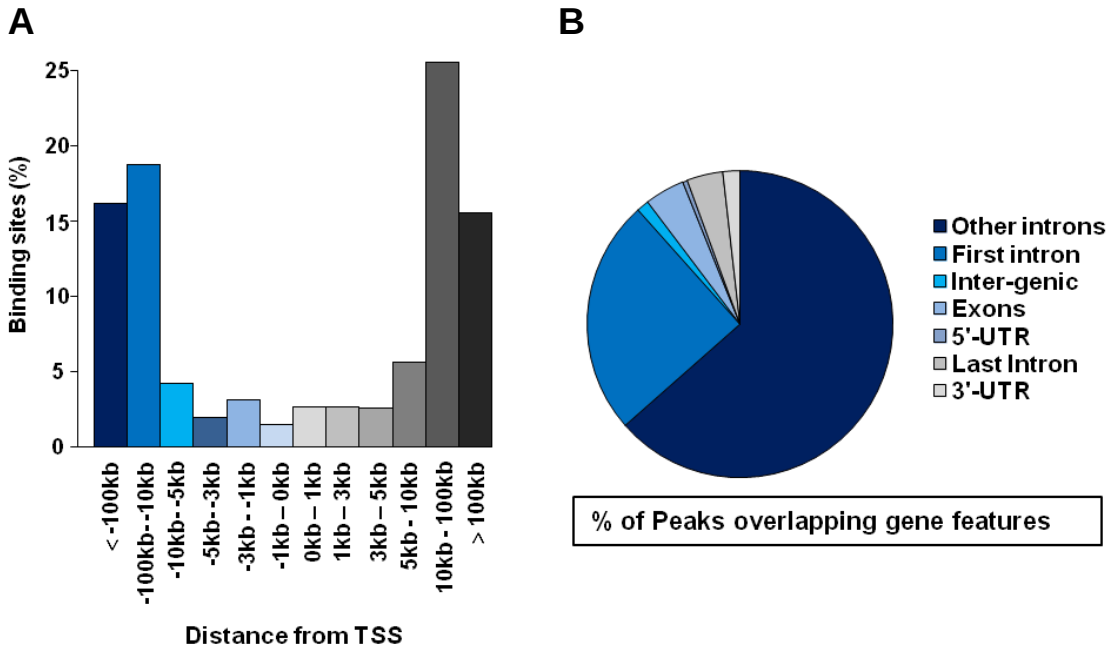

Figure 10: Distribution of TRF1 peaks in the *Trf1*$^{+/+}$ *p53*$^{-/-}$-Cre vs *Trf1*$^{\Delta/\Delta}$ *p53*$^{-/-}$-Cre comparison. (A) Distance from genes transcription start sites (TSS). Note that most of the peaks are >10 kbp from the genes TSS. **(B)** Distribution of peaks that mapped inside a gene. Note that 88.4% of the peaks are intronic.

1.2. Overlapping with mouse RAP1 ChIP-seq

To further analyze whether TRF1 binding to chromatin is restricted to telomeres in mice, we compared our TRF1 ChIP-seq data with that previously published by us for RAP1 (Martinez et al., 2010) and sought peaks that overlapped in both experiments. Just a few TRF1 regions (14 sites, 1.6% of the 875 peaks from the comparison *Trf1*$^{+/+}$ *p53*$^{-/-}$-Cre vs *Trf1*$^{\Delta/\Delta}$ *p53*$^{-/-}$-Cre) were found to overlap with RAP1 binding sites and only five of them contained telomeric $(TTAGGG)_{n\geq2}$ tracks (**Table 6**). While dozens of peaks associated with ITSs were found in RAP1 ChIP-seq, in TRF1 ChIP-seq we only detected a few peaks in ITSs and with no statitistical significance. In this comparison, we also noticed that peaks obtained in TRF1 ChIP-seq were much longer than RAP1 peaks (RAP1 peaks had an average width of 75 bp, while TRF1 peaks were 576 bp long on average). This distribution in broad peaks suggests that peaks obtained in this experiment were peaks associated with background instead of peaks showing real binding of TRF1. Lastly, RAP1 ChIP-seq showed a much higher number of RAP1 binding peaks, 30,000 peaks, compared to the 1,165 peaks from TRF1 ChIP-seq experiment.

Table 6: Peaks that overlap with RAP1 ChIP-seq in the *Trf1*$^{+/+}$ *p53*$^{-/-}$-Cre vs *Trf1*$^{\Delta/\Delta}$ *p53*$^{-/-}$ -Cre comparison and that contain tracks with $(TTAGGG)_{n\geq2}$ repeats

Chr	RAP1 peak number	Start	End	TRF1 peak number	Start	End	FDR (%)
2	4	28,040,118	28,040,149	603	28,039,717	28,040,535	100
2	1	57,482,074	57,482,124	620	57,481,892	57,482,277	100
6	2027	4,873,918	4,873,946	874	4,873,501	4,874,305	100
8	2	73,957,000	73,957,029	980	73,956,797	73,957,467	100
9	7	95,326,334	95,326,363	1073	95,326,167	95,326,779	100

1.3. Chip-seq validation by qRT-PCR

Even though none of the TRF1 peaks obtained by ChiP-seq passed the statistical significance threshold, we decided to further study those TRF1 peaks in ITSs that overlapped with the RAP1 ChIP-seq peaks to be certain that TRF1 does not show binding outside of telomeres. We tested the five peaks associated with TTAGGG repeats that overlapped with RAP1 (peaks 603, 620, 874, 980 and 1073) (**Table 6**). In addition, we also selected for validation peaks in the subtelomeric regions of chromosome 4 and 8, which were the chromosomes that showed a slight enrichment in peaks in the S regions (peaks 804, 805 806, 807, 1014, 1015 and 1016) (**Table 7**).

Table 7: Peaks from subtelomeres of chromosomes 4 and 8, which are the chromosomes that showed higher enrichment of peaks in S regions in the comparison *Trf1*$^{+/+}$ *p53*$^{-/-}$-Cre vs *Trf1*$^{\Delta/\Delta}$ *p53*$^{-/-}$ -Cre.

Chr	Peak number	Start	End	FDR (%)
4	804	153,217,553	153,218,190	100
4	805	154,765,741	154,766,224	100
4	806	155,161,073	155,161,670	100
4	807	155,334,959	155,335,528	100
8	1014	128,849,051	128,849,629	100
8	1015	129,108,238	129,108,707	100
8	1016	129,423,259	129,423,839	100

To study TRF1 binding to these peaks, we carried out independent ChIP experiments with our anti-TRF1 antibody in two MEF lines per genotype; *Trf1*$^{+/+}$ *p53*$^{-/-}$-Cre MEFs and *Trf1*$^{\Delta/\Delta}$ *p53*$^{-/-}$-Cre MEFs deficient for *Trf1* as negative control for peak specificity, followed by qPCR analysis with primers for the extra-telomeric regions mentioned above (see primer sequences in Experimental Procedures, **Table 2**). We failed to detect TRF1 binding to the indicated ITSs (**Fig. 11, left panel**) or to subtelomeric regions (**Fig. 11, right panel**), thus confirming that the peaks obtained in the ChIP-seq were false positives in agreement with the FDR indicator. Taking all these results together, we conclude that mouse TRF1 does not bind to chromosomal regions other than telomeres, at least in wild-type MEFs.

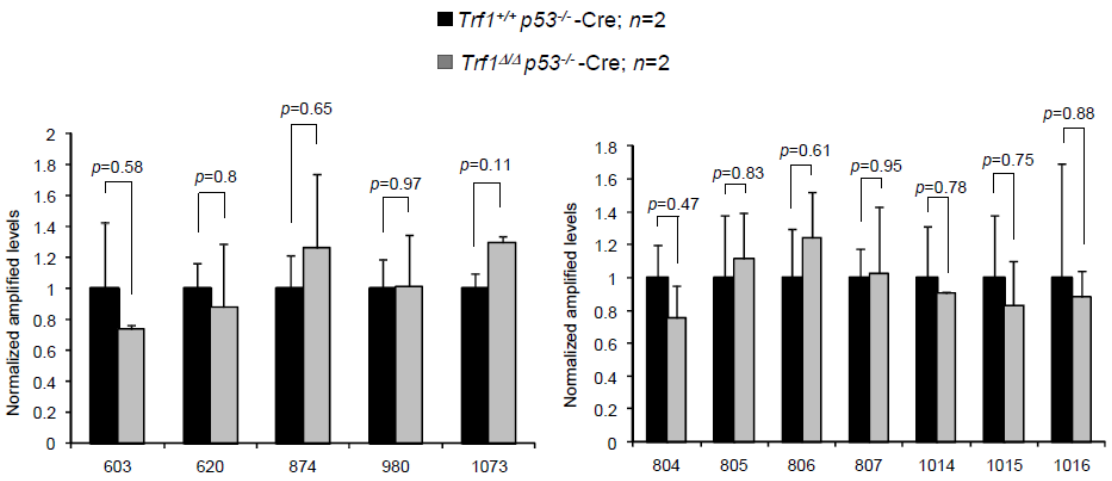

Figure 11: Validation of TRF1-binding peaks by ChIP with anti-TRF1 antibody followed by qPCR. The peak ranks of the regions tested are indicated on the *x* axis. Validation of peaks that overlapped with RAP1 ChIP-seq and contain $(TTAGGG)_{n\geq 2}$ repeats (**Left panel**). Validation of peaks from subtelomeric regions of chromosomes 4 and 8 (**Right panel**). The results were normalized to the input and relativized to wild-type levels. No decrease in TRF1 binding was detected in *Trf1*-null MEFs. *n*= number of independent MEFs analyzed. Error bars: s.e.m. Statistical analysis: Two sided Student's *t*-test.

1.4. Identification of TRF1 binding sites upon telomere shortening by ChIP-sequencing

Interestingly, in yeast telomeric alterations can lead to delocalization from telomeres of Rap1-associated heterochromatin factors that are able to operate at interstitial genomic sites (Maillet et al., 1996; Marcand et al., 1996). It is also known that gradual reduction in the telomere length associated with aging is linked to global deregulation of the transcriptome and loss of maintenance of epigenetic silencing mechanisms (Schoeftner et al., 2009). Knowing that in normal conditions TRF1 does not bind outside telomeres, we hypothesized that upon telomere attrition TRF1 could delocalize from telomeres to other regions of the genome, having additional functions independent from telomere biology and contributing to the gene expression changes associated with aging. To address this, we performed a second ChIP-seq experiment in MEFs deficient for *Terc*, the gene that codifies the telomerase RNA component, for

successive mouse generations (Blasco et al. 1997). Samples used were *Trf1*$^{+/+}$ MEFs *Terc*$^{+/+}$ (wild-type) and *Terc*$^{-/-}$ of the first (*Terc*$^{-/-}$ G1) and third (*Terc*$^{-/-}$ G3) generations, which display progressively shorter telomeres, senescence and chromosomal aberrations like end-to-end fusions in advanced generations.

Again, we first confirmed the enrichment in telomeric repeats before sequence alignment with mouse genome in wild-type, *Terc*$^{-/-}$ G1 and *Terc*$^{-/-}$ G3 MEFs compared to their corresponding input DNA (input pool 2). In agreement with shorter telomeres owing to telomerase deficiency, *Terc*$^{-/-}$ G1 and G3 samples showed gradual decrease in the percentage of reads containing 5 perfect telomeric repeats (**Fig. 12**). A similar enrichment was seen for 2, 3, 4 and 6 repeats of the TTAGGG or CCCTAA sequences (**Table 8**).

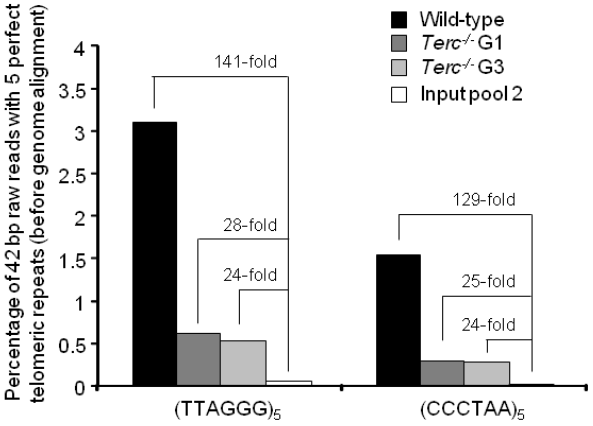

Figure 12: Enrichment of telomere sequences bound to TRF1 in ChIP-seq experiment. The percentage of 42-bp raw reads before alignment with mouse genome containing perfect $(TTAGGG)_5$ or $(CCCTAA)_5$ repeats is shown for the different samples. Input pool 2 is a combination of input DNA from wild-type, *Terc*$^{-/-}$ G1 and *Terc*$^{-/-}$ G3 samples.

This ChIP-seq experiment yielded >14 x 10^6 uniquely mapped short reads for wild-type, >16 x 10^6 for *Terc*$^{-/-}$ G1, >15 x 10^6 for *Terc*$^{-/-}$ G3 and >21 x 10^6 for input pool 2 (**Table 9**). Peak detection and statistical analysis was done as described above. We compared *Terc*$^{-/-}$ G3 vs wild-type, *Terc*$^{-/-}$ G1 vs wild-type and *Terc*$^{-/-}$ G3 vs *Terc*$^{-/-}$ G1, so as to obtain new TRF1 binding sites to the genome while telomeres get shorter. We obtained 2,179 peaks in the comparison *Terc*$^{-/-}$ G3 vs wild-type, 2,207 peaks in the comparison *Terc*$^{-/-}$ G1 vs wild-type and 2,524 peaks in the comparison *Terc*$^{-/-}$ G3 vs *Terc*$^{-/-}$ G1. However, none of these peaks were of statistical significance and were discarded from the analysis. Once again, we did not see any enrichment in S regions in

the comparison *Terc*$^{-/-}$ G3 vs wild-type (1.93% compared to 2.27% of the random average) (**Fig. 13**), suggesting that telomeric shortening and the consequent decreased binding of TRF1 to telomeres does not induce TRF1 interaction with other regions of the genome.

Table 8: Total number of reads with $(TTAGGG)_{1,2,3,4,5,6}$ or $(CCCTAA)_{1,2,3,4,5,6}$ repeats in wild-type, *Terc*$^{-/-}$ G1, *Terc*$^{-/-}$ G3 and input pool 2 samples from the second ChIP-seq experiment before alignment with mouse genome.

	wild-type		*Terc*$^{-/-}$ G1		*Terc*$^{-/-}$ G3		Input pool 2	
Repeats	**nº of reads**	**%**	**nº of reads**	**%**	**nº of reads**	**%**	**nº of reads**	**%**
$(TTAGGG)_1$	951,647	3.843	331,362	1.271	296,587	1.147	197,186	0.680
$(TTAGGG)_2$	809,239	3.268	169,543	0.650	143,595	0.556	7,259	0.025
$(TTAGGG)_3$	806,879	3.258	168,810	0.647	142,801	0.552	6,849	0.024
$(TTAGGG)_4$	787,802	3.181	166,154	0.637	140,420	0.543	6,607	0.023
$(TTAGGG)_5$	767,623	3.100	161,835	0.621	136,804	0.529	6,377	0.022
$(TTAGGG)_6$	742,038	2.996	154,517	0.592	132,819	0.514	6,161	0.021
$(CCCTAA)_1$	540,729	2.184	242,641	0.930	231,604	0.896	196,350	0.678
$(CCCTAA)_2$	398,057	1.607	81,759	0.313	75,774	0.293	4,066	0.014
$(CCCTAA)_3$	397,172	1.604	81,389	0.312	75,280	0.291	3,717	0.013
$(CCCTAA)_4$	389,551	1.573	80,366	0.308	74,212	0.287	3,576	0.012
$(CCCTAA)_5$	382,186	1.543	78,819	0.302	72,793	0.282	3,469	0.012
$(CCCTAA)_6$	373,401	1.508	75,939	0.291	71,232	0.276	3,372	0.012
$(TTAGGG)_1 + (CCCTAA)_1$	1,492,376	6.026	574,003	2.201	528,191	2.044	393,536	1.358
$(TTAGGG)_2 + (CCCTAA)_2$	1,207,296	4.875	251,302	0.964	219,369	0.849	11,325	0.039
$(TTAGGG)_3 + (CCCTAA)_3$	1,204,051	4.862	250,199	0.959	218,081	0.844	10,566	0.036
$(TTAGGG)_4 + (CCCTAA)_4$	1,177,353	4.754	246,520	0.945	214,632	0.830	10,183	0.035
$(TTAGGG)_5 + (CCCTAA)_5$	1,149,809	4.643	240,654	0.923	209,597	0.811	9,846	0.034
$(TTAGGG)_6 + (CCCTAA)_6$	1,115,439	4.504	230,456	0.884	204,051	0.789	9,533	0.033
Total nº of reads	24,763,644		26,079,916		25,846,525		28,980,120	

Table 9: Summary of second ChIP-seq experiment. Overall number of reads obtained and their size. % of alignment (PF) is the percentage of filtered reads that were uniquely aligned to the reference. In this second experiment,the read length is 42 bp.

Sample	Raw sequenced reads	Size of raw sequenced reads (bp)	% of alignment (PF)	Uniquely mapped reads	Size of uniquely mapped reads (bp)
Wildtype	29,609,663	1,243,605,846	58.54	14,498,028	608,917,176
Terc$^{-/-}$ G1	31,473,982	1,321,907,244	63.43	16,542,830	694,798,860
Terc$^{-/-}$ G3	30,741,283	1,291,133,886	59.88	15,476,230	650,001,660
Input Pool 2	35,229,238	1,479,627,996	73.78	21,381,218	898,011,156

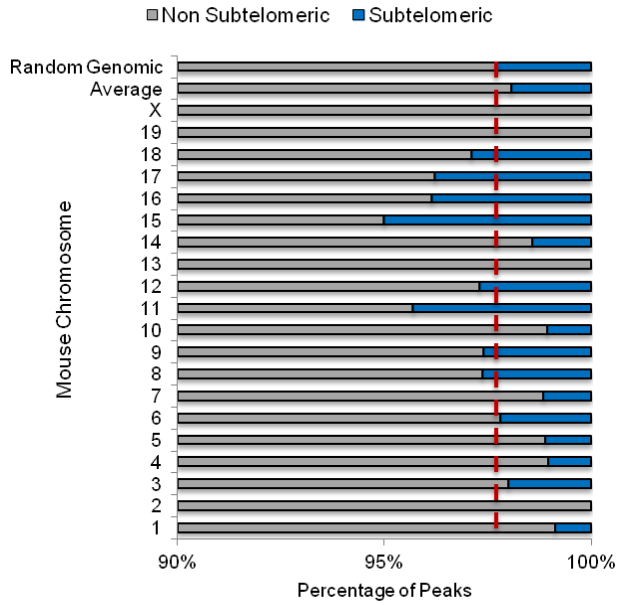

Figure 13: Percentage of peaks from the *Terc*$^{-/-}$ G3 vs wild-type comparison that are located in non subtelomeric and subtelomeric regions (-3 Mbp from telomeres). There is no enrichment in peaks in subtelomeres comparing with the random average of enrichment in any other region in the genome.

2. Dissecting the reprogramming process: shelterins and telomerase in iPS cell generation

Differentiated cells can be reprogrammed to a more pluripotent state by a process named nuclear reprogramming. The most recent approach for nuclear reprogramming consists in the overexpression of a combination of four core transcription factors (*Oct3/4*, *Sox2*, *Klf4* and *c-Myc*), leading to the so-called induced pluripotent stem (iPS) cells, which closely resemble ES cells (Takahashi and Yamanaka, 2006). It is known that during this process telomeres are also reprogrammed, resulting in a telomere elongation that is mainly telomerase-dependent (Marion et al., 2009b). The feasibility of clinical applications of iPS cells is dependent on the quality of these cells and the maintenance of their genomic stability, in order to avoid the danger of transformation. In this sense, ensuring telomere protection and capping during the formation and maintenance of iPS cells is crucial. In this thesis we set forth to study the role and dynamics of different proteins associated with telomere biology during nuclear reprogramming.

2. 1. TRF1 is essential for reprogramming

As we explained before, TRF1 has fundamental roles in telomere protection and replication, since its deletion in MEFs causes telomere fragility, chromosomal aberrations, replication fork stalling and a DDR leading to severe cell cycle arrest and senescence (Martinez et al., 2009; Sfeir et al., 2009). Moreover, TRF1 has been established as a stem cell marker that is significantly upregulated in ES and iPS cells compared to the starting cell populations both in humans and mice (Boue et al., 2010; Ginis et al., 2004; Hosseinpour et al., 2013; Schneider et al., 2013). Based on this, we decided to study the effect of *Trf1* abrogation during the reprogramming process. To this end, we reprogrammed MEFs knockout for *Trf1* in order to determine if TRF1 was essential for reprogramming. A scheme of the experiment is shown in **Fig. 14**.

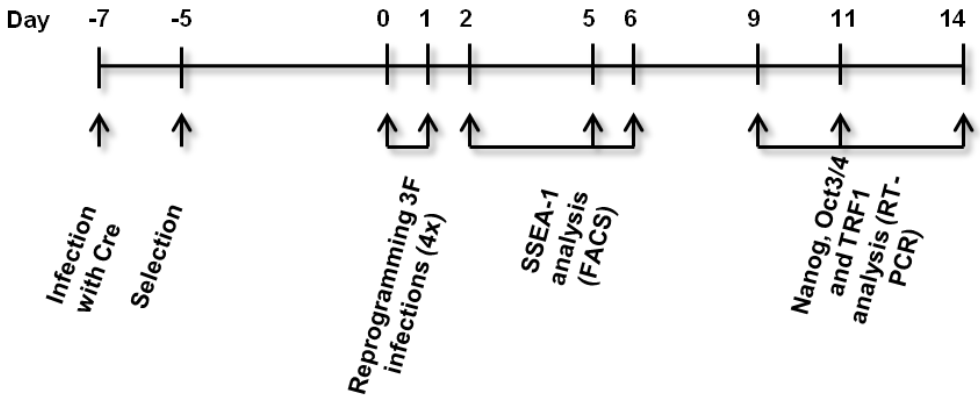

Figure 14: Scheme of the reprogramming approach.

As we have already explained, *p53* abrogation rescues proliferative defects associated with *Trf1* deficiency (Martinez et al., 2009). On top of that, p53 has been described as a barrier for reprogramming. In this way, its abrogation during reprogramming increases the efficiency of this process, by facilitating the reprogramming of cells with severe DNA damage (Hong et al., 2009; Kawamura et al., 2009; Li et al., 2009; Marion et al., 2009a; Utikal et al., 2009). Hence, we reprogrammed MEFs simultaneously deficient for *Trf1* and *p53*. Prior to reprogramming, $Trf1^{+/+}$ $p53^{-/-}$ and $Trf1^{lox/lox}$ $p53^{-/-}$ MEFs were infected with pBabe-puro-Cre and selected with puromycin for one week. TRF1 decrease was confirmed by Western blot (**Fig. 15**). As addition of *c-Myc* in the reprogramming cocktail was previously shown to be dispensable for the obtaining of iPS cells, for telomerase activation and for the elongation of telomeres associated with the reprogramming process (Wernig et al. 2007; Marion 2009a), we reprogrammed 200,000 cells per MEF line by four consecutive infections (Day 0 and 1) of the three retroviral Yamanaka factors *Oct3/4*, *Sox2* and *Klf4*. In parallel, we also infected cells with retroviral pBabe-GFP plasmid and checked infection efficiency by flow cytometry so as to calculate the reprogramming efficiency.

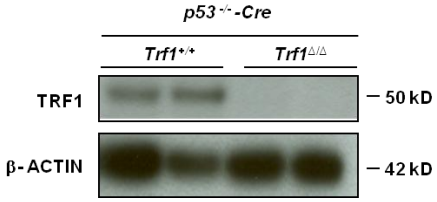

Figure 15: Western blot for TRF1 protein.

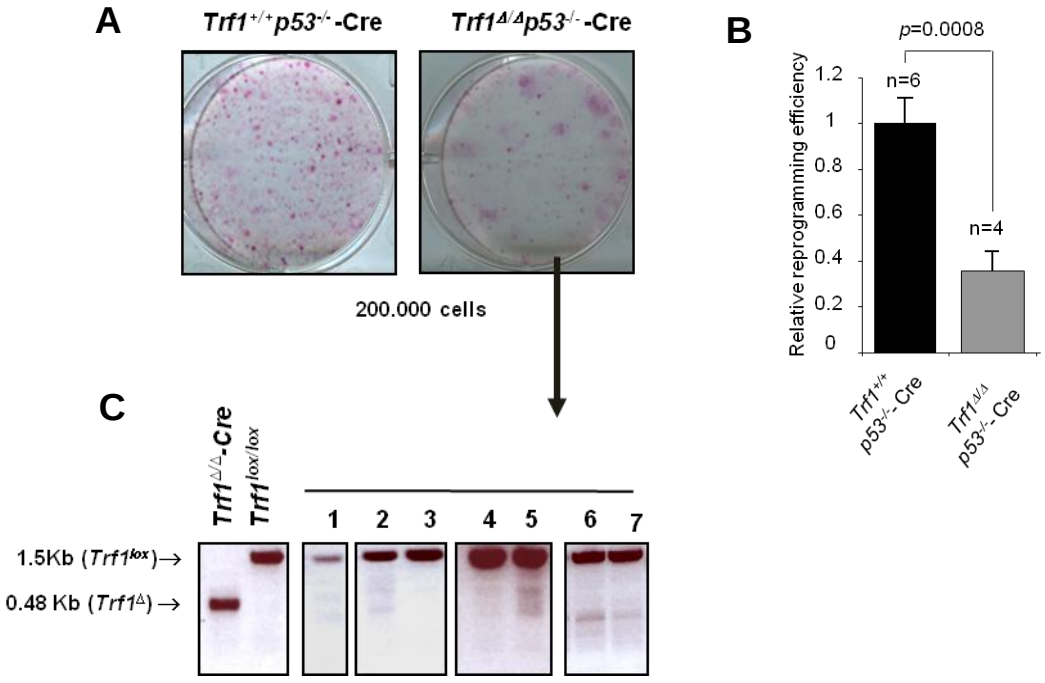

Figure 16: Reprogramming of *Trf1* ablated MEFs. (A) Reprogramming plates stained with alkaline phosphatase (AP). The number of parental MEFs used is indicated. **(B)** Relative reprogramming efficiencies of the indicated cells. n= number of independent MEF lines. Error bars: s.e.m. Statistical analysis: Two sided Student's *t*-test. **(C)** Analysis of *Trf1* excision in iPS colonies obtained from $Trf1^{\Delta/\Delta}$ $p53^{-/-}$-Cre MEFs by PCR. Note that all the clones keep the *Trf1* locus.

After two weeks, we failed to obtain any iPS cell colonies in the majority of the $Trf1^{\Delta/\Delta}$ $p53^{-/-}$-*Cre* cultures. In some of the wells, we obtained a few colonies with the same timing of $Trf1^{+/+}$ $p53^{-/-}$-Cre. The number of alkaline phosphatase positive colonies, which are the true pluripotent colonies, was scored after two weeks to

calculate reprogramming efficiency (**Fig. 16A)**. A decreased of three times in the reprogramming efficiency was seen in *Trf1*$^{\Delta/\Delta}$ *p53*$^{-/-}$-Cre MEFs compared to *Trf1*$^{+/+}$ *p53*$^{-/-}$-Cre MEFs (**Fig. 16B**). Colonies of both genotypes were picked in feeders and amplified to check the excision. All the iPS colonies obtained in the case of *Trf1*$^{\Delta/\Delta}$ *p53*$^{-/-}$*-Cre* cultures retained the *Trf1*^{lox} allele, indicating that those colonies were wild-type escapers of the infection with Cre recombinase (**Fig. 16C**). Therefore, we conclude that *Trf1* deficiency completely blocks reprogramming, even in the absence of p53.

Some of the key events associated with reprogramming are the upregulation of pluripotency markers. The surface antigen Stage-Specific Embryonic Antigen 1 (SSEA-1) is expressed in ES cells (Cui et al. 2004) and is upregulated at early time-points during reprogramming, whereas the increase in the expression of endogenous pluripotency genes *Nanog* and *Oct3/4* is a late step during reprogramming, being considered markers of fully reprogrammed cells (Brambrink et al., 2008; Stadtfeld et al., 2008a). We checked these pluripotency markers at different time-points during reprogramming by flow cytometry (SSEA-1) or by qRT-PCR (*Nanog* and *Oct3/4*). *Trf1* deficiency prevented the appearance of SSEA-1 positive clones, while wild-type control reprogramming cells started expressing SSEA-1 by day 5 of reprogramming (**Fig. 17A**). As expected, we detected increased expression of *Nanog* and *Oct3/4* before the appearance of the first iPS clones (11-14 days post-infection), while *Trf1*$^{\Delta/\Delta}$ *p53*$^{-/-}$-Cre did not show this increase, concordantly with reduced *Trf1* mRNA levels. We detected a slight increase in these markers in the *Trf1*$^{\Delta/\Delta}$ *p53*$^{-/-}$-Cre MEFs concomitant with an increase in *Trf1* expression from days 9 to 14, probably corresponding to MEFs that escaped the excision (**Fig. 17B**).

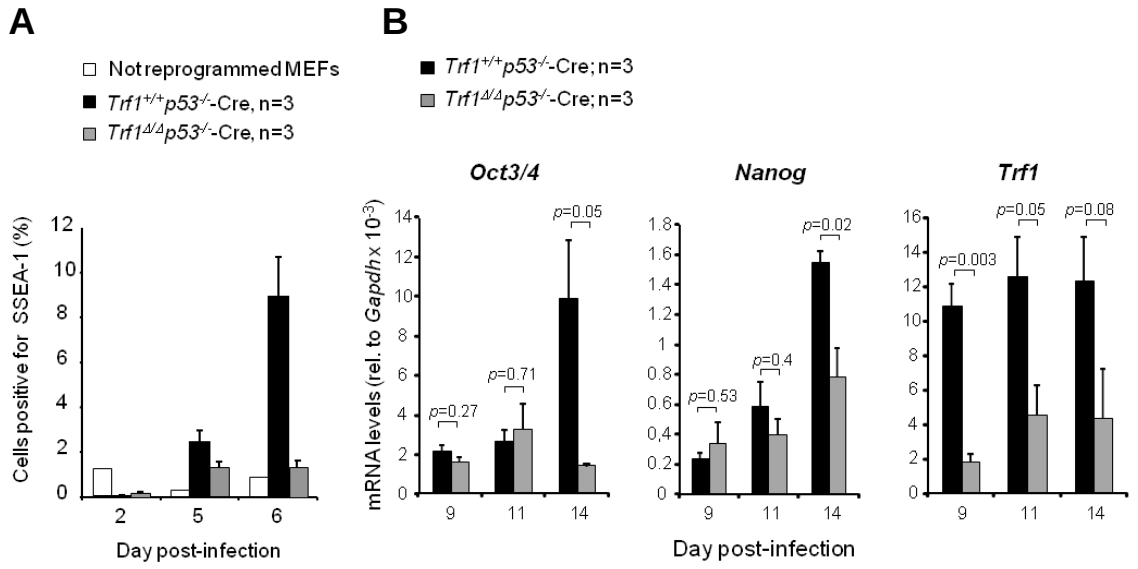

Figure 17: *Trf1*-null MEFs do not express SSEA-1, *Nanog* and *Oct3/4* pluripotency markers upon infection with 3F. (**A**) Kinetics of expression of SSEA-1 pluripotency marker during reprogramming, as measured by flow cytometry. Non-reprogrammed MEFs are shown as negative control. n= number of independent MEF lines. Error bars: s.e.m. (**B**) mRNA levels of *Oct3/4*, *Nanog* and *Trf1* at days 9, 11 and 14 of reprogramming, before appearance of iPS colonies. The mRNA levels are measured by qRT-PCR relative to *Gapdh* mRNA levels. n= number of independent MEF lines. Error bars: s.e.m. Statistical analysis: two sided Student's *t*-test.

2.2. *Trf1* knockdown MEFs reprogram with lower efficiency

In view that *Trf1* deficiency completely blocks reprogramming, even in the absence of p53, we set to confirm this essential role of TRF1 in reprogramming by knocking down *Trf1* expression during the reprogramming process. To this end, *p53*$^{-/-}$ MEFs were reprogrammed using a cocktail of retroviral vectors expressing the three reprogramming factors (*Oct3/4, Klf4* and *Sox2*) and a lentiviral vector expressing either *Trf1* shRNA or a scramble shRNA as a control. As expected, reduced expression of *Trf1* during reprogramming strongly decreased the reprogramming capacity of the cells (**Fig.18A-B**). To confirm that the colonies obtained in the sh*Trf1* treatment were not escapers, we picked colonies, amplified them and analyzed TRF1 levels by Western blot (**Fig. 18C-D**). We observed a decreased in TRF1 protein levels in the two colonies with the sh*Trf1* compared to those with the scramble, concluding that cells with low levels of TRF1 are capable to reprogram, but with a lower efficiency than wild-type cells.

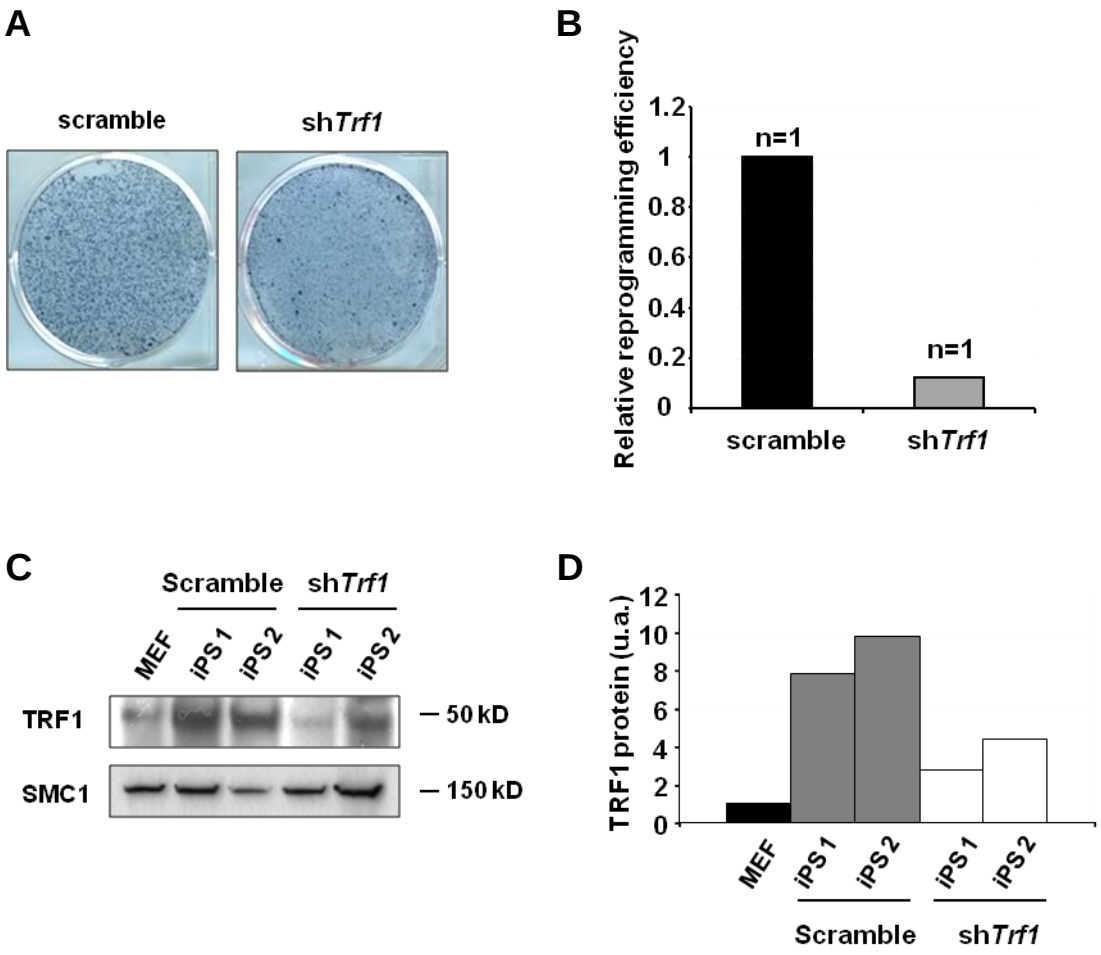

Figure 18: Down-regulation of TRF1 during reprogramming decreases dramatically the reprogramming efficiency. (**A**) Reprogramming plates stained with alkaline phosphatase. (**B**) Relative reprogramming efficiency of the indicated cells. Note that sh*Trf1*-transduced MEF line shows decreased reprogramming capacity. n= number of independent MEF lines. (**C**) Western blot for TRF1 in nuclear extracts from iPS colonies obtained from MEFs infected with scramble or sh*Trf1*. Two iPS clones per treatment were picked. MEFs were included as a control. (**D**) Quantification of the Western blot shown in **C**. Values are in arbitrary units (a.u.).

As *Trf1* deficiency results in activation of a DDR at telomeres, we checked for DNA damage foci by co-staining of γH2AX and TRF1. In line with this, we found an increased intensity of γH2AX per nucleus in cells with reduced levels of TRF1 at day 8 post-infection (**Fig. 19A**), suggesting that increased DNA damage may be responsible for the deficient reprogramming capacity of these cells. We have previously described that *Trf1* deletion leads to chromosome instability in MEFs, characterized by the presence of aberrations like chromosome or chromatid end-to-end fusions and

multitelomeric signals (MTS), which reflect telomere uncapping and fragility, respectively. We observed a significant increase in MTS at day 17 post-infection (p.i.), but not at an earlier time-point (day 10 p.i.), in cells with *Trf1* downregulation when compared to cells with normal levels of TRF1 (**Fig. 19B**), suggesting that accumulation of MTS may be associated with the number of cell doublings to form an iPS cell colony.

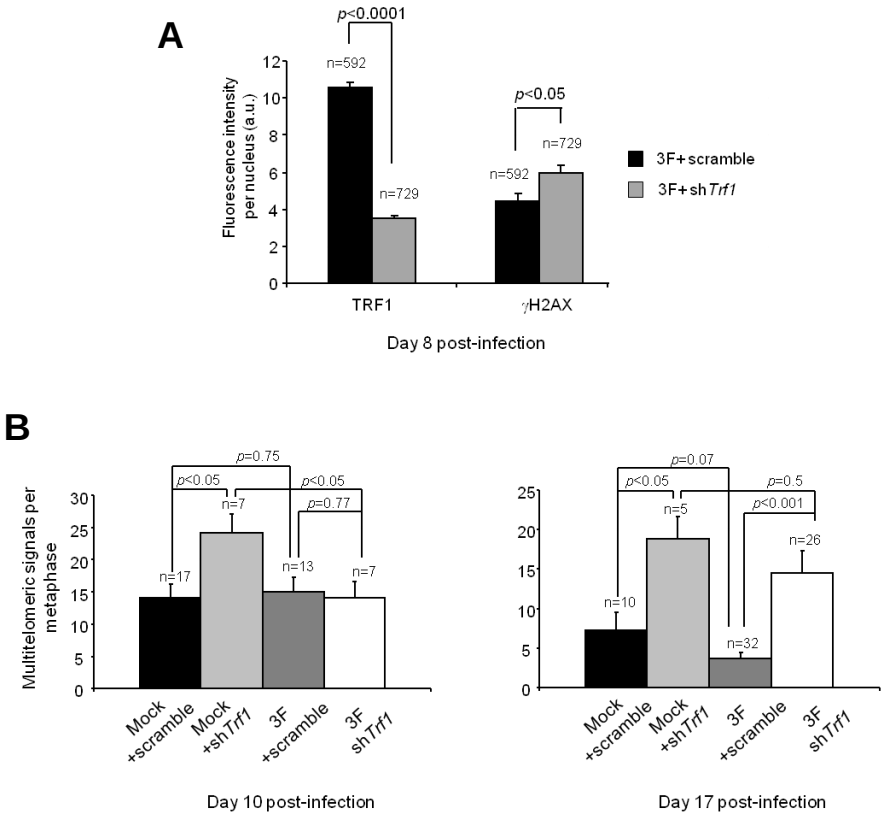

Figure 19: Downregulation of *Trf1* during reprogramming induces DNA damage and telomere aberrations. (**A**) Quantification of TRF1 and γH2AX immunofluorescence after infection with the indicated viral cocktails (day 8 p.i). n=number of cells analyzed. Error bars: s.e.m. Statistical analysis: two sided Student's *t*-test. (**B**) Frequency of multitelomeric signals in cells 10 days (no presence of iPS colonies) or 17 days (presence of iPS cells) after infection with the indicated viral cocktails. n= number of metaphases analyzed. Error bars: s.e.m. Statistical analysis: two sided Student's *t*-test.

2.3. Induction of apoptosis, chromosomal aberrations and DDR activation in *Trf1*-deficient iPS cells

Next, we wondered whether TRF1 could be essential not only during the acquisition of pluripotency, but also for the maintenance of the pluripotent state. To this end, we generated *Trf1*-null iPS cells using primary MEFs carrying the aforementioned conditional *lox*P-flanked *Trf1* allele and a Cre recombinase allele ubiquitously expressed under the control of the locus encoding the large subunit of RNA polymerase II (*RERTn*) (Guerra et al., 2003). This Cre recombinase is merged to the binding domain of the modified estrogen receptor (ERT2), being translocated to the nucleus upon treatment with the synthetic steroid 4-hydroxytamoxifen (4-OHT). After reprogramming of $Trf1^{+/+}RERTn^{+/ERT}$ and $Trf1^{lox/lox}RERTn^{+/ERT}$ MEFs by infections with the three OSK factors (as previously described), the resultant iPS cells were picked, replated and treated with 0.2 μM 4-OHT to obtain *Trf1* wild-type and *Trf1*-null iPS cells, respectively. IPS medium with 4-OHT was changed every day (**Fig. 20**).

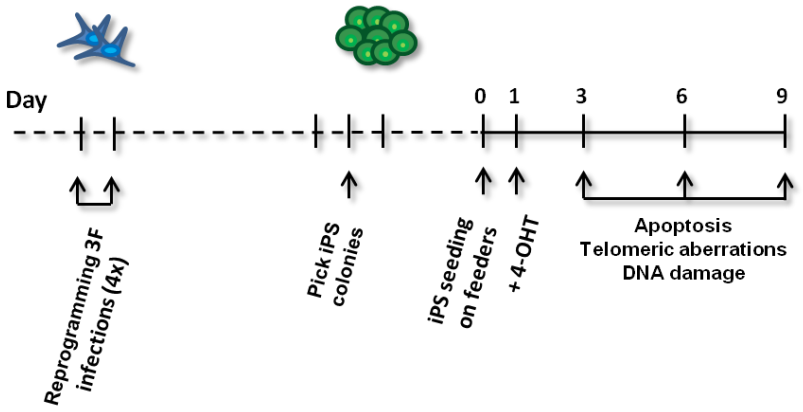

Figure 20: Scheme of the approach for the obtaining of conditional *Trf1* knockout iPS cells.

The phenotype of *Trf1* deletion in iPS cells was fast and severe, since practically all the *Trf1*-null iPS colonies were death by day 6 of 4-OHT treatment **(Fig. 21A)**. We confirmed *Trf1* abrogation in $Trf1^{\Delta/\Delta}RERTn^{+/ERTOHT}$ iPS cells by qRT-PCR at day 3 and 6 of 4-OHT treatment (**Fig. 21B**).

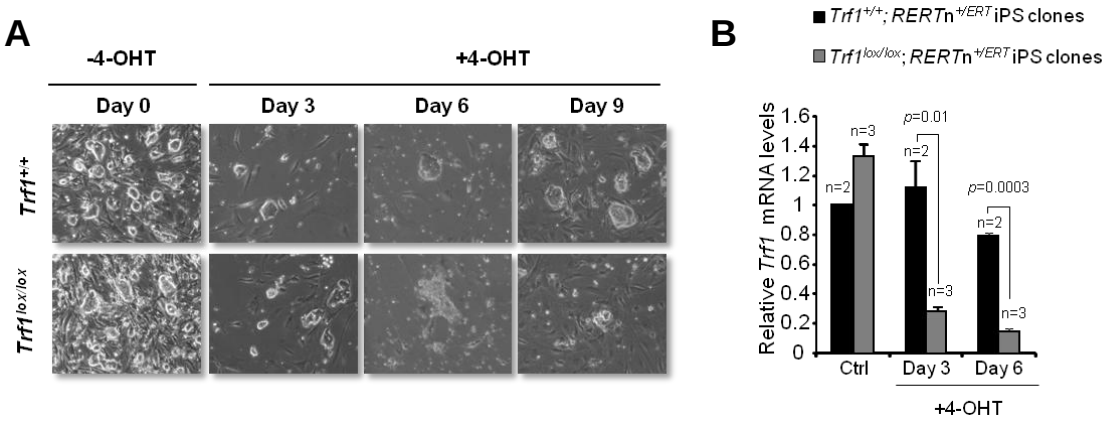

Figure 21: Conditional *Trf1* deletion in iPS cells. (A) Representative bright-field images showing the effect of *Trf1* abrogation in iPS cells. (**B)** *Trf1* mRNA levels decrease with time of 4-OHT treatment at day 3 and day 6. Ctrl are control treated cells at day 3 where no difference in the *Trf1* mRNA levels was detected. n= number of iPS cell clones. Error bars: s.e.m. Statistical analysis: Two sided Student's *t*-test.

Thereafter, we wanted to know whether this *Trf1*-deletion induced cell death in iPS cells was mediated by apoptosis. To this end, we checked Annexin-V staining by flow cytometry at day 3 and 6 of 4-OHT treatment. Even if the initial levels were abnormally high in both genotypes, we observed a robust increase in apoptosis in $Trf1^{\Delta/\Delta}$ $RERTn^{+/ERTOHT}$ iPS cells compared to the $Trf1^{+/+}$ $RERTn^{+/ERTOHT}$ iPS cells by day 6 of treatment (**Fig. 22A-B**).

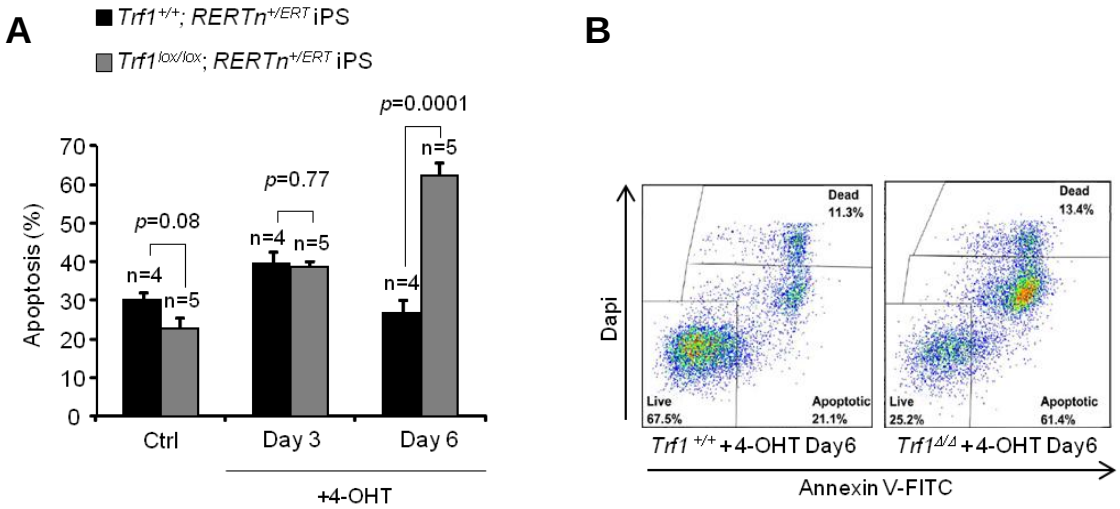

Figure 22: Induction of apoptosis in *Trf1* knockout iPS cells. (**A**) Apoptosis was determined on control treated iPS cells and iPS cells at day 3 and 6 of 4-OHT treatment. n= number of iPS clones analyzed. Error bars: s.e.m. Statistical analysis: Two sided Student's *t*-test. (**B**) Representative FACS profiles at day 6 of 4-OHT treatment.

To address whether *Trf1* deficiency causes telomeric aberrations in iPS cells, we performed Q-FISH by hybridization with a telomeric $(TTAGGG)_3$ probe. For this, iPS cells were arrested in metaphase by three hours treatment with colcemid, which prevents spindle formation during mitosis. As expected, $Trf1^{\Delta/\Delta}$ $RERTn^{+/ERTOHT}$ iPS cells showed higher levels of multitelomeric signals, sister-chromatid and chromosome end-to-end fusions at day 3 and 6 after 4-OHT treatment (**Fig. 23**), suggesting increased telomere fragility and telomere uncapping due to *Trf1* abrogation.

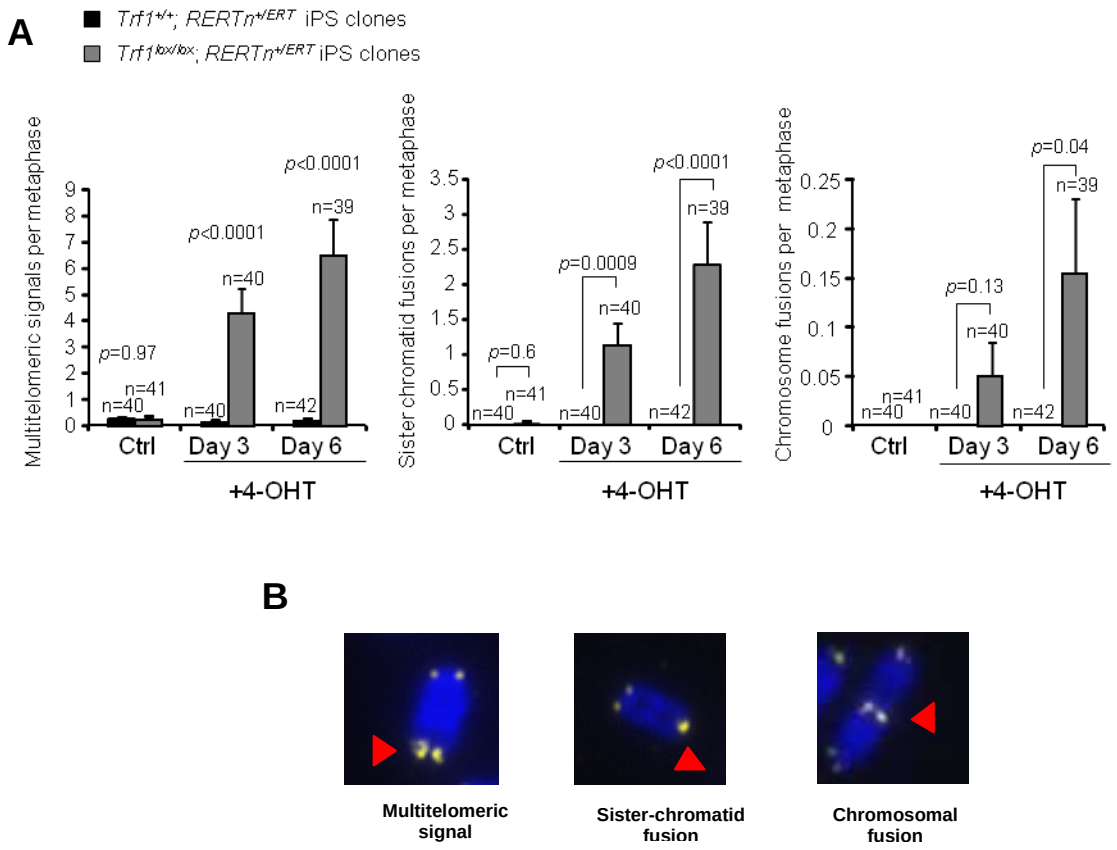

Figure 23: ***Trf1*-null iPS cells show chromosomal aberrations.** (**A**) Frequency of aberrations in metaphase spreads of the indicated genotypes and conditions. n= number of metaphases from a total of two iPS clones per genotype. Error bars: s.e.m. Statistical analysis: Two sided Student's *t*-test. (**B**) Representative images of the aberrations. Red arrows highlight the indicated aberrations; Yellow: telomeres $(TTAGGG)_3$ probe; Blue: Dapi.

Finally, we analyzed DDR activation by immunofluorescent co-staining of γH2AX and TRF1 in iPS cells at day 3 of 4-OHT treatment. We detected a considerable increase in the percentage of γH2AX positive cells (**Fig. 24**) in $Trf1^{\Delta/\Delta}RERTn^{+/ERTOHT}$ with low levels of TRF1 compared to $Trf1^{+/+}RERTn^{+/ERTOHT}$ and $Trf1^{\Delta/\Delta}RERTn^{+/ERTOHT}$ with high levels of TRF1, in agreement with the results from *Trf1*-null MEFs.

Together, these findings indicate that TRF1 is essential both for the induction and maintenance of pluripotency in iPS cells.

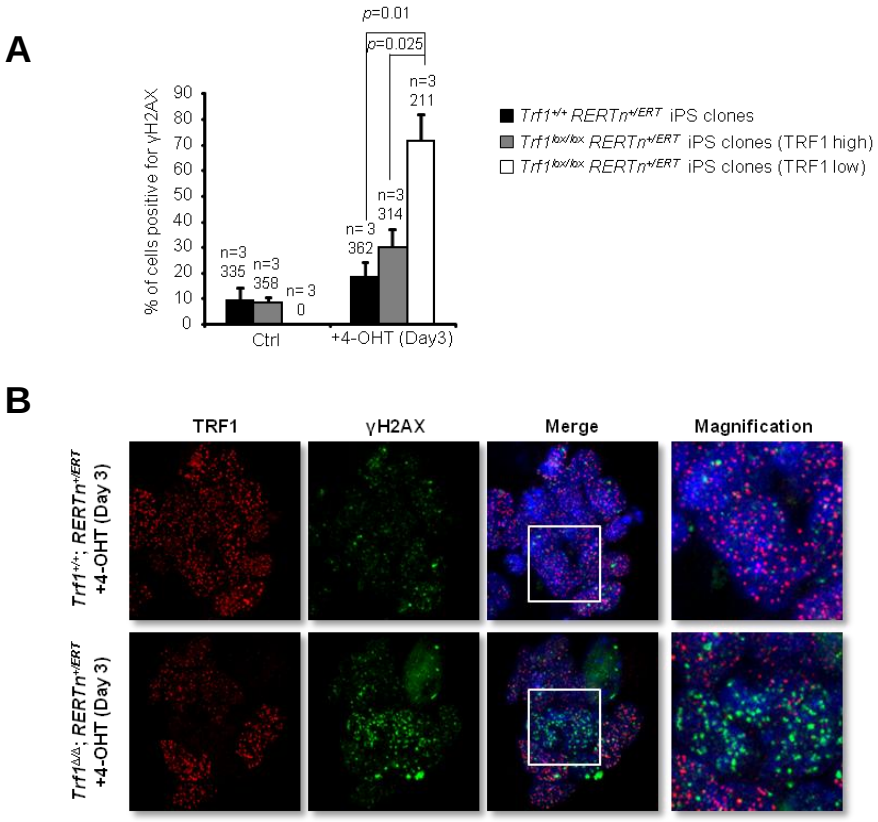

Figure 24: *Trf1*-null iPS cells show DNA damage. (**A**) Percentage of γH2AX positive cells in non-treated (Ctrl) and 4-OHT treated (Day 3) iPS cells. n= number of iPS clones used for the analysis. The total number of cells analyzed per genotype is shown. Error bars: s.e.m. Statistical analysis: Two sided Student's *t*-test. (**B**) Representative images of TRF1 and γH2AX immunofluorescence co-staining.

2.4. Ectopic expression of *Trf1* does not affect reprogramming efficiency or replace any of the OSK factors during reprogramming

High TRF1 levels are observed not only in established ES cells but also in cultured ICM cells before telomere elongation, probably to assure telomeres protection as they are elongated (Varela et al., 2011). As we said before, TRF1 levels dramatically increase in iPS cells compared to differentiated cells. It has been previously demonstrated by us that this TRF1 increase is uncoupled from telomere elongation, as *Tpp1*$^{\Delta/\Delta}$ *Cre-shp53* iPS cells, which show impaired telomere elongation (Tejera et al., 2010), exhibit TRF1 levels similar to those of wild-type iPS cells, implying a role of TRF1 protein apart from telomere maintenance (Schneider et al., 2013). Besides, it has been reported that the ectopic expression of factors that protect telomeres, such as *Zscan4*, can increase efficiency of reprogramming (Jiang et al. 2013). Once we demonstrated that *Trf1* is essential for reprogramming and maintenance of iPS cells, we wondered whether ectopic expression of this protein could modulate reprogramming efficiency. On top of that, we also wanted to know if *Trf1* could replace any of the three Yamanaka factors (*Oct3/4*, *Sox2*, *Klf4*) in the reprogramming cocktail. To address this, we carried out a reprogramming assay with MEFs overexpressing *Trf1* (**Fig. 25**).

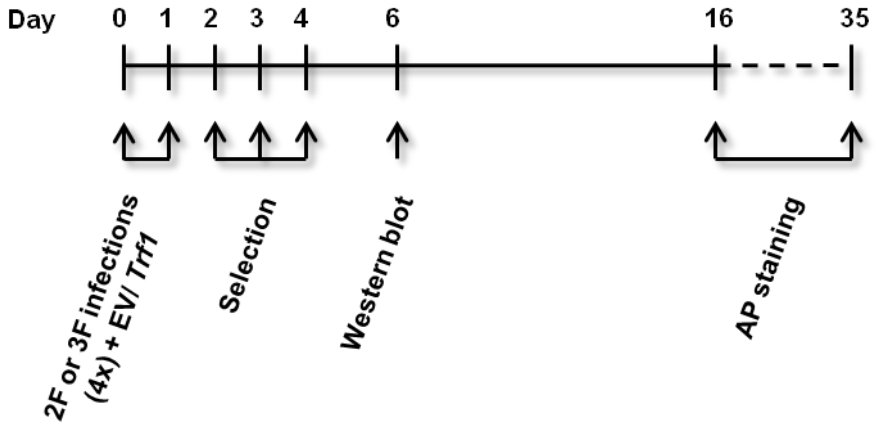

Figure 25: Scheme of the approach for reprogramming of MEFs overexpressing *Trf1*

To this end, we cloned mouse *Trf1* cDNA in a retroviral pBabe-puro-Empty Vector (EV) backbone with puromycin selection. Our approach was to infect wild-type MEFs with the three Yamanaka factors (OSK, 3F) in combination with pBabe-puro-

Trf1 or the corresponding pBabe-puro-EV mock control and selected them with puromycin. Besides, we also infected MEFs with two Yamanaka factors (OK, OS and SK) combined with either pBabe-puro-*Trf1* or pBabe-puro-EV. We began by testing our plasmid by Western blot for TRF1 at day 6 of reprogramming, confirming TRF1 overexpression (**Fig. 26A**). In the case of reprogramming with 3F, iPS colonies appeared at the same time in both control and *Trf1* overexpressing MEFs at day 14 post-infection (**Fig. 26B**). *Trf1* overexpression did not affect the reprogramming efficiency either, as it is shown in the alkaline phosphatase staining from day 16 (**Fig. 26C-D**). In contrast, we did not obtain any colonies in the 2F reprogrammings by day 35 (**Fig. 26C**), indicating that *Trf1* is not able to replace any of the OSK factors in the cocktail of reprogramming.

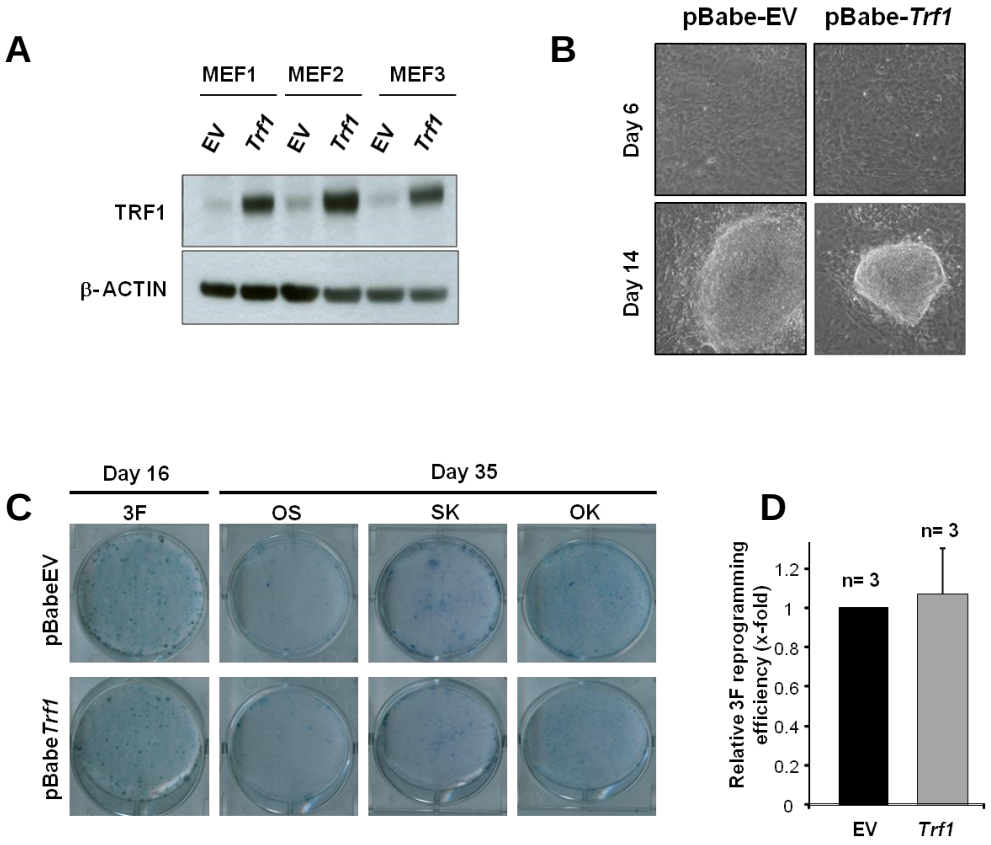

Figure 26: Reprogramming of MEFs overexpressing *Trf1*. (A) Western blot showing increased levels of TRF1 in MEFs infected with pBabe-puro-*Trf1*. (**B**) Bright-field images at day 6 and 14 of reprogramming. (**C**) Alkaline phosphatase staining of MEFs infected with 3F (OSK) at day 16 and with 2F (OS, SK and OK) at day 35 of reprogramming. Note that no iPS colonies appeared in the case of 2F reprogramming. (**D**) Relative reprogramming efficiency of MEFs infected with pBabe-puro-*Trf1* compared to the control infected with pBabe-puro-EV. n= number of independent MEF lines. Error bars= s.e.m.

As we mentioned before, iPS cell formation is associated with an increase in telomerase activity (Takahashi and Yamanaka, 2006), which takes place late in the reprogramming process (Stadtfeld et al., 2008a). Consequently, telomeres elongate during reprogramming, specially post-reprogramming (Marion et al., 2009b) and this elongation has been described to be crucial for the proliferative capacity, stability and differentiation potential of the resultant iPS cells. On top of that, ectopic expression of the catalytic subunit of telomerase *Tert* confers growth advantages in MEFs. This effect is independent of telomere elongation and seems to be related with a role of *Tert* through inhibition of the TGF-β pathway (Geserick et al., 2006). Besides, mice *Tert*$^{-/-}$ tail-tip fibroblasts (TTFs) have been shown to reprogram with lower efficiency, also independent of their telomere length (Kinoshita et al., 2014). This evidence suggests that TERT could have extra-telomeric functions that positively modulate reprogramming capacity.

Factors that can regulate telomerase expression, recruitment or activity are also expected to play a significant part in iPS cell formation. TPP1 interaction with telomerase has been described to be necessary for high processivity of telomerase enzyme (Zaug et al., 2010). Moreover, TPP1 is essential for the telomere elongation that takes place during reprogramming by facilitating the recruitment of telomerase (Tejera et al., 2010).

Based on this, we wanted to know if *Tert* overexpression, alone or in combination with *Tpp1* overexpression during reprogramming could influence reprogramming efficiency. To test this, we cloned mouse *Tert* and *Tpp1* cDNAs in a lentiviral vector and overexpressed them during reprogramming. Since c-MYC is a well characterized regulator of *Tert* (Flores et al., 2006), we carried out our reprogramming assay both in the presence and absence of *c-Myc* in the reprogramming cocktail. Wild-type MEFs from low passages were infected with 3 (OSK) and 4 (OSKM) reprogramming factors in combination with pLVX-EV, pLVX-*Tert*, pLVX-*Tpp1* or pLVX-*Tert* + pLVX-*Tpp1*. Reprogramming efficiency was tested by alkaline phosphatase staining at day 9 (4F) or day 11 (3F) post-infection (**Fig. 27**). As expected, MEFs infected with 4F reprogrammed much faster and with higher efficiency than with 3F, since c-MYC enhances reprogramming efficiency although it is dispensable for the obtaining of iPS

cells (Wernig et al., 2008). However, no differences in the reprogramming efficiency or colony appearance timing were observed in any of the conditions tested, concluding that *Tpp1* or *Tert* overexpression does not affect reprogramming efficiency.

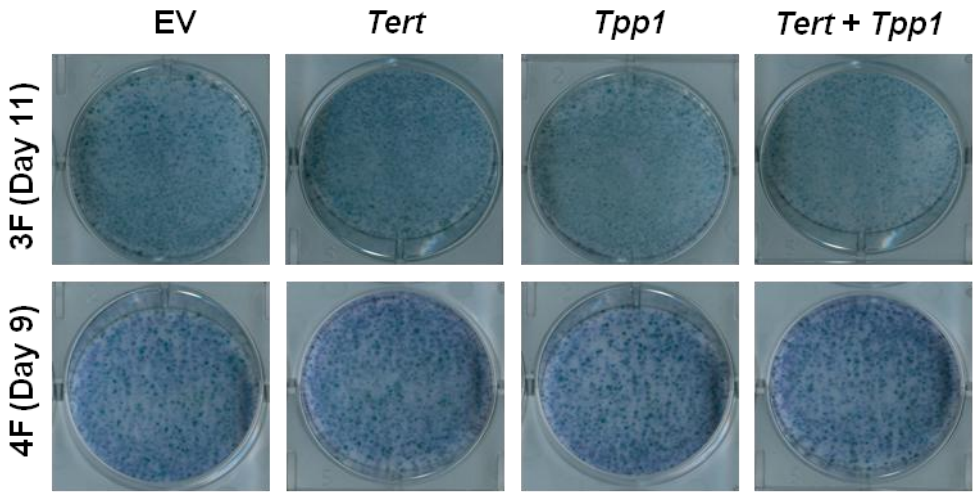

Figure 27: Reprogramming of MEFs overexpressing *Tert* and/or *Tpp1*. Alkaline phosphatase staining at day 9 (4F) and day 11 (3F) post-infection. Note that reprogramming efficiency is much higher in MEFs reprogrammed with 4F.

We checked the increase in both *Tert* and *Tpp1* mRNA levels by qRT-PCR at day 4 of reprogramming relative to day 0 (**Fig. 28**). In the case of *Tert*, we showed a robust increase in pLVX-*Tert* and pLVX-*Tert* + pLVX-*Tpp1* infected MEFs compared to control MEFs with EV in 3F reprogramming. Surprisingly, *Tert* overexpression was milder in 4F reprogramming (**Fig. 28, left**). *Tpp1* also showed a higher upregulation in the 3F approach compared to 4F (**Fig 28, right**). These differences between 3F and 4F could be due to the silencing of the lentivirus, one of the late events of the reprogramming process (Stadtfeld et al., 2008a), associated with the faster reprogramming of MEFs infected with 4F.

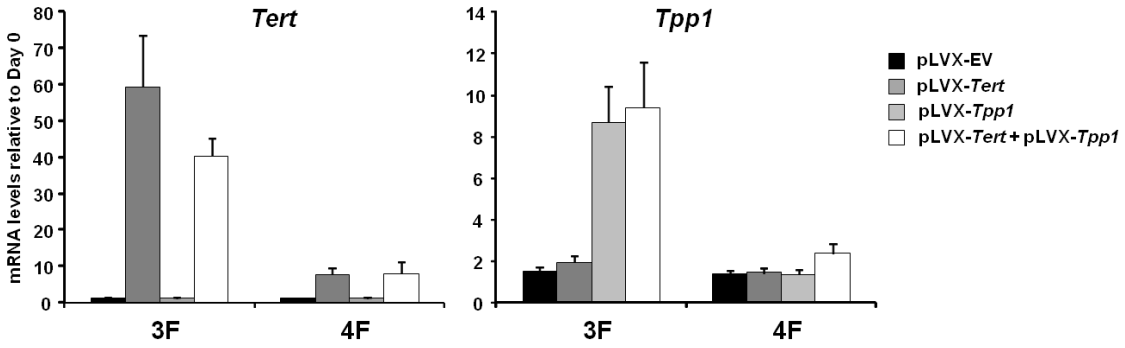

Figure 28: *Tert* and *Tpp1* mRNA levels at day 4 of reprogramming relative to day 0. n= 3 independent MEF lines. Error bars= s.e.m.

2.6. Shelterins and telomerase dynamics during reprogramming

A lot of effort has been made in the field of reprogramming trying to unveil the steps leading to the formation of iPS cells. It is clear that there is a connection between telomerase and reprogramming, but little is known about the dynamics of shelterins during this process. At least two of the proteins of the shelterin complex, TRF1 and TRF2, have been described to be upregulated in ES and iPS cells, being considered as stem cell markers (Boue et al., 2010; Ginis et al., 2004; Hosseinpour et al., 2013; Schneider et al., 2013). Besides, we recently showed that *Trf1* upregulation takes place early in reprogramming (Schneider, 2013). However, nothing is known about the rest of the shelterins.

In the last years, several publications have been released dissecting the pluripotency roadmap by the use of high-throughput techniques (Buganim et al., 2012; Hansson et al., 2012; Mah et al., 2011; O'Malley et al., 2013; Polo et al., 2012; Soufi et al., 2012). Polo and collegues examined defined intermediate cell populations poised to becoming iPSCs by genome-wide analyses. They reported that induced pluripotency elicits two transcriptional waves, which are driven by c-MYC/KLF4 (first wave) and OCT3/4/SOX2/KLF4 (second wave) (Polo et al., 2012). Using these microarray data, we checked shelterins and telomerase dynamics during the reprogramming process. As it is seen in **Fig. 29**, *Trf1* and *Tin2* showed an obvious increase, more pronounced at the beginning and at the end of reprogramming. *Trf2* and *Rap1* displayed a similar pattern

of expression, as they decreased during the process of reprogramming. Surprisingly, no increase was detected in the case of *Tert* expression. The same happened with *Tpp1*. Lastly, in the case of *Pot1a*, a mild increase was shown.

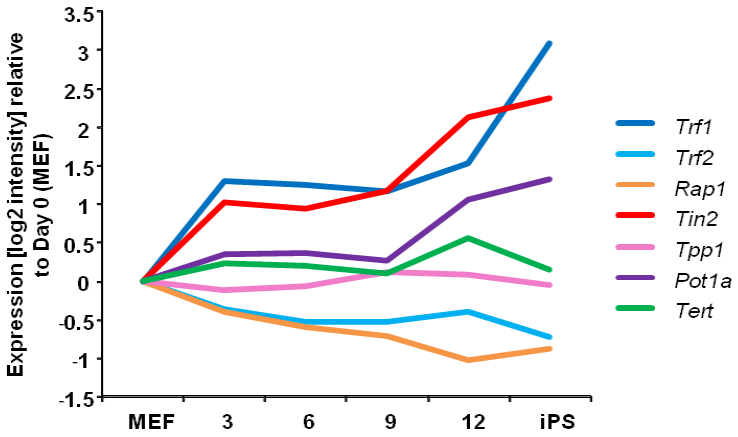

Figure 29: Expression analysis of the indicated genes at day 0 (MEF), 3, 6, 9 and 12 of reprogramming and in established iPS cells. Cells were sorted based on THY, SSEA-1 and Oct-GFP markers, selecting for cells undergoing successful reprogramming at day 3, 6 and 9 (THY^-/ $SSEA\text{-}1^+$) and day 12 (THY^-/ $SSEA\text{-}1^+$/ $Oct\text{-}GFP^+$) (Adapted from Polo et al. 2012).

In order to validate these results, we analyzed the expression of these genes during reprogramming by qRT-PCR. We took advantage of a "reprogrammable" transgenic mouse strain (inducible four factors, i4F) from the laboratory of Manuel Serrano, which is a useful tool that allows us to reprogram MEFs faster and more homogeneously (Abad et al., 2013). This reprogramming system consists in MEFs carrying the doxycycline-inducible transcriptional transactivator (rtTa) and a single copy of a lentiviral polycistronic cassette encoding the four murine reprogramming factors (*Oct3/4*, *Sox2*, *Klf4* and *c-Myc*) under the control of the tetO element. Upon doxycycline addition, iPS colonies appear after one week. A scheme of the experiment is depicted in **Fig. 30**.

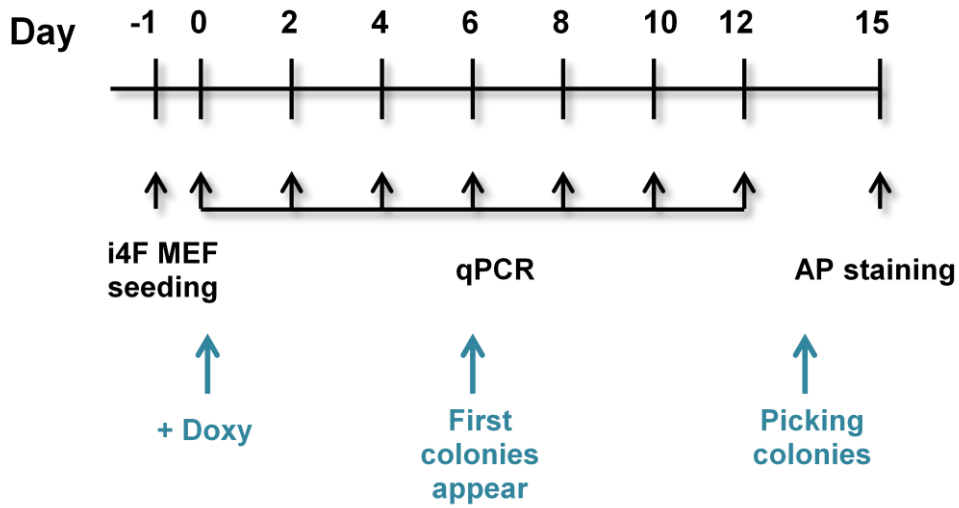

Figure 30: Scheme of the reprogramming approach with the reprogrammable i4F MEFs

We added doxycycline one day after MEF seeding (day 0) and analyzed shelterins and telomerase components expression by qRT-PCR every two days (day 0, 2, 4, 6, 8, 10 and 12) and in established iPS cells obtained from these MEFs **(Fig. 31).** *Nanog* expression was checked to confirm the dynamics of the reprogramming. In regards to telomerase components, we observed an increase in *Tert* expression at the beginning of reprogramming. By contrast, *Terc* progressively increases during the reprogramming, reaching over an 8-fold upregulation in iPS cells compared to MEFs. Regarding shelterins, we noticed a slight increase at the beginning of reprogramming (day 0 to day 4) in all the shelterins, although most of them came back to the initial levels in established iPS cells, except *Trf1* and *Pot1a.* In the case of *Trf1*, we observed an increase of around four times in iPS cells compared to MEFs. We have previously described that OCT3/4 is able to directly bind to *Trf1* promoter regulating its expression in pluripotent cells, both ES and iPS cells (Schneider et al., 2013). Further studies are needed to elucidate whether the expression of the rest of the shelterins is also regulated by reprogramming factors.

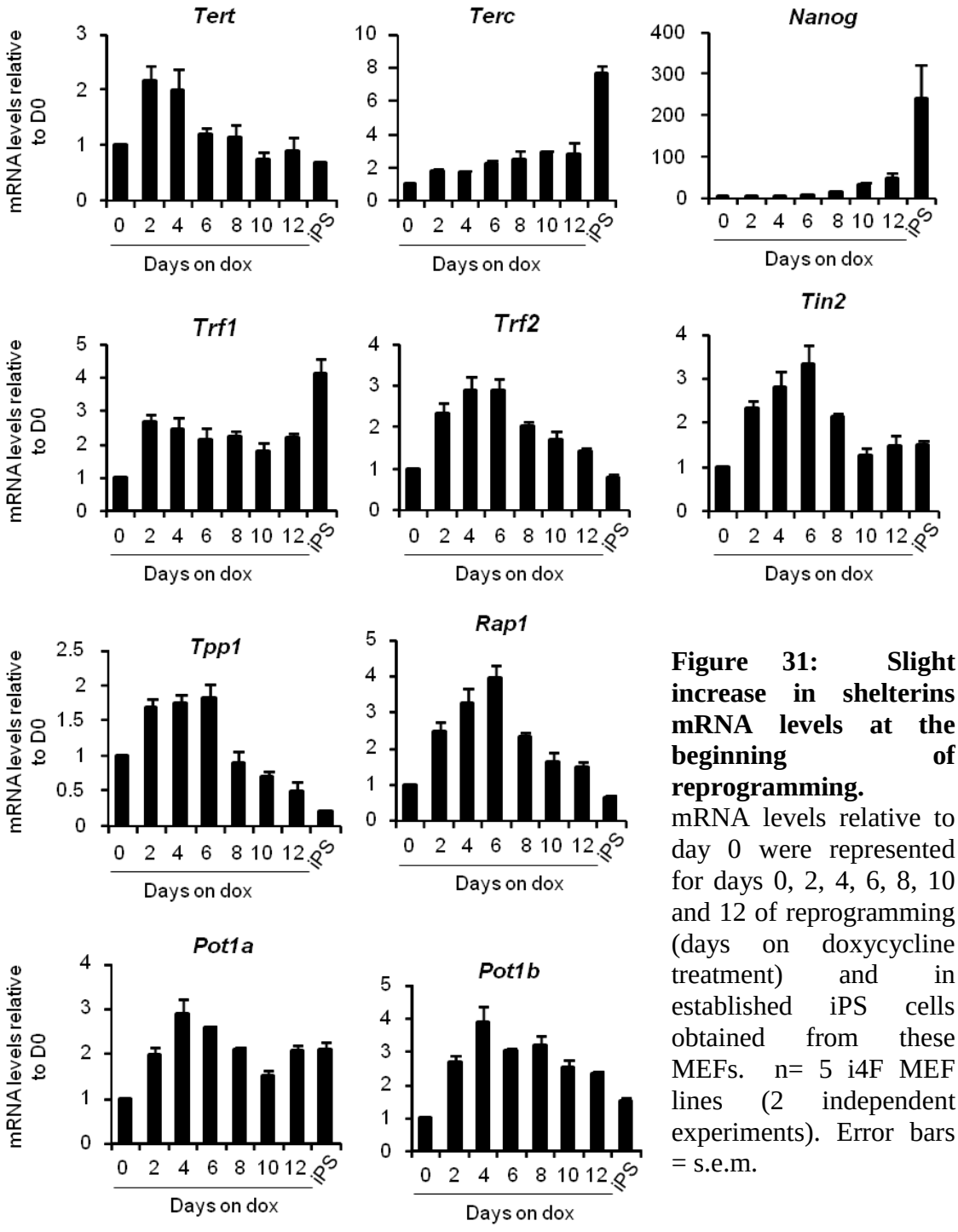

Figure 31: Slight increase in shelterins mRNA levels at the beginning of reprogramming.
mRNA levels relative to day 0 were represented for days 0, 2, 4, 6, 8, 10 and 12 of reprogramming (days on doxycycline treatment) and in established iPS cells obtained from these MEFs. n= 5 i4F MEF lines (2 independent experiments). Error bars = s.e.m.

Discussion

1. Identification of putative extra-telomeric binding of TRF1

Restricted binding of TRF1 to telomeres in normal conditions and upon telomere shortening in mice

The aim of this study was to establish the genome-wide DNA binding patterns of the telomeric dsDNA binding protein TRF1 in MEFs and find out whether telomere shortening could induce delocalization of TRF1 from telomeres and binding to other regions in the genome. When we analyzed TRF1 specific binding sites by ChIP sequencing, however, none of the peaks obtained had enough statistical significance and were statistically considered false positives. In agreement with this, we could not validate the TRF1 peaks by ChIP-qRT-PCR, further indicating that mouse TRF1 binding to chromatin is restricted to telomeres, at least in MEFs.

This is in apparent conflict with what was previously observed in a work done in humans, where they identified a limited number of extra-telomeric TRF1 binding sites that largely comprised ITSs in human tumor cell lines (Simonet et al., 2011). Another group also reported binding of TRF1 to an ITS that form a common fragile site, also in humans (Bosco and de Lange, 2012). Simonet and colleagues used BJ-HELTRas^{mc} tumor cell line, which are Ras-transformed BJ-HELT fibroblasts (SV40/hTERT-immortalized human BJ fibroblasts) where TRF2 seems to have a role in oncogenesis mediated by extra-telomeric binding (Biroccio et al. 2013). This fact suggests that TRF1 could also have additional functions in these cells. It is well established that both TRF1 and TRF2 are overexpressed in several cancers, suggesting that they could carry out extra-telomeric functions different from non transformed cells. In the second study from Bosco and de Lange, also done in transformed human fibroblasts, they described the binding of TRF1 to an especial ITS located in the human chromosome region 2q14 and associated with a fragile site, which was originated from a telomere-telomere fusion of two ancestral ape chromosomes. We have to take into consideration that not only protein binding profiles but also ITSs structure and length differ between humans and mice, which may explain the differences in TRF1 binding observed in both species. The fact that the human studies were performed in transformed cell lines, while we studied TRF1 binding to chromatin in normal primary cells, may also account for the different

results, as the specific cellular context could have an effect on TRF1 levels and determine its ability to bind to certain regions.

It has also been reported that TRF1 binds to ITSs in immortalized Chinese hamster cells, where it is involved in the stability of these repeated sequences (Krutilina et al., 2001; Krutilina et al., 2003). Unlike mouse cells, however, the Chinese hamster cells contain large blocks of cytologically detectable het-ITSs that correspond to 5% of their genome, which probably have completely different stabilization and protection mechanisms, and this may also explain the differences with our study.

Finally, we found very few TRF1 peaks associated with ITSs in MEFs when compared with an analogous RAP1 ChIP-seq also in MEFs and we could not validate them by ChIP-RT-PCR, suggesting that indeed those putative TRF1 peaks may be artifacts of the sequencing technique owing to erroneous alignment of telomeres to ITSs rather than *bona fide* TRF1 binding sites. When studying genome-wide DNA binding profiles, protein concentration can be critical in the identification of statistically significant peaks. In fact, in a ChIP-seq experiment done with anti-TRF2 and anti-RAP1 antibodies in humans, they demonstrated that TRF2 concentration could considerably influence this protein's binding to ITSs (Yang et al., 2011). Even so, we previously published a TRF1 ChIP-seq done in iPS cells, which display high TRF1 levels, showing no significant TRF1 binding to putative regulatory regions nor intragenic binding of this protein outside telomeric regions (Schneider et al., 2013).

Given our negative findings with TRF1, it would be interesting to study the genome-wide DNA binding profiles for TRF2, which also binds to dsDNA and recruits RAP1 to telomeres. In fact, we previously demonstrated that TRF2 binds to TTAGGG-rich extra-telomeric RAP1 binding sites (Martinez et al., 2010). It is well established that TRF1 and TRF2 share the binding domain to DNA but they do not interact and bind independently to the DNA. We expected that TRF1 would have similar binding to ITSs similar to TRF2. Nevertheless it has been published that these two proteins recognize the DNA in a different way, as TRF1 binds slightly more strongly to DNA than TRF2 (Hanaoka et al., 2005) and they use different mechanisms to find telomeric DNA (Lin et al., 2014). Apart from the slight dissimilarities in binding to DNA, TRF1 and TRF2 differ in their N-terminal domain, which is acidic in TRF1 and basic in

TRF2. This could equally influence the distinct binding and functions of these two proteins.

Telomere shortening is accompanied by a change in the architecture of telomeric and subtelomeric chromatin leading to a more "open" chromatin state. However, this loss of telomeric repeats in G2 and G5 *Terc*$^{-/-}$ MEFs has no effect on TRF1 density at telomeres, inferring that no alterations of TRF1 binding to telomeres are associated with telomere shortening (Benetti et al., 2007). Besides, it is known that TRF1 protein levels are significantly reduced in late generation *Terc*$^{-/-}$ mice (Franco et al., 2002). These two data together with our results suggest that TRF1 expression and degradation are tightly regulated in mice and that telomeric shortening induces a decrease in TRF1 levels rather than a relocalization of this protein to other regions in the genome. In fact, TRF1 release from telomeres induces its ubiquitylation and subsequent degradation via proteosome (Chang et al., 2003). Nevertheless, it is known that a fraction of TRF1 can also exist free in the nucleus (McKerlie and Zhu, 2011). In humans, CDK1 phosphorylates TRF1 at T371 (pT371), keeping TRF1 free of telomere chromatin and protected from proteasome-mediated protein degradation. This phosphorylation is upregulated during mitosis but during interphase, in response to ionizing radiation (IR), phosphorylated TRF1 is recruited to sites of DSB and forms damage-induced foci, promoting the repair of these IR-induced DSBs by homologous recombination (HR) (McKerlie et al., 2013). It would be interesting to clarify if this extra-telomeric function of TRF1 is preserved in mice after DNA damage induction. In this way, further studies of the extra-telomeric binding of TRF1 and other shelterins in a context of telomere shortening, other pathological conditions or DNA damage induction are needed. Besides, a deeper knowledge of the structure, function and stability of these ITSs in the different species will help us to understand the dissimilar binding of shelterins to these regions.

2. Dissecting the reprogramming process: shelterins and telomerase in iPS cell generation

Regarding therapeutic purposes, iPS cells bypass the ethical issues that limit application of ES cells, as they avoid the need for blastocyst-derived ES-cells. Besides, since they are derived from the patient's own cells, they are thought to represent a renewable and immunologically compatible cell source for cell replacement therapy. In this way, iPS cells have the potential to be used in age-related infertility and age-related diseases. Moreover, generation of iPS cells from patients provides *in vitro* models to understand the mechanisms involved in the development of diseases, as it is the case of iPS obtained from dyskeratosis congenita patients.

In addition to the applications in regenerative medicine, iPS cells serve as a tool for studying developmental processes at earliest embryonic stages. It is known that telomere status changes during embryo development and ES cells derivation. At the preimplantation embryo-stage, telomeres are effectively elongated by ALT-like mechanism from totipotent zygote to blastocist and then telomerase is used to maintain telomere length during ontogenesis in adult stem cells (Liu et al., 2007). Hence, the study of telomere remodeling during reprogramming could also help us to understand the mechanisms underlying telomerase and shelterin dynamics *in vivo* in the embryonic development.

Functional telomeres are essential for maintaining stemness and genome stability in ES and iPS cells and possible markers for evaluating pluripotency. In this way, further understanding of telomere reprogramming and maintenance is crucial to guarantee the quality of iPS cells and their clinical applications.

TRF1 is essential for the acquisition and maintenance of pluripotency

TRF1 is a well-established stem cell marker, since it is among the most upregulated genes associated with pluripotency (Boue et al., 2010; Ginis et al., 2004; Hosseinpour et al., 2013). The fact that we showed that higher levels of TRF1 in iPS cells correlated with higher levels of the stem cell marker NANOG and with a higher

degree of pluripotency (Schneider et al., 2013), encouraged us to study the role of TRF1 during reprogramming. On the one hand, *Trf1* deletion induces uncapping, fragility and a massive DNA damage response at telomeres, resulting in p53 and RB pathways activation and ensuing cell cycle arrest. In this way, *p53* deletion partially rescues the proliferative defects of *Trf1* deficiency (Martínez et al. 2009). On the other hand, the ectopic expression of the reprogramming factors OCT3/4, KLF4, SOX2 and cMYC triggers senescence or apoptosis by upregulating p53, $p16^{INK4a}$ and $p21^{CIP1}$ (Banito et al., 2009). Hence, these tumor suppressors have been defined as a barrier for reprogramming, as they prevent the reprogramming of cells presenting DNA damage in order to maintain genome stability. *p53* deletion results in an increase in the reprogramming efficiency and allows the reprogramming of cells with telomere damage, like G3 $Terc^{-/-}$ MEFs (Marion et al., 2009b). Thus, we tried to reprogram *Trf1* knockout MEFs in a *p53*-null background. However, *Trf1*-deficient MEFs completely failed to reprogram, even in the absence of *p53*. This is in contrast with what was shown before with another shelterin, TPP1. *Tpp1* knockout MEFs display telomeric aberrations similar to those of *Trf1* knockout MEFs, like multitelomeric signals and end-to-end fusions. Nevertheless, they are amenable to reprogram, although with lower efficiency than wild-type MEFs (Tejera et al., 2010).

Furthermore, conditional deletion of *Trf1* in already established iPS cells lead to rapid elimination of iPS colonies coincidental with increased DNA damage and apoptosis, demonstrating that protection from telomere damage by TRF1 is essential for the maintenance of pluripotency. IPS cells have been described to be highly sensitive to DNA damage (Momcilovic et al., 2010). It is known that pluripotent stem cells have higher levels of p53 than differentiated cells (Sabapathy et al., 1997), but the majority of it is located in the cytoplasm (Solozobova et al., 2009), suggesting that p53 regulation may differ between ES and somatic cells. Thus, it would be interesting to study whether the apoptosis seen after *Trf1* deletion in iPS cells is p53-dependent. Similar experiments were done in ES cells with a milder phenotype, as the majority of the conditional *Trf1*-deficient ES cells survived in culture. *Trf1*-deficient ES cells showed growth defects and chromosomal instability, with a moderate increase in the levels of apoptosis (Iwano et al., 2004). These differences could be due to more sensitivity to genome instability in iPS cells compared to ES cells, but also to the fact that they removed the 4-OHT after

two days, while we maintained the treatment. Moreover, it has been published that some of the phenotypes in *Trf1* knockout mouse ES cells can be partially rescued by the overexpression of other components of the shelterin complex (Okamoto et al., 2008). Further studies are needed to confirm this in iPS cells and during the reprogramming process.

Together, these results suggest that TRF1 is a key factor for reprogramming of differentiated cells into iPS cells as well as for the maintenance of pluripotency.

Trf1 overexpression during reprogramming has no effect in the reprogramming efficiency

The reprogramming process is a very slow and inefficient process and this is one of the main limitations for the clinical applications of iPS cells. In this regard, overexpression of factors that could positively affect reprogramming efficiency is a good strategy for the amelioration of the reprogramming technique.

In line with a role for TRF1 in stemness, it was previously described that TRF1 upregulation during the process of induction of pluripotency is uncoupled from net telomere elongation, as indicated by induction of TRF1 in iPS cells defective for the shelterin component TPP1, previously shown by us to fail to elongate telomeres during reprogramming (Schneider et al., 2013; Tejera et al., 2010). This notion suggests that TRF1 could also have functions independent from telomere maintenance during reprogramming. Based on this, we reprogrammed MEFs adding TRF1 to the three Yamanaka factors cocktail or with combinations of two of the factors. Strikingly, overexpression of *Trf1* during reprogramming had no effect in the reprogramming efficiency. Similarly, TRF1 was not able to replace any of the Yamanaka factors in the reprogramming cocktail. Thus, we conclude that even if TRF1 is essential for reprogramming and significantly upregulated during this process, its ectopic expression at the beginning of the reprogramming does not improve the efficiency of iPS cell generation.

Trf1 overexpression has been reported to have several adverse effects. TRF1 protein has been described as a negative regulator of telomere length, apparently regulating telomerase in cis without affecting its expression (Ancelin et al., 2002; Smogorzewska et al., 2000; van Steensel and de Lange, 1997). In addition, transgenic *K5-Trf1* mice which overexpress *Trf1* in the epithelial tissues, showing 2 to 4 more TRF1 density at telomeres, display shorter telomeres in the epidermis, indicating that TRF1 also acts as a negative regulator of telomere length in mice. Besides, *K5-Trf1* cells show increased end-to-end, chromosomal fusions, multitelomeric signals and increased telomere recombination, implying an impact of TRF1 overexpression on telomere integrity (Muñoz et al. 2009). Furthermore, TRF1 is a mediator of telomere associations in mammalian cells and its overexpression in mouse ES cells prevents proper telomere resolution during mitosis and results in telomere anaphase bridges.

As telomeres elongate during the reprogramming process, TRF1 could be essential for the correct capping and telomere replication. Nevertheless, it remains unclear which is the regulation and function of TRF1 in the absence of telomeric elongation during the reprogramming of *Tpp1*$^{\Delta/\Delta}$-Cre MEFs. Recently, it has been reported in telomerase immortalized human fibroblasts that at the initial phases of transformation both TRF1 and TRF2 proteins are in vast excess with respect to telomere length, pointing to a role of these proteins in tumorigenesis (Chiodi et al., 2013). It would be interesting to study if the density of TRF1 in these iPS cells is higher than in wild-type iPS cells and if this could affect the integrity of telomeres in these cells.

Tert and *Tpp1* overexpression during reprogramming

Wnt/ β-catenin pathway has a role in maintenance of ESCs both in humans and mice. β-catenin is constitutively phosphorylated by Glycogen synthase kinase-3 (GSK-3), inducing its ubiquitylation and degradation. However, the presence of Wnt3a leads to GSK-3 inhibition and activation of β-catenin. It has been reported that stimulation of the Wnt/ β-catenin pathway by the addition of the soluble factor Wnt3a to the medium enhances reprogramming (Marson et al., 2008). Besides, addition of GSK-3 inhibitors like CHIR has been demonstrated to sustain the pluripotent state of ESCs (Sato N,

2004) and to facilitate transition to naive pluripotency in partially reprogrammed (pre-iPS) cells (Theunissen et al., 2011). β-catenin overexpression, especially at the initial stages of reprogramming, also increases the efficiency of this process (Zhang et al., 2014). TERT directly modulates Wnt/β-catenin signalling by serving as a cofactor in a β-catenin transcriptional complex (Park et al., 2009). In this sense, *Tert* overexpression during reprogramming could positively modulate reprogramming efficiency by activation of β-catenin. As TPP1 is necessary for the recruitment of telomerase and the subsequent telomere elongation during the formation of iPS cells (Tejera et al., 2010), its overexpression could also influence the process of reprogramming. Strikingly, we showed that overexpression of *Tert*, *Tpp1* or the combination of both during reprogramming did not have any effect in the reprogramming efficiency.

C-MYC is a well described trancriptional activator of *Tert* (Flores et al., 2006) Surprisingly, we showed a higher increase in *Tert* expression in MEFs reprogrammed with 3F than with 4F. We have to take into account that MEFs infected with 4F reprogram much faster than 3F MEFs. Besides, addition of c-MYC to the reprogramming cocktail induces a lot of cell death at the beginning, which could explain the differences. On top of that, a recent publication described for the first time dual roles of c-MYC in the regulation of human telomerase, as they showed activation of *hTERT* promoter upon c-MYC/MAX downregulation. Thus, they concluded that c-MYC/Max is involved not only in activating *hTERT* transcription but also in maintaining the repressive states of *hTERT* promoter in somatic cells (Zhao et al., 2014). It would be interesting to study if this phenomenon is reproduced in mice.

As we said before, TERT has extra-telomeric functions, some of them dependent on the formation of the TERT/*Terc* complex. For instance, the telomere length-independent positive effects shown in growth upon *Tert* overexpression in MEFs are dependent of the formation of the TERT/*Terc* complex (Geserick et al., 2006). *Terc* is also required for the tumor-promoting effects of *Tert* overexpression in K5-*Tert* mice. Furthermore, increased expression of *Tert* in a T*erc*$^{-/-}$ context has inhibitory effects, independently of telomere length or telomerase activity (Cayuela et al., 2005). *Tert* expression has been described to be the limiting factor for telomere maintenance in studies done in ES cells (Liu et al., 2000). In contrast, another group published that it

was *Terc* and not *Tert* what limits telomere elongation during embryonic and early postnatal *in vivo* development (Chiang et al., 2004). In this sense, it is possible that *Terc* overexpression combined with *Tert* overexpression during reprogramming had a positive effect in reprogramming efficiency.

As we said before, *Tert*$^{-/-}$ cells were reprogrammed with lower efficiency than wild-type cells even if they had similar telomere length, suggesting that TERT has extra-telomeric functions during reprogramming (Kinoshita et al., 2014). Nevertheless, these experiments were done in TTFs, which have been described to follow different dynamics in the overexpression of telomerase components during reprogramming (Zuo et al., 2012). In this paper, they overexpressed *Tert* in *Terc*$^{-/-}$ TTFs, but they did not report anything about the effect of *Tert* overexpression in wild-type TTFs. It would be interesting to study if *Tert* overexpression has the same effect on TTFs than in MEFs in reprogramming efficiency.

In contrast to what we show in MEFs, *TERT* overexpression in human keratinocyte cell lines leads to an increase in reprogramming efficiency (Utikal et al., 2009). TERT induces immortalization in human cells. Thus, the long-term proliferative potential and not higher growth rates is what leads to an enhancement of the reprogramming ability in these cells. In mice *Tert* overexpression alone does not lead to immortalization of MEFs. Nevertheless, it facilitates their spontaneous immortalization and increases their colony-forming capacity upon activation of oncogenes (Geserick et al., 2006). It would be interesting to overexpress *Tert* in senescent MEFs at higher passages.

The long and stable telomeres of pluripotent cells might be an additional mechanism to protect chromosome integrity. *Tert* overexpression confers greater resistance to oxidative stress in mouse ES cells (Armstrong et al., 2005). Since iPS cells are very sensitive to DNA damage compared to somatic cells, *Tert* overexpression could be determinant for the maintenance of genomic stability in IPS cells. Further studies in iPS cells obtained from MEFs overexpressing *Tert* during reprogramming are needed to analyze their genomic stability and differentiation potential.

Shelterin and telomerase dynamics during reprogramming

Regarding telomerase components, we showed a marked increased in *Terc* at the end of reprogramming, which is maintained in established iPS cells. *Terc* promoter is regulated by OCT3/4 and NANOG in pluripotent cells (Agarwal et al., 2010). In this sense, the increase seen in *Terc* could be explained by OCT3/4 acting in a second wave at the end of reprogramming, as described by Polo and colleagues Overexpression of *Tert* was seen at the beginning of reprogramming, coincidental with c-MYC and KLF4, known activators of *Tert* transcription, acting in the first wave during reprogramming (Polo et al., 2012). Nevertheless, *Tert* levels decreased at the end of reprogramming, showing a similar expression in MEFs and iPS cells. There has been controversy in relation with *Tert* expression during reprogramming. While TERT upregulation was described to be a late event in the reprogramming process (Stadtfeld et al., 2008a), other publications have shown an early activation of this gene (Wang et al., 2012; Zuo et al., 2012). In this way, both telomere length and telomerase activity have been described to show high heterogeneity among the different iPS clones. Besides, telomerase activity is not only dependent on *Tert* and *Terc* expression, but also on other factors like recruitment to telomeres, localization in Cajal bodies or interaction with DKC1, which is also increased in human iPS cells (Batista et al., 2011; Mah et al., 2011).

With respect to shelterins, we showed a slight increased in all the shelterins at the beginning of reprogramming. As they have essential roles in telomere protection, elongation, DDR inhibition and replication, it makes sense that they also increased during the process of reprogramming. Nevertheless, most of them come back to initial levels in iPS cells. This suggests that shelterins could also suffer post-transcriptional regulation in the process of reprogramming. TRF1 and POT1A are the only shelterins that appeared to show higher expression in IPS cells. In a paper from 2012, they reported a map of OCT3/4, SOX2, KLF4 and c-MYC on the human genome during the first 48 hours of fibroblasts reprogramming by ChIP-seq (Soufi et al., 2012). In another work done in mouse, they carried out genome-wide analysis of the binding of the four transcription factors in ES cells, iPS cells and partially reprogrammed iPS cells (Sridharan et al., 2009). In order to set light into the regulation of shelterins and

telomerase, we studied the binding of the reprogramming factors to these proteins promoters in these data (**Table 10-11**).

Table 10: Chromatin ocuppancy within 20 kb upstream TSS and gene body (peaks called with MACS at 0.005 FDR, * peaks within the OCT3/4, SOX2, KLF4 and c-MYC coding regions were not considered). +: bound; -= not bound (Adapted from Soufi et al., 2012).

Gene	Occupancy of O, S, K and M at 48 hr			
	O	**S**	**K**	**M**
TRF1	+	+	+	-
TRF2	-	+	-	+
TPP1	-	-	-	-
POT1	-	-	-	-
RAP1	+	+	+	+
TERT	-	-	-	-
DKC1	-	-	-	-

Table 11: Average binding data of O, S, K and M to the promoters of shelterins and telomerase in ES, iPS and pre-iPS cells += bound; -= not bound. Adapted from (Sridharan et al., 2009).

Gene	Occupancy of O, S, K and M											
	ES cells				iPS cells				pre-iPS cells			
	O	**S**	**K**	**M**	**O**	**S**	**K**	**M**	**O**	**S**	**K**	**M**
Trf1	-	-	-	-	-	-	-	-	-	-	-	-
Trf2	-	+	-	+	-	-	-	-	-	-	-	+
Tpp1	-	-	-	-	-	-	-	-	-	-	-	-
Pot1a	-	-	-	+	-	-	-	+	-	-	-	+
Rap1	-	-	-	-	-	-	-	-	-	-	-	-
Tin2	-	-	-	-	-	-	-	-	-	-	-	-
Tert	-	-	-	+	-	-	-	-	-	-	-	-
Dkc1	-	-	-	+	-	-	-	+	-	-	-	+

Surprisingly, they did not see binding of OCT3/4 to the *Trf1* promoter in ES and iPS cells (**Table 11**). This is in controversy with what we previously showed (Schneider et al.) 2013), indicating that these data need to be validated. Nevertheless, we showed binding of c-MYC to *Pot1a* promoter in ES, iPS and pre-iPS cells and of SOX2 and c-MYC to *Trf2* promoter in ES cells. Validation of these data by ChIP would give us information about the regulation of these shelterins during reprogramming.

Conclusions

1. The component of the shelterin complex TRF1 show restricted binding to telomeres *in vivo* in MEFs, both in normal conditions and in a context of telomere shortening.

2. TRF1 protein is essential for the process of nuclear reprogramming to iPS cells and for the maintenance of already established iPS cells and its downregulation decreases dramatically the efficiency of reprogramming.

3. Even if it is considered as a stem cell marker and highly overexpressed in iPS cells, ectopic expression of TRF1 in the cocktail of reprogramming does not modulate reprogramming efficiency.

4. TRF1 is not able to replace any of the three Yamanaka factors during reprogramming.

5. *Tert* overexpression alone or in combination with *Tpp1*, the shelterin that facilitates its recruitment to telomeres, does not enhance reprogramming efficiency in MEFs.

6. During reprogramming, there is a slight transcriptional upregulation of all the components of the shelterin complex, concomitant with an upregulation of the components of telomerase, *Tert* and *Terc*.

Conclusiones

1. El componente del complejo shelterina TRF1 se une exclusivamente a telómeros in vivo en MEFs, tanto en condiciones normales como en un contexto de acortamiento telomérico.

2. La proteína TRF1 es esencial para la adquisición y mantenimiento de la pluripotencia y una disminución en su expresión reduce dramáticamente la eficiencia de reprogramación

3. Aunque esté considerado como un marcador de células madre altamente sobreexpresado en células iPS, la sobreexpresión de *Trf1* en el cocktail de reprogramación no aumenta la eficiencia de reprogramación.

4. TRF1 no es capaz de reemplazar a ninguno de los factores de "Yamanaka" durante la reprogramación.

5. La sobreexpresión de *Tert*, sólo o en combinación con *Tpp1*, la shelterina que facilita el reclutamiento de la telomerasa al telómero, no aumenta la eficiencia de reprogramación en MEFs.

6. Durante la reprogramación, hay un ligero aumento transcripcional de todos los componentes del complejo *shelterin*, coincidente con un aumento de los componentes de la telomerasa, *Tert* y *Terc*.

References

Abad, M., Mosteiro, L., Pantoja, C., Canamero, M., Rayon, T., Ors, I., Grana, O., Megias, D., Dominguez, O., Martinez, D., *et al.* (2013). Reprogramming in vivo produces teratomas and iPS cells with totipotency features. Nature *502*, 340-345.

Agarwal, S., Loh, Y.H., McLoughlin, E.M., Huang, J., Park, I.H., Miller, J.D., Huo, H., Okuka, M., Dos Reis, R.M., Loewer, S., *et al.* (2010). Telomere elongation in induced pluripotent stem cells from dyskeratosis congenita patients. Nature *464*, 292-296.

Allsopp, R.C., Morin, G.B., DePinho, R., Harley, C.B., and Weissman, I.L. (2003). Telomerase is required to slow telomere shortening and extend replicative lifespan of HSCs during serial transplantation. Blood *102*, 517-520.

Amabile, G., and Meissner, A. (2009). Induced pluripotent stem cells: current progress and potential for regenerative medicine. Trends Mol Med *15*, 59-68.

Ancelin, K., Brunori, M., Bauwens, S., Koering, C.E., Brun, C., Ricoul, M., Pommier, J.P., Sabatier, L., and Gilson, E. (2002). Targeting assay to study the cis functions of human telomeric proteins: evidence for inhibition of telomerase by TRF1 and for activation of telomere degradation by TRF2. Mol Cell Biol *22*, 3474-3487.

Anokye-Danso, F., Trivedi, C.M., Juhr, D., Gupta, M., Cui, Z., Tian, Y., Zhang, Y., Yang, W., Gruber, P.J., Epstein, J.A., *et al.* (2012). Highly efficient miRNA-mediated reprogramming of mouse and human somatic cells to pluripotency. Cell Stem Cell *8*, 376-388.

Armanios, M., and Blackburn, E.H. (2012). The telomere syndromes. Nat Rev Genet *13*, 693-704.

Armanios, M.Y., Chen, J.J., Cogan, J.D., Alder, J.K., Ingersoll, R.G., Markin, C., Lawson, W.E., Xie, M., Vulto, I., Phillips, J.A., 3rd, *et al.* (2007). Telomerase mutations in families with idiopathic pulmonary fibrosis. N Engl J Med *356*, 1317-1326.

Armstrong, L., Saretzki, G., Peters, H., Wappler, I., Evans, J., Hole, N., von Zglinicki, T., and Lako, M. (2005). Overexpression of telomerase confers growth advantage, stress resistance, and enhanced differentiation of ESCs toward the hematopoietic lineage. Stem Cells *23*, 516-529.

Artandi, S.E., Chang, S., Lee, S.L., Alson, S., Gottlieb, G.J., Chin, L., and DePinho, R.A. (2000). Telomere dysfunction promotes non-reciprocal translocations and epithelial cancers in mice. Nature *406*, 641-645.

Banito, A., Rashid, S.T., Acosta, J.C., Li, S., Pereira, C.F., Geti, I., Pinho, S., Silva, J.C., Azuara, V., Walsh, M., *et al.* (2009). Senescence impairs successful reprogramming to pluripotent stem cells. Genes Dev *23*, 2134-2139.

Batista, L.F., Pech, M.F., Zhong, F.L., Nguyen, H.N., Xie, K.T., Zaug, A.J., Crary, S.M., Choi, J., Sebastiano, V., Cherry, A., *et al.* (2011). Telomere shortening and

loss of self-renewal in dyskeratosis congenita induced pluripotent stem cells. Nature *474*, 399-402.

Baumann, P., and Cech, T.R. (2001). Pot1, the putative telomere end-binding protein in fission yeast and humans. Science *292*, 1171-1175.

Becker, K.A., Ghule, P.N., Therrien, J.A., Lian, J.B., Stein, J.L., van Wijnen, A.J., and Stein, G.S. (2006). Self-renewal of human embryonic stem cells is supported by a shortened G1 cell cycle phase. J Cell Physiol *209*, 883-893.

Benetti, R., Garcia-Cao, M., and Blasco, M.A. (2007). Telomere length regulates the epigenetic status of mammalian telomeres and subtelomeres. Nat Genet *39*, 243-250.

Bernardes de Jesus, B., Vera, E., Schneeberger, K., Tejera, A.M., Ayuso, E., Bosch, F., and Blasco, M.A. (2012). Telomerase gene therapy in adult and old mice delays aging and increases longevity without increasing cancer. EMBO Mol Med *4*, 691-704.

Bianchi, A., Smith, S., Chong, L., Elias, P., and de Lange, T. (1997). TRF1 is a dimer and bends telomeric DNA. EMBO J *16*, 1785-1794.

Blackburn, E.H. (2001). Switching and signaling at the telomere. Cell *106*, 661-673.

Blasco, M.A. (2005). Telomeres and human disease: ageing, cancer and beyond. Nat Rev Genet *6*, 611-622.

Blasco, M.A. (2007). Telomere length, stem cells and aging. Nat Chem Biol *3*, 640-649.

Blasco, M.A., Funk, W., Villeponteau, B., and Greider, C.W. (1995). Functional characterization and developmental regulation of mouse telomerase RNA. Science *269*, 1267-1270.

Blasco, M.A., Lee, H.W., Hande, M.P., Samper, E., Lansdorp, P.M., DePinho, R.A., and Greider, C.W. (1997). Telomere shortening and tumor formation by mouse cells lacking telomerase RNA. Cell *91*, 25-34.

Bodnar, A.G., Ouellette, M., Frolkis, M., Holt, S.E., Chiu, C.P., Morin, G.B., Harley, C.B., Shay, J.W., Lichtsteiner, S., and Wright, W.E. (1998). Extension of life-span by introduction of telomerase into normal human cells. Science *279*, 349-352.

Bosco, N., and de Lange, T. (2012). A TRF1-controlled common fragile site containing interstitial telomeric sequences. Chromosoma *121*, 465-474.

Boue, S., Paramonov, I., Barrero, M.J., and Izpisua Belmonte, J.C. (2010). Analysis of human and mouse reprogramming of somatic cells to induced pluripotent stem cells. What is in the plate? PLoS One *5*.

Brambrink, T., Foreman, R., Welstead, G.G., Lengner, C.J., Wernig, M., Suh, H., and Jaenisch, R. (2008). Sequential expression of pluripotency markers during direct reprogramming of mouse somatic cells. Cell Stem Cell *2*, 151-159.

Broccoli, D., Smogorzewska, A., Chong, L., and de Lange, T. (1997). Human telomeres contain two distinct Myb-related proteins, TRF1 and TRF2. Nat Genet *17*, 231-235.

Buchman, A.R., Lue, N.F., and Kornberg, R.D. (1988). Connections between transcriptional activators, silencers, and telomeres as revealed by functional analysis of a yeast DNA-binding protein. Mol Cell Biol *8*, 5086-5099.

Buganim, Y., Faddah, D.A., Cheng, A.W., Itskovich, E., Markoulaki, S., Ganz, K., Klemm, S.L., van Oudenaarden, A., and Jaenisch, R. (2012). Single-cell expression analyses during cellular reprogramming reveal an early stochastic and a late hierarchic phase. Cell *150*, 1209-1222.

Capieaux, E., Vignais, M.L., Sentenac, A., and Goffeau, A. (1989). The yeast H+-ATPase gene is controlled by the promoter binding factor TUF. J Biol Chem *264*, 7437-7446.

Cayuela, M.L., Flores, J.M., and Blasco, M.A. (2005). The telomerase RNA component Terc is required for the tumour-promoting effects of Tert overexpression. EMBO Rep *6*, 268-274.

Celli, G.B., and de Lange, T. (2005). DNA processing is not required for ATM-mediated telomere damage response after TRF2 deletion. Nat Cell Biol *7*, 712-718.

Cifuentes-Rojas, C., and Shippen, D.E. (2012). Telomerase regulation. Mutat Res *730*, 20-27.

Collins, K., and Mitchell, J.R. (2002). Telomerase in the human organism. Oncogene *21*, 564-579.

Cook, B.D., Dynek, J.N., Chang, W., Shostak, G., and Smith, S. (2002). Role for the related poly(ADP-Ribose) polymerases tankyrase 1 and 2 at human telomeres. Mol Cell Biol *22*, 332-342.

Cooper, J.P., Nimmo, E.R., Allshire, R.C., and Cech, T.R. (1997). Regulation of telomere length and function by a Myb-domain protein in fission yeast. Nature *385*, 744-747.

Court, R., Chapman, L., Fairall, L., and Rhodes, D. (2005). How the human telomeric proteins TRF1 and TRF2 recognize telomeric DNA: a view from high-resolution crystal structures. EMBO Rep *6*, 39-45.

Chan, S.W., and Blackburn, E.H. (2002). New ways not to make ends meet: telomerase, DNA damage proteins and heterochromatin. Oncogene *21*, 553-563.

Chang, W., Dynek, J.N., and Smith, S. (2003). TRF1 is degraded by ubiquitin-mediated proteolysis after release from telomeres. Genes Dev *17*, 1328-1333.

Chen, Y., Yang, Y., van Overbeek, M., Donigian, J.R., Baciu, P., de Lange, T., and Lei, M. (2008). A shared docking motif in TRF1 and TRF2 used for differential recruitment of telomeric proteins. Science *319*, 1092-1096.

Chiang, Y.J., Hemann, M.T., Hathcock, K.S., Tessarollo, L., Feigenbaum, L., Hahn, W.C., and Hodes, R.J. (2004). Expression of telomerase RNA template, but not telomerase reverse transcriptase, is limiting for telomere length maintenance in vivo. Mol Cell Biol *24*, 7024-7031.

Chiodi, I., Belgiovine, C., Zongaro, S., Ricotti, R., Horard, B., Lossani, A., Focher, F., Gilson, E., Giulotto, E., and Mondello, C. (2013). Super-telomeres in transformed human fibroblasts. Biochim Biophys Acta *1833*, 1885-1893.

d'Adda di Fagagna, F., Hande, M.P., Tong, W.M., Roth, D., Lansdorp, P.M., Wang, Z.Q., and Jackson, S.P. (2001). Effects of DNA nonhomologous end-joining factors on telomere length and chromosomal stability in mammalian cells. Curr Biol *11*, 1192-1196.

d'Adda di Fagagna, F., Reaper, P.M., Clay-Farrace, L., Fiegler, H., Carr, P., Von Zglinicki, T., Saretzki, G., Carter, N.P., and Jackson, S.P. (2003). A DNA damage checkpoint response in telomere-initiated senescence. Nature *426*, 194-198.

d'Alcontres, M.S., Palacios, J.A., Mejias, D., and Blasco, M.A. (2014). TopoIIalpha prevents telomere fragility and formation of ultra thin DNA bridges during mitosis through TRF1-dependent binding to telomeres. Cell Cycle *13*, 1463-1481.

Daniel, M., Peek, G.W., and Tollefsbol, T.O. (2012). Regulation of the human catalytic subunit of telomerase (hTERT). Gene *498*, 135-146.

Dantzer, F., Giraud-Panis, M.J., Jaco, I., Ame, J.C., Schultz, I., Blasco, M., Koering, C.E., Gilson, E., Menissier-de Murcia, J., de Murcia, G., *et al.* (2004). Functional interaction between poly(ADP-Ribose) polymerase 2 (PARP-2) and TRF2: PARP activity negatively regulates TRF2. Mol Cell Biol *24*, 1595-1607.

Day, J.P., Limoli, C.L., and Morgan, W.F. (1998). Recombination involving interstitial telomere repeat-like sequences promotes chromosomal instability in Chinese hamster cells. Carcinogenesis *19*, 259-265.

de Lange, T. (2005). Shelterin: the protein complex that shapes and safeguards human telomeres. Genes Dev *19*, 2100-2110.

de Lange, T. (2009). How telomeres solve the end-protection problem. Science *326*, 948-952.

de Lange, T., and DePinho, R.A. (1999). Unlimited mileage from telomerase? Science *283*, 947-949.

Denchi, E.L. (2009). Give me a break: how telomeres suppress the DNA damage response. DNA Repair (Amst) *8*, 1118-1126.

Diotti, R., and Loayza, D. (2011). Shelterin complex and associated factors at human telomeres. Nucleus *2*, 119-135.

Dokal, I. (2000). Dyskeratosis congenita in all its forms. Br J Haematol *110*, 768-779.

Donate, L.E., and Blasco, M.A. (2011). Telomeres in cancer and ageing. Philos Trans R Soc Lond B Biol Sci *366*, 76-84.

Donigian, J.R., and de Lange, T. (2007). The role of the poly(ADP-ribose) polymerase tankyrase1 in telomere length control by the TRF1 component of the shelterin complex. J Biol Chem *282*, 22662-22667.

Drissi, R., Zindy, F., Roussel, M.F., and Cleveland, J.L. (2001). c-Myc-mediated regulation of telomerase activity is disabled in immortalized cells. J Biol Chem *276*, 29994-30001.

Dunham, M.A., Neumann, A.A., Fasching, C.L., and Reddel, R.R. (2000). Telomere maintenance by recombination in human cells. Nat Genet *26*, 447-450.

Dynek, J.N., and Smith, S. (2004). Resolution of sister telomere association is required for progression through mitosis. Science *304*, 97-100.

Evans, M.J., and Kaufman, M.H. (1981). Establishment in culture of pluripotential cells from mouse embryos. Nature *292*, 154-156.

Fairall, L., Chapman, L., Moss, H., de Lange, T., and Rhodes, D. (2001). Structure of the TRFH dimerization domain of the human telomeric proteins TRF1 and TRF2. Mol Cell *8*, 351-361.

Feng, J., Liu, T., Qin, B., Zhang, Y., and Liu, X.S. (2012). Identifying ChIP-seq enrichment using MACS. Nat Protoc *7*, 1728-1740.

Flores, I., Canela, A., Vera, E., Tejera, A., Cotsarelis, G., and Blasco, M.A. (2008). The longest telomeres: a general signature of adult stem cell compartments. Genes Dev *22*, 654-667.

Flores, I., Evan, G., and Blasco, M.A. (2006). Genetic analysis of myc and telomerase interactions in vivo. Mol Cell Biol *26*, 6130-6138.

Forsyth, N.R., Wright, W.E., and Shay, J.W. (2002). Telomerase and differentiation in multicellular organisms: turn it off, turn it on, and turn it off again. Differentiation *69*, 188-197.

Franco, S., Alsheimer, M., Herrera, E., Benavente, R., and Blasco, M.A. (2002). Mammalian meiotic telomeres: composition and ultrastructure in telomerase-deficient mice. Eur J Cell Biol *81*, 335-340.

Garcia-Cao, M., O'Sullivan, R., Peters, A.H., Jenuwein, T., and Blasco, M.A. (2004). Epigenetic regulation of telomere length in mammalian cells by the Suv39h1 and Suv39h2 histone methyltransferases. Nat Genet *36*, 94-99.

Geserick, C., Tejera, A., Gonzalez-Suarez, E., Klatt, P., and Blasco, M.A. (2006). Expression of mTert in primary murine cells links the growth-promoting effects of telomerase to transforming growth factor-beta signaling. Oncogene *25*, 4310-4319.

Giachino, C., Orlando, L., and Turinetto, V. (2013). Maintenance of genomic stability in mouse embryonic stem cells: relevance in aging and disease. Int J Mol Sci *14*, 2617-2636.

Ginis, I., Luo, Y., Miura, T., Thies, S., Brandenberger, R., Gerecht-Nir, S., Amit, M., Hoke, A., Carpenter, M.K., Itskovitz-Eldor, J., *et al.* (2004). Differences between human and mouse embryonic stem cells. Dev Biol *269*, 360-380.

Gonzalez-Suarez, E., Flores, J.M., and Blasco, M.A. (2002). Cooperation between p53 mutation and high telomerase transgenic expression in spontaneous cancer development. Mol Cell Biol *22*, 7291-7301.

Gonzalez-Suarez, E., Samper, E., Ramirez, A., Flores, J.M., Martin-Caballero, J., Jorcano, J.L., and Blasco, M.A. (2001). Increased epidermal tumors and increased skin wound healing in transgenic mice overexpressing the catalytic subunit of telomerase, mTERT, in basal keratinocytes. EMBO J *20*, 2619-2630.

Greenberg, R.A., Allsopp, R.C., Chin, L., Morin, G.B., and DePinho, R.A. (1998). Expression of mouse telomerase reverse transcriptase during development, differentiation and proliferation. Oncogene *16*, 1723-1730.

Greenberg, R.A., O'Hagan, R.C., Deng, H., Xiao, Q., Hann, S.R., Adams, R.R., Lichtsteiner, S., Chin, L., Morin, G.B., and DePinho, R.A. (1999). Telomerase reverse transcriptase gene is a direct target of c-Myc but is not functionally equivalent in cellular transformation. Oncogene *18*, 1219-1226.

Greider, C.W., and Blackburn, E.H. (1985). Identification of a specific telomere terminal transferase activity in Tetrahymena extracts. Cell *43*, 405-413.

Griffith, J.D., Comeau, L., Rosenfield, S., Stansel, R.M., Bianchi, A., Moss, H., and de Lange, T. (1999). Mammalian telomeres end in a large duplex loop. Cell *97*, 503-514.

Guerra, C., Mijimolle, N., Dhawahir, A., Dubus, P., Barradas, M., Serrano, M., Campuzano, V., and Barbacid, M. (2003). Tumor induction by an endogenous K-ras oncogene is highly dependent on cellular context. Cancer Cell *4*, 111-120.

Gurdon, J.B., and Melton, D.A. (2008). Nuclear reprogramming in cells. Science *322*, 1811-1815.

Hanahan, D., and Weinberg, R.A. (2000). The hallmarks of cancer. Cell *100*, 57-70.

Hanahan, D., and Weinberg, R.A. (2011). Hallmarks of cancer: the next generation. Cell *144*, 646-674.

Hanaoka, S., Nagadoi, A., and Nishimura, Y. (2005). Comparison between TRF2 and TRF1 of their telomeric DNA-bound structures and DNA-binding activities. Protein Sci *14*, 119-130.

Hansson, J., Rafiee, M.R., Reiland, S., Polo, J.M., Gehring, J., Okawa, S., Huber, W., Hochedlinger, K., and Krijgsveld, J. (2012). Highly coordinated proteome

dynamics during reprogramming of somatic cells to pluripotency. Cell Rep *2*, 1579-1592.

Hayflick, L. (1965). The Limited in Vitro Lifetime of Human Diploid Cell Strains. Exp Cell Res *37*, 614-636.

Henson, J.D., Neumann, A.A., Yeager, T.R., and Reddel, R.R. (2002). Alternative lengthening of telomeres in mammalian cells. Oncogene *21*, 598-610.

Herrera, E., Samper, E., and Blasco, M.A. (1999a). Telomere shortening in mTR-/- embryos is associated with failure to close the neural tube. EMBO J *18*, 1172-1181.

Herrera, E., Samper, E., Martin-Caballero, J., Flores, J.M., Lee, H.W., and Blasco, M.A. (1999b). Disease states associated with telomerase deficiency appear earlier in mice with short telomeres. EMBO J *18*, 2950-2960.

Hiyama, E., and Hiyama, K. (2002). Clinical utility of telomerase in cancer. Oncogene *21*, 643-649.

Hockemeyer, D., Daniels, J.P., Takai, H., and de Lange, T. (2006). Recent expansion of the telomeric complex in rodents: Two distinct POT1 proteins protect mouse telomeres. Cell *126*, 63-77.

Hochedlinger, K., and Plath, K. (2009). Epigenetic reprogramming and induced pluripotency. Development *136*, 509-523.

Hoffmeyer, K., Raggioli, A., Rudloff, S., Anton, R., Hierholzer, A., Del Valle, I., Hein, K., Vogt, R., and Kemler, R. (2012). Wnt/beta-catenin signaling regulates telomerase in stem cells and cancer cells. Science *336*, 1549-1554.

Hong, H., Takahashi, K., Ichisaka, T., Aoi, T., Kanagawa, O., Nakagawa, M., Okita, K., and Yamanaka, S. (2009). Suppression of induced pluripotent stem cell generation by the p53-p21 pathway. Nature *460*, 1132-1135.

Hosseinpour, B., Bakhtiarizadeh, M.R., Khosravi, P., and Ebrahimie, E. (2013). Predicting distinct organization of transcription factor binding sites on the promoter regions: a new genome-based approach to expand human embryonic stem cell regulatory network. Gene *531*, 212-219.

Hou, P., Li, Y., Zhang, X., Liu, C., Guan, J., Li, H., Zhao, T., Ye, J., Yang, W., Liu, K., *et al.* (2013). Pluripotent stem cells induced from mouse somatic cells by small-molecule compounds. Science *341*, 651-654.

Huang, J., Wang, F., Okuka, M., Liu, N., Ji, G., Ye, X., Zuo, B., Li, M., Liang, P., Ge, W.W., *et al.* (2011). Association of telomere length with authentic pluripotency of ES/iPS cells. Cell Res *21*, 779-792.

Huang, Y., Liang, P., Liu, D., Huang, J., and Songyang, Z. (2014). Telomere regulation in pluripotent stem cells. Protein Cell *5*, 194-202.

Iwano, T., Tachibana, M., Reth, M., and Shinkai, Y. (2004). Importance of TRF1 for functional telomere structure. J Biol Chem *279*, 1442-1448.

Jaskelioff, M., Muller, F.L., Paik, J.H., Thomas, E., Jiang, S., Adams, A.C., Sahin, E., Kost-Alimova, M., Protopopov, A., Cadinanos, J., *et al.* (2011). Telomerase reactivation reverses tissue degeneration in aged telomerase-deficient mice. Nature *469*, 102-106.

Kaji, K., Norrby, K., Paca, A., Mileikovsky, M., Mohseni, P., and Woltjen, K. (2009). Virus-free induction of pluripotency and subsequent excision of reprogramming factors. Nature *458*, 771-775.

Kang, L., Wang, J., Zhang, Y., Kou, Z., and Gao, S. (2009). iPS cells can support full-term development of tetraploid blastocyst-complemented embryos. Cell Stem Cell *5*, 135-138.

Kanoh, J., and Ishikawa, F. (2001). spRap1 and spRif1, recruited to telomeres by Taz1, are essential for telomere function in fission yeast. Curr Biol *11*, 1624-1630.

Karlseder, J., Kachatrian, L., Takai, H., Mercer, K., Hingorani, S., Jacks, T., and de Lange, T. (2003). Targeted deletion reveals an essential function for the telomere length regulator Trf1. Mol Cell Biol *23*, 6533-6541.

Kawamura, T., Suzuki, J., Wang, Y.V., Menendez, S., Morera, L.B., Raya, A., Wahl, G.M., and Izpisua Belmonte, J.C. (2009). Linking the p53 tumour suppressor pathway to somatic cell reprogramming. Nature *460*, 1140-1144.

Kim, S.H., Beausejour, C., Davalos, A.R., Kaminker, P., Heo, S.J., and Campisi, J. (2004). TIN2 mediates functions of TRF2 at human telomeres. J Biol Chem *279*, 43799-43804.

Kinoshita, T., Nagamatsu, G., Saito, S., Takubo, K., Horimoto, K., and Suda, T. (2014). Telomerase reverse transcriptase has an extratelomeric function in somatic cell reprogramming. J Biol Chem *289*, 15776-15787.

Kovalenko, O.A., Kaplunov, J., Herbig, U., Detoledo, S., Azzam, E.I., and Santos, J.H. (2010). Expression of (NES-)hTERT in cancer cells delays cell cycle progression and increases sensitivity to genotoxic stress. PLoS One *5*, e10812.

Krutilina, R.I., Oei, S., Buchlow, G., Yau, P.M., Zalensky, A.O., Zalenskaya, I.A., Bradbury, E.M., and Tomilin, N.V. (2001). A negative regulator of telomere-length protein trf1 is associated with interstitial (TTAGGG)n blocks in immortal Chinese hamster ovary cells. Biochem Biophys Res Commun *280*, 471-475.

Krutilina, R.I., Smirnova, A.N., Mudrak, O.S., Pleskach, N.M., Svetlova, M.P., Oei, S.L., Yau, P.M., Bradbury, E.M., Zalensky, A.O., and Tomilin, N.V. (2003). Protection of internal (TTAGGG)n repeats in Chinese hamster cells by telomeric protein TRF1. Oncogene *22*, 6690-6698.

Lee, H.W., Blasco, M.A., Gottlieb, G.J., Horner, J.W., 2nd, Greider, C.W., and DePinho, R.A. (1998). Essential role of mouse telomerase in highly proliferative organs. Nature *392*, 569-574.

Lei, M., Podell, E.R., and Cech, T.R. (2004). Structure of human POT1 bound to telomeric single-stranded DNA provides a model for chromosome end-protection. Nat Struct Mol Biol *11*, 1223-1229.

Li, B., and de Lange, T. (2003). Rap1 affects the length and heterogeneity of human telomeres. Mol Biol Cell *14*, 5060-5068.

Li, H., Cao, Y., Berndt, M.C., Funder, J.W., and Liu, J.P. (1999). Molecular interactions between telomerase and the tumor suppressor protein p53 in vitro. Oncogene *18*, 6785-6794.

Li, H., Collado, M., Villasante, A., Strati, K., Ortega, S., Canamero, M., Blasco, M.A., and Serrano, M. (2009). The Ink4/Arf locus is a barrier for iPS cell reprogramming. Nature *460*, 1136-1139.

Li, W., Tian, E., Chen, Z.X., Sun, G., Ye, P., Yang, S., Lu, D., Xie, J., Ho, T.V., Tsark, W.M., *et al.* (2012). Identification of Oct4-activating compounds that enhance reprogramming efficiency. Proc Natl Acad Sci U S A *109*, 20853-20858.

Li, Y., Zhang, Q., Yin, X., Yang, W., Du, Y., Hou, P., Ge, J., Liu, C., Zhang, W., Zhang, X., *et al.* (2011). Generation of iPSCs from mouse fibroblasts with a single gene, Oct4, and small molecules. Cell Res *21*, 196-204.

Lin, J., Countryman, P., Buncher, N., Kaur, P., E, L., Zhang, Y., Gibson, G., You, C., Watkins, S.C., Piehler, J., *et al.* (2014). TRF1 and TRF2 use different mechanisms to find telomeric DNA but share a novel mechanism to search for protein partners at telomeres. Nucleic Acids Res *42*, 2493-2504.

Lipps, H.J., and Rhodes, D. (2009). G-quadruplex structures: in vivo evidence and function. Trends Cell Biol *19*, 414-422.

Lisaingo, K., Uringa, E.J., and Lansdorp, P.M. (2014). Resolution of telomere associations by TRF1 cleavage in mouse embryonic stem cells. Mol Biol Cell *25*, 1958-1968.

Liu, D., Safari, A., O'Connor, M.S., Chan, D.W., Laegeler, A., Qin, J., and Songyang, Z. (2004). PTOP interacts with POT1 and regulates its localization to telomeres. Nat Cell Biol *6*, 673-680.

Liu, L., Bailey, S.M., Okuka, M., Munoz, P., Li, C., Zhou, L., Wu, C., Czerwiec, E., Sandler, L., Seyfang, A., *et al.* (2007). Telomere lengthening early in development. Nat Cell Biol *9*, 1436-1441.

Liu, Y., Snow, B.E., Hande, M.P., Yeung, D., Erdmann, N.J., Wakeham, A., Itie, A., Siderovski, D.P., Lansdorp, P.M., Robinson, M.O., *et al.* (2000). The telomerase reverse transcriptase is limiting and necessary for telomerase function in vivo. Curr Biol *10*, 1459-1462.

Loayza, D., and De Lange, T. (2003). POT1 as a terminal transducer of TRF1 telomere length control. Nature *423*, 1013-1018.

Loayza, D., Parsons, H., Donigian, J., Hoke, K., and de Lange, T. (2004). DNA binding features of human POT1: a nonamer 5'-TAGGGTTAG-3' minimal binding site, sequence specificity, and internal binding to multimeric sites. J Biol Chem *279*, 13241-13248.

Lopez-Otin, C., Blasco, M.A., Partridge, L., Serrano, M., and Kroemer, G. (2013). The hallmarks of aging. Cell *153*, 1194-1217.

Low, K.C., and Tergaonkar, V. (2013). Telomerase: central regulator of all of the hallmarks of cancer. Trends Biochem Sci *38*, 426-434.

Mah, N., Wang, Y., Liao, M.C., Prigione, A., Jozefczuk, J., Lichtner, B., Wolfrum, K., Haltmeier, M., Flottmann, M., Schaefer, M., *et al.* (2011). Molecular insights into reprogramming-initiation events mediated by the OSKM gene regulatory network. PLoS One *6*, e24351.

Maillet, L., Boscheron, C., Gotta, M., Marcand, S., Gilson, E., and Gasser, S.M. (1996). Evidence for silencing compartments within the yeast nucleus: a role for telomere proximity and Sir protein concentration in silencer-mediated repression. Genes Dev *10*, 1796-1811.

Makarov, V.L., Hirose, Y., and Langmore, J.P. (1997). Long G tails at both ends of human chromosomes suggest a C strand degradation mechanism for telomere shortening. Cell *88*, 657-666.

Marcand, S., Buck, S.W., Moretti, P., Gilson, E., and Shore, D. (1996). Silencing of genes at nontelomeric sites in yeast is controlled by sequestration of silencing factors at telomeres by Rap 1 protein. Genes Dev *10*, 1297-1309.

Marion, R.M., Strati, K., Li, H., Murga, M., Blanco, R., Ortega, S., Fernandez-Capetillo, O., Serrano, M., and Blasco, M.A. (2009a). A p53-mediated DNA damage response limits reprogramming to ensure iPS cell genomic integrity. Nature *460*, 1149-1153.

Marion, R.M., Strati, K., Li, H., Tejera, A., Schoeftner, S., Ortega, S., Serrano, M., and Blasco, M.A. (2009b). Telomeres acquire embryonic stem cell characteristics in induced pluripotent stem cells. Cell Stem Cell *4*, 141-154.

Marson, A., Foreman, R., Chevalier, B., Bilodeau, S., Kahn, M., Young, R.A., and Jaenisch, R. (2008). Wnt signaling promotes reprogramming of somatic cells to pluripotency. Cell Stem Cell *3*, 132-135.

Martin, G.R. (1981). Isolation of a pluripotent cell line from early mouse embryos cultured in medium conditioned by teratocarcinoma stem cells. Proc Natl Acad Sci U S A *78*, 7634-7638.

Martinez, P., and Blasco, M.A. (2011). Telomeric and extra-telomeric roles for telomerase and the telomere-binding proteins. Nat Rev Cancer *11*, 161-176.

Martinez, P., Thanasoula, M., Carlos, A.R., Gomez-Lopez, G., Tejera, A.M., Schoeftner, S., Dominguez, O., Pisano, D.G., Tarsounas, M., and Blasco, M.A.

(2010). Mammalian Rap1 controls telomere function and gene expression through binding to telomeric and extratelomeric sites. Nat Cell Biol *12*, 768-780.

Martinez, P., Thanasoula, M., Munoz, P., Liao, C., Tejera, A., McNees, C., Flores, J.M., Fernandez-Capetillo, O., Tarsounas, M., and Blasco, M.A. (2009). Increased telomere fragility and fusions resulting from TRF1 deficiency lead to degenerative pathologies and increased cancer in mice. Genes Dev *23*, 2060-2075.

Mathew, R., Jia, W., Sharma, A., Zhao, Y., Clarke, L.E., Cheng, X., Wang, H., Salli, U., Vrana, K.E., Robertson, G.P., *et al.* (2010). Robust activation of the human but not mouse telomerase gene during the induction of pluripotency. FASEB J *24*, 2702-2715.

McClintock, B. (1941). The Stability of Broken Ends of Chromosomes in Zea Mays. Genetics *26*, 234-282.

McKerlie, M., Walker, J.R., Mitchell, T.R., Wilson, F.R., and Zhu, X.D. (2013). Phosphorylated (pT371)TRF1 is recruited to sites of DNA damage to facilitate homologous recombination and checkpoint activation. Nucleic Acids Res *41*, 10268-10282.

McKerlie, M., and Zhu, X.D. (2011). Cyclin B-dependent kinase 1 regulates human TRF1 to modulate the resolution of sister telomeres. Nat Commun *2*, 371.

Messier, W., Li, S.H., and Stewart, C.B. (1996). The birth of microsatellites. Nature *381*, 483.

Meyne, J., Baker, R.J., Hobart, H.H., Hsu, T.C., Ryder, O.A., Ward, O.G., Wiley, J.E., Wurster-Hill, D.H., Yates, T.L., and Moyzis, R.K. (1990). Distribution of non-telomeric sites of the (TTAGGG)n telomeric sequence in vertebrate chromosomes. Chromosoma *99*, 3-10.

Miyoshi, N., Ishii, H., Nagano, H., Haraguchi, N., Dewi, D.L., Kano, Y., Nishikawa, S., Tanemura, M., Mimori, K., Tanaka, F., *et al.* (2011). Reprogramming of mouse and human cells to pluripotency using mature microRNAs. Cell Stem Cell *8*, 633-638.

Momcilovic, O., Knobloch, L., Fornsaglio, J., Varum, S., Easley, C., and Schatten, G. (2010). DNA damage responses in human induced pluripotent stem cells and embryonic stem cells. PLoS One *5*, e13410.

Montgomery, R.K., Carlone, D.L., Richmond, C.A., Farilla, L., Kranendonk, M.E., Henderson, D.E., Baffour-Awuah, N.Y., Ambruzs, D.M., Fogli, L.K., Algra, S., *et al.* (2011). Mouse telomerase reverse transcriptase (mTert) expression marks slowly cycling intestinal stem cells. Proc Natl Acad Sci U S A *108*, 179-184.

Munoz, P., Blanco, R., de Carcer, G., Schoeftner, S., Benetti, R., Flores, J.M., Malumbres, M., and Blasco, M.A. (2009). TRF1 controls telomere length and mitotic fidelity in epithelial homeostasis. Mol Cell Biol *29*, 1608-1625.

Munoz, P., Blanco, R., Flores, J.M., and Blasco, M.A. (2005). XPF nuclease-dependent telomere loss and increased DNA damage in mice overexpressing TRF2 result in premature aging and cancer. Nat Genet *37*, 1063-1071.

Nakagawa, M., Koyanagi, M., Tanabe, K., Takahashi, K., Ichisaka, T., Aoi, T., Okita, K., Mochiduki, Y., Takizawa, N., and Yamanaka, S. (2008). Generation of induced pluripotent stem cells without Myc from mouse and human fibroblasts. Nat Biotechnol *26*, 101-106.

Nandakumar, J., and Cech, T.R. (2013). Finding the end: recruitment of telomerase to telomeres. Nat Rev Mol Cell Biol *14*, 69-82.

Nergadze, S.G., Santagostino, M.A., Salzano, A., Mondello, C., and Giulotto, E. (2007). Contribution of telomerase RNA retrotranscription to DNA double-strand break repair during mammalian genome evolution. Genome Biol *8*, R260.

Neumann, A.A., Watson, C.M., Noble, J.R., Pickett, H.A., Tam, P.P., and Reddel, R.R. (2013). Alternative lengthening of telomeres in normal mammalian somatic cells. Genes Dev *27*, 18-23.

O'Malley, J., Skylaki, S., Iwabuchi, K.A., Chantzoura, E., Ruetz, T., Johnsson, A., Tomlinson, S.R., Linnarsson, S., and Kaji, K. (2013). High-resolution analysis with novel cell-surface markers identifies routes to iPS cells. Nature *499*, 88-91.

Ohki, R., Tsurimoto, T., and Ishikawa, F. (2001). In vitro reconstitution of the end replication problem. Mol Cell Biol *21*, 5753-5766.

Okamoto, K., Iwano, T., Tachibana, M., and Shinkai, Y. (2008). Distinct roles of TRF1 in the regulation of telomere structure and lengthening. J Biol Chem *283*, 23981-23988.

Okazaki, R., Okazaki, T., Sakabe, K., and Sugimoto, K. (1967). Mechanism of DNA replication possible discontinuity of DNA chain growth. Jpn J Med Sci Biol *20*, 255-260.

Okita, K., Matsumura, Y., Sato, Y., Okada, A., Morizane, A., Okamoto, S., Hong, H., Nakagawa, M., Tanabe, K., Tezuka, K., *et al.* (2011). A more efficient method to generate integration-free human iPS cells. Nat Methods *8*, 409-412.

Okita, K., Nakagawa, M., Hyenjong, H., Ichisaka, T., and Yamanaka, S. (2008). Generation of mouse induced pluripotent stem cells without viral vectors. Science *322*, 949-953.

Opresko, P.L., von Kobbe, C., Laine, J.P., Harrigan, J., Hickson, I.D., and Bohr, V.A. (2002). Telomere-binding protein TRF2 binds to and stimulates the Werner and Bloom syndrome helicases. J Biol Chem *277*, 41110-41119.

Park, J.I., Venteicher, A.S., Hong, J.Y., Choi, J., Jun, S., Shkreli, M., Chang, W., Meng, Z., Cheung, P., Ji, H., *et al.* (2009). Telomerase modulates Wnt signalling by association with target gene chromatin. Nature *460*, 66-72.

Polo, J.M., Anderssen, E., Walsh, R.M., Schwarz, B.A., Nefzger, C.M., Lim, S.M., Borkent, M., Apostolou, E., Alaei, S., Cloutier, J., *et al.* (2012). A molecular roadmap of reprogramming somatic cells into iPS cells. Cell *151*, 1617-1632.

Poulet, A., Pisano, S., Faivre-Moskalenko, C., Pei, B., Tauran, Y., Haftek-Terreau, Z., Brunet, F., Le Bihan, Y.V., Ledu, M.H., Montel, F., *et al.* (2012). The N-terminal domains of TRF1 and TRF2 regulate their ability to condense telomeric DNA. Nucleic Acids Res *40*, 2566-2576.

Pucci, F., Gardano, L., and Harrington, L. (2013). Short telomeres in ESCs lead to unstable differentiation. Cell Stem Cell *12*, 479-486.

Quail, M.A., Kozarewa, I., Smith, F., Scally, A., Stephens, P.J., Durbin, R., Swerdlow, H., and Turner, D.J. (2008). A large genome center's improvements to the Illumina sequencing system. Nat Methods *5*, 1005-1010.

Rideout, W.M., 3rd, Eggan, K., and Jaenisch, R. (2001). Nuclear cloning and epigenetic reprogramming of the genome. Science *293*, 1093-1098.

Ruiz-Herrera, A., Nergadze, S.G., Santagostino, M., and Giulotto, E. (2008). Telomeric repeats far from the ends: mechanisms of origin and role in evolution. Cytogenet Genome Res *122*, 219-228.

Sabapathy, K., Klemm, M., Jaenisch, R., and Wagner, E.F. (1997). Regulation of ES cell differentiation by functional and conformational modulation of p53. EMBO J *16*, 6217-6229.

Sahin, E., Colla, S., Liesa, M., Moslehi, J., Muller, F.L., Guo, M., Cooper, M., Kotton, D., Fabian, A.J., Walkey, C., *et al.* (2011). Telomere dysfunction induces metabolic and mitochondrial compromise. Nature *470*, 359-365.

Samper, E., Goytisolo, F.A., Slijepcevic, P., van Buul, P.P., and Blasco, M.A. (2000). Mammalian Ku86 protein prevents telomeric fusions independently of the length of TTAGGG repeats and the G-strand overhang. EMBO Rep *1*, 244-252.

Santos, J.H., Meyer, J.N., Skorvaga, M., Annab, L.A., and Van Houten, B. (2004). Mitochondrial hTERT exacerbates free-radical-mediated mtDNA damage. Aging Cell *3*, 399-411.

Santos, J.H., Meyer, J.N., and Van Houten, B. (2006). Mitochondrial localization of telomerase as a determinant for hydrogen peroxide-induced mitochondrial DNA damage and apoptosis. Hum Mol Genet *15*, 1757-1768.

Schepers, A.G., Vries, R., van den Born, M., van de Wetering, M., and Clevers, H. (2011). Lgr5 intestinal stem cells have high telomerase activity and randomly segregate their chromosomes. EMBO J *30*, 1104-1109.

Schneider, R.P., Garrobo, I., Foronda, M., Palacios, J.A., Marion, R.M., Flores, I., Ortega, S., and Blasco, M.A. (2013). TRF1 is a stem cell marker and is essential for the generation of induced pluripotent stem cells. Nat Commun *4*, 1946.

Schoeftner, S., Blanco, R., Lopez de Silanes, I., Munoz, P., Gomez-Lopez, G., Flores, J.M., and Blasco, M.A. (2009). Telomere shortening relaxes X chromosome inactivation and forces global transcriptome alterations. Proc Natl Acad Sci U S A *106*, 19393-19398.

Sfeir, A., Kosiyatrakul, S.T., Hockemeyer, D., MacRae, S.L., Karlseder, J., Schildkraut, C.L., and de Lange, T. (2009). Mammalian telomeres resemble fragile sites and require TRF1 for efficient replication. Cell *138*, 90-103.

Sharov, A.A., Masui, S., Sharova, L.V., Piao, Y., Aiba, K., Matoba, R., Xin, L., Niwa, H., and Ko, M.S. (2008). Identification of Pou5f1, Sox2, and Nanog downstream target genes with statistical confidence by applying a novel algorithm to time course microarray and genome-wide chromatin immunoprecipitation data. BMC Genomics *9*, 269.

Simonet, T., Zaragosi, L.E., Philippe, C., Lebrigand, K., Schouteden, C., Augereau, A., Bauwens, S., Ye, J., Santagostino, M., Giulotto, E., *et al.* (2011). The human TTAGGG repeat factors 1 and 2 bind to a subset of interstitial telomeric sequences and satellite repeats. Cell Res *21*, 1028-1038.

Smith, S., and de Lange, T. (1997). TRF1, a mammalian telomeric protein. Trends Genet *13*, 21-26.

Smith, S., Giriat, I., Schmitt, A., and de Lange, T. (1998). Tankyrase, a poly(ADP-ribose) polymerase at human telomeres. Science *282*, 1484-1487.

Smogorzewska, A., van Steensel, B., Bianchi, A., Oelmann, S., Schaefer, M.R., Schnapp, G., and de Lange, T. (2000). Control of human telomere length by TRF1 and TRF2. Mol Cell Biol *20*, 1659-1668.

Solozobova, V., Rolletschek, A., and Blattner, C. (2009). Nuclear accumulation and activation of p53 in embryonic stem cells after DNA damage. BMC Cell Biol *10*, 46.

Soohoo, C.Y., Shi, R., Lee, T.H., Huang, P., Lu, K.P., and Zhou, X.Z. (2011). Telomerase inhibitor PinX1 provides a link between TRF1 and telomerase to prevent telomere elongation. J Biol Chem *286*, 3894-3906.

Soufi, A., Donahue, G., and Zaret, K.S. (2012). Facilitators and impediments of the pluripotency reprogramming factors' initial engagement with the genome. Cell *151*, 994-1004.

Sridharan, R., Tchieu, J., Mason, M.J., Yachechko, R., Kuoy, E., Horvath, S., Zhou, Q., and Plath, K. (2009). Role of the murine reprogramming factors in the induction of pluripotency. Cell *136*, 364-377.

Stadtfeld, M., Maherali, N., Breault, D.T., and Hochedlinger, K. (2008a). Defining molecular cornerstones during fibroblast to iPS cell reprogramming in mouse. Cell Stem Cell *2*, 230-240.

Stadtfeld, M., Nagaya, M., Utikal, J., Weir, G., and Hochedlinger, K. (2008b). Induced pluripotent stem cells generated without viral integration. Science *322*, 945-949.

Suhr, S.T., Chang, E.A., Rodriguez, R.M., Wang, K., Ross, P.J., Beyhan, Z., Murthy, S., and Cibelli, J.B. (2009). Telomere dynamics in human cells reprogrammed to pluripotency. PLoS One *4*, e8124.

Sutherland, G.R., Baker, E., and Richards, R.I. (1998). Fragile sites still breaking. Trends Genet *14*, 501-506.

Tada, M., Takahama, Y., Abe, K., Nakatsuji, N., and Tada, T. (2001). Nuclear reprogramming of somatic cells by in vitro hybridization with ES cells. Curr Biol *11*, 1553-1558.

Takahashi, K., Okita, K., Nakagawa, M., and Yamanaka, S. (2007). Induction of pluripotent stem cells from fibroblast cultures. Nat Protoc *2*, 3081-3089.

Takahashi, K., and Yamanaka, S. (2006). Induction of pluripotent stem cells from mouse embryonic and adult fibroblast cultures by defined factors. Cell *126*, 663-676.

Tazumi, A., Fukuura, M., Nakato, R., Kishimoto, A., Takenaka, T., Ogawa, S., Song, J.H., Takahashi, T.S., Nakagawa, T., Shirahige, K., *et al.* (2012). Telomere-binding protein Taz1 controls global replication timing through its localization near late replication origins in fission yeast. Genes Dev *26*, 2050-2062.

Tejera, A.M., Stagno d'Alcontres, M., Thanasoula, M., Marion, R.M., Martinez, P., Liao, C., Flores, J.M., Tarsounas, M., and Blasco, M.A. (2010). TPP1 is required for TERT recruitment, telomere elongation during nuclear reprogramming, and normal skin development in mice. Dev Cell *18*, 775-789.

Theunissen, T.W., van Oosten, A.L., Castelo-Branco, G., Hall, J., Smith, A., and Silva, J.C. (2011). Nanog overcomes reprogramming barriers and induces pluripotency in minimal conditions. Curr Biol *21*, 65-71.

Tomas-Loba, A., Flores, I., Fernandez-Marcos, P.J., Cayuela, M.L., Maraver, A., Tejera, A., Borras, C., Matheu, A., Klatt, P., Flores, J.M., *et al.* (2008). Telomerase reverse transcriptase delays aging in cancer-resistant mice. Cell *135*, 609-622.

Tsakiri, K.D., Cronkhite, J.T., Kuan, P.J., Xing, C., Raghu, G., Weissler, J.C., Rosenblatt, R.L., Shay, J.W., and Garcia, C.K. (2007). Adult-onset pulmonary fibrosis caused by mutations in telomerase. Proc Natl Acad Sci U S A *104*, 7552-7557.

Utikal, J., Polo, J.M., Stadtfeld, M., Maherali, N., Kulalert, W., Walsh, R.M., Khalil, A., Rheinwald, J.G., and Hochedlinger, K. (2009). Immortalization eliminates a roadblock during cellular reprogramming into iPS cells. Nature *460*, 1145-1148.

van Steensel, B., and de Lange, T. (1997). Control of telomere length by the human telomeric protein TRF1. Nature *385*, 740-743.

Varela, E., Schneider, R.P., Ortega, S., and Blasco, M.A. (2011). Different telomere-length dynamics at the inner cell mass versus established embryonic stem (ES) cells. Proc Natl Acad Sci U S A *108*, 15207-15212.

Vaziri, H., Chapman, K.B., Guigova, A., Teichroeb, J., Lacher, M.D., Sternberg, H., Singec, I., Briggs, L., Wheeler, J., Sampathkumar, J., *et al.* (2010). Spontaneous reversal of the developmental aging of normal human cells following transcriptional reprogramming. Regen Med *5*, 345-363.

Walker, J.R., and Zhu, X.D. (2012). Post-translational modifications of TRF1 and TRF2 and their roles in telomere maintenance. Mech Ageing Dev *133*, 421-434.

Wang, F., Yin, Y., Ye, X., Liu, K., Zhu, H., Wang, L., Chiourea, M., Okuka, M., Ji, G., Dan, J., *et al.* (2012). Molecular insights into the heterogeneity of telomere reprogramming in induced pluripotent stem cells. Cell Res *22*, 757-768.

Wang, Y., Chen, J., Hu, J.L., Wei, X.X., Qin, D., Gao, J., Zhang, L., Jiang, J., Li, J.S., Liu, J., *et al.* (2011). Reprogramming of mouse and human somatic cells by high-performance engineered factors. EMBO Rep *12*, 373-378.

Wernig, M., Meissner, A., Cassady, J.P., and Jaenisch, R. (2008). c-Myc is dispensable for direct reprogramming of mouse fibroblasts. Cell Stem Cell *2*, 10-12.

Wilmut, I., Schnieke, A.E., McWhir, J., Kind, A.J., and Campbell, K.H. (1997). Viable offspring derived from fetal and adult mammalian cells. Nature *385*, 810-813.

Woltjen, K., Michael, I.P., Mohseni, P., Desai, R., Mileikovsky, M., Hamalainen, R., Cowling, R., Wang, W., Liu, P., Gertsenstein, M., *et al.* (2009). piggyBac transposition reprograms fibroblasts to induced pluripotent stem cells. Nature *458*, 766-770.

Wong, C.W., Hou, P.S., Tseng, S.F., Chien, C.L., Wu, K.J., Chen, H.F., Ho, H.N., Kyo, S., and Teng, S.C. (2010). Kruppel-like transcription factor 4 contributes to maintenance of telomerase activity in stem cells. Stem Cells *28*, 1510-1517.

Wong, L.H., Ren, H., Williams, E., McGhie, J., Ahn, S., Sim, M., Tam, A., Earle, E., Anderson, M.A., Mann, J., *et al.* (2009). Histone H3.3 incorporation provides a unique and functionally essential telomeric chromatin in embryonic stem cells. Genome Res *19*, 404-414.

Wu, K.J., Grandori, C., Amacker, M., Simon-Vermot, N., Polack, A., Lingner, J., and Dalla-Favera, R. (1999). Direct activation of TERT transcription by c-MYC. Nat Genet *21*, 220-224.

Wu, P., Takai, H., and de Lange, T. (2012). Telomeric 3' overhangs derive from resection by Exo1 and Apollo and fill-in by POT1b-associated CST. Cell *150*, 39-52.

Xin, H., Liu, D., Wan, M., Safari, A., Kim, H., Sun, W., O'Connor, M.S., and Songyang, Z. (2007). TPP1 is a homologue of ciliate TEBP-beta and interacts with POT1 to recruit telomerase. Nature *445*, 559-562.

Yang, C., Przyborski, S., Cooke, M.J., Zhang, X., Stewart, R., Anyfantis, G., Atkinson, S.P., Saretzki, G., Armstrong, L., and Lako, M. (2008). A key role for telomerase reverse transcriptase unit in modulating human embryonic stem cell proliferation, cell cycle dynamics, and in vitro differentiation. Stem Cells *26*, 850-863.

Yang, C.R., Yeh, S., Leskov, K., Odegaard, E., Hsu, H.L., Chang, C., Kinsella, T.J., Chen, D.J., and Boothman, D.A. (1999). Isolation of Ku70-binding proteins (KUBs). Nucleic Acids Res *27*, 2165-2174.

Yang, D., Xiong, Y., Kim, H., He, Q., Li, Y., Chen, R., and Songyang, Z. (2011). Human telomeric proteins occupy selective interstitial sites. Cell Res *21*, 1013-1027.

Yang, X., and Smith, S.L. (2007). ES cells derived from cloned embryos in monkey--a jump toward human therapeutic cloning. Cell Res *17*, 969-970.

Ye, J.Z., Donigian, J.R., van Overbeek, M., Loayza, D., Luo, Y., Krutchinsky, A.N., Chait, B.T., and de Lange, T. (2004a). TIN2 binds TRF1 and TRF2 simultaneously and stabilizes the TRF2 complex on telomeres. J Biol Chem *279*, 47264-47271.

Ye, J.Z., Hockemeyer, D., Krutchinsky, A.N., Loayza, D., Hooper, S.M., Chait, B.T., and de Lange, T. (2004b). POT1-interacting protein PIP1: a telomere length regulator that recruits POT1 to the TIN2/TRF1 complex. Genes Dev *18*, 1649-1654.

Yehezkel, S., Rebibo-Sabbah, A., Segev, Y., Tzukerman, M., Shaked, R., Huber, I., Gepstein, L., Skorecki, K., and Selig, S. (2011). Reprogramming of telomeric regions during the generation of human induced pluripotent stem cells and subsequent differentiation into fibroblast-like derivatives. Epigenetics *6*, 63-75.

Yin, L., Hubbard, A.K., and Giardina, C. (2000). NF-kappa B regulates transcription of the mouse telomerase catalytic subunit. J Biol Chem *275*, 36671-36675.

Yoo, J.E., Park, Y.N., and Oh, B.K. (2014). PinX1, a telomere repeat-binding factor 1 (TRF1)-interacting protein, maintains telomere integrity by modulating TRF1 homeostasis, the process in which human telomerase reverse Transcriptase (hTERT) plays dual roles. J Biol Chem *289*, 6886-6898.

Yu, J., Hu, K., Smuga-Otto, K., Tian, S., Stewart, R., Slukvin, II, and Thomson, J.A. (2009). Human induced pluripotent stem cells free of vector and transgene sequences. Science *324*, 797-801.

Yu, J., Vodyanik, M.A., Smuga-Otto, K., Antosiewicz-Bourget, J., Frane, J.L., Tian, S., Nie, J., Jonsdottir, G.A., Ruotti, V., Stewart, R., *et al.* (2007). Induced pluripotent stem cell lines derived from human somatic cells. Science *318*, 1917-1920.

Zaug, A.J., Podell, E.R., Nandakumar, J., and Cech, T.R. (2010). Functional interaction between telomere protein TPP1 and telomerase. Genes Dev *24*, 613-622.

Zhang, P., Chang, W.H., Fong, B., Gao, F., Liu, C., Al Alam, D., Bellusci, S., and Lu, W. (2014). Regulation of induced pluripotent stem (iPS) cell induction by Wnt/beta-catenin signaling. J Biol Chem *289*, 9221-9232.

Zhang, Y., Toh, L., Lau, P., and Wang, X. (2012). Human telomerase reverse transcriptase (hTERT) is a novel target of the Wnt/beta-catenin pathway in human cancer. J Biol Chem *287*, 32494-32511.

Zhao, X.Y., Li, W., Lv, Z., Liu, L., Tong, M., Hai, T., Hao, J., Guo, C.L., Ma, Q.W., Wang, L., *et al.* (2009). iPS cells produce viable mice through tetraploid complementation. Nature *461*, 86-90.

Zhao, Y., Cheng, D., Wang, S., and Zhu, J. (2014). Dual roles of c-Myc in the regulation of hTERT gene. Nucleic Acids Res *42*, 10385-10398.

Zhong, Z., Shiue, L., Kaplan, S., and de Lange, T. (1992). A mammalian factor that binds telomeric TTAGGG repeats in vitro. Mol Cell Biol *12*, 4834-4843.

Zhu, S., Wei, W., and Ding, S. (2011). Chemical strategies for stem cell biology and regenerative medicine. Annu Rev Biomed Eng *13*, 73-90.

Zhu, X.D., Kuster, B., Mann, M., Petrini, J.H., and de Lange, T. (2000). Cell-cycle-regulated association of RAD50/MRE11/NBS1 with TRF2 and human telomeres. Nat Genet *25*, 347-352.

Zhu, X.D., Niedernhofer, L., Kuster, B., Mann, M., Hoeijmakers, J.H., and de Lange, T. (2003). ERCC1/XPF removes the 3' overhang from uncapped telomeres and represses formation of telomeric DNA-containing double minute chromosomes. Mol Cell *12*, 1489-1498.

Zuo, B., Yang, J., Wang, F., Wang, L., Yin, Y., Dan, J., Liu, N., and Liu, L. (2012). Influences of lamin A levels on induction of pluripotent stem cells. Biol Open *1*, 1118-1127.

Annex

Published articles directly related to this thesis:

Schneider R, **Garrobo I**, Foronda M, Palacios JA, Marión RM, Flores I, Ortega S, Blasco MA. "TRF1 is a stem cell marker and is essential for the generation of induced pluripotent stem cells." *Nature Communications.* 4: 1946 (2013).

Garrobo I, Marión RM, Domínguez O, Pisano D and Blasco MA. Genome-wide analysis of *in vivo* TRF1 binding to chromatin restricts its location exclusively to telomeric repeats. *Cell Cycle*. Accepted, 2014.